technische universität
dortmund

Arbeit zur Erlangung des akademischen Grades
Dr. rer. nat.

Towards reducing uncertainties in the applied effective dose for two specialized radiotherapy techniques: Total body irradiation and proton therapy

Lena Heuchel
geboren in Essen

2023

Fakultät Physik
Technische Universität Dortmund

Von der Fakultät Physik zur Veröffentlichung angenommene Dissertation zur Erlangung des akademischen Grades eines Doktors der Naturwissenschaften (Doctor rerum naturalium).

Erstgutachter:	Prof. Dr. Armin Lühr
Zweitgutachter:	PD Dr. Christian Bäumer
Vorsitzender der Prüfungskommission:	Prof. Dr. Kevin Krönninger
Vertretung der wissenschaftlichen Mitarbeitenden:	Dr. Sergiu Anghel
Abgabedatum:	December 20th 2023
Datum der mündlichen Prüfung:	April 17th 2024

Abstract

Radiotherapy is a high-precision treatment of malignant diseases. However, for some specialized techniques, e.g., total body irradiation (TBI) and proton therapy, considerable uncertainties remain regarding the applied effective dose. For some TBI techniques, no CT-based treatment planning is performed, therefore 3D dose distributions are unavailable. For proton therapy, the relative biological effectiveness (RBE) compared to standard photon irradiation is variable and subject to high uncertainties, particularly at the end of the proton range. Clinically, however, a constant RBE of 1.1 is assumed, since precise knowledge of the RBE distribution in patients, and therefore of the applied biological effective dose, is lacking. Two surveys among German and European clinics were performed to analyze the current clinical practice for TBI and proton therapy, respectively. These surveys showed that participating centers wish for new and improved guidelines for treatment planning, but important tools for analyzing the needed clinical data are missing. Therefore, these necessary tools were developed and tested by performing in silico patient irradiation studies. For TBI, a Monte Carlo-based simulation workflow was developed allowing for 3D dose calculations for non-CT-based TBI techniques. For proton therapy, a novel concept was introduced allowing for the reduction of dose components associated with high RBE uncertainties.

Kurzfassung

Die Strahlentherapie ist eine hochpräzise Behandlung von bösartigen Erkrankungen. Bei einigen speziellen Techniken, z.B. der Ganzkörperbestrahlung (GKB) und der Protonentherapie, bestehen jedoch nach wie vor erhebliche Unsicherheiten hinsichtlich der applizierten effektiven Dosis. Bei einigen GKB-Techniken wird keine CT-basierte Planung durchgeführt, weswegen 3D Dosisverteilungen nicht bekannt sind. Bei der Protonentherapie ist die relative biologische Wirksamkeit (RBW) im Vergleich zur Standard-Photonenbestrahlung variabel und insbesondere am Ende des Protonenreichweite mit großen Unsicherheiten behaftet. Klinisch wird jedoch eine konstante RBW von 1,1 angenommen, da genaue Kenntnisse über die RBW-Verteilung in Patienten, und damit über die applizierte biologisch wirksame Dosis, fehlen. Zunächst wurden zwei Umfragen unter deutschen und europäischen Kliniken durchgeführt, um das derzeitige klinische Vorgehen für TBI bzw. Protonentherapie zu analysieren. Diese Umfragen haben gezeigt, dass die teilnehmende Zentren sich neue und verbesserte Richtlinien bezogen auf die Behandlungsplanung wünschen, hierfür allerdings wichtige Hilfsmittel zur Analyse der benötogten klinischen Daten fehlen. Aus diesem Grund wurden diese benötigten Hilfsmittel entwickelt und anhand von in silico Patientenstudien getestet. Für die GKB wurden ein Monte Carlo-basierter Simulationsworkflow entwickelt, der die 3D Dosisberechnung für nicht CT-basierte GKB-Techniken erlaubt. Für die Protonentherapie wurde ein neues Konzept vorgestellt, welches die Reduzierung des mit hohen RBW-Unsicherheiten behafteten Dosisanteils erlaubt.

Contents

1 Introduction **1**

2 Theoretical background **3**
2.1 Radiation physics . . . 3
2.2 Radiation biology . . . 8
2.3 Irradiation techniques . . . 10
2.4 Treatment planning . . . 15

3 Project photons: Total body irradiation **21**
3.1 Survey . . . 21
3.1.1 Material and methods . . . 21
3.1.2 Results . . . 22
3.1.3 Discussion . . . 27
3.2 In silico study . . . 29
3.2.1 Material and methods . . . 30
3.2.2 Results . . . 33
3.2.3 Discussion . . . 42
3.3 Conclusion . . . 44

4 Project protons: Variable relative biological effectiveness **46**
4.1 Survey . . . 46
4.1.1 Material and methods . . . 46
4.1.2 Results . . . 48
4.1.3 Discussion . . . 53
4.2 In silico study . . . 56
4.2.1 Material and methods . . . 56
4.2.2 Results . . . 61
4.2.3 Discussion . . . 74
4.3 Conclusion . . . 79

5 Summary and Conclusion **80**

A Appendix **83**

References **121**

List of Publications **134**

Danksagung **137**

List of Figures

2.1 Photon depth dose curves . . . 4
2.2 Proton depth dose curve . . . 6
2.3 Proton spread-out Bragg peak . . . 6
2.4 Dose and LET of a proton Bragg peak . . . 8
2.5 Dose, LET and variable RBE-weighted dose of an SOBP . . . 10
2.6 Photon energy spectra of clinical linacs . . . 11
2.7 Head of a clinical linac . . . 12
2.8 Extended SSD and translational couch appa-TBI . . . 14
2.9 Pencil beam scanning system . . . 15
2.10 Beam-zone method . . . 18

3.1 Number of patients and children treated with TBI . . . 23
3.2 Used irradiation TBI techniques . . . 24
3.3 Prescribed dose definition and CT usage for TBI . . . 26
3.4 Set-up of the translational couch and extended SSD technique . . . 31
3.5 DVH for the translational couch technique . . . 34
3.6 Dose on CT slice for the translational couch technique . . . 35
3.7 DVH for the validation of the beam-zone method . . . 37
3.8 DVH for the comparison of TBI techniques . . . 40
3.9 Dose on CT slice for the comparison of TBI techniques . . . 41

4.1 Map of Europe . . . 47
4.2 Minimum number of treatment fields . . . 50
4.3 Number of centers using constant RBE and applying measures . . . 50
4.4 RBE-relevant sites and applied measures . . . 51
4.5 Calculated quantities and software used . . . 53
4.6 Two-step planning approach . . . 57
4.7 Used water phantoms . . . 59
4.8 Line profiles in an SOBP . . . 62
4.9 Total, dirty, and clean dose on a water phantom CT slice . . . 63
4.10 Differences between DDopt and RefPlan in the water phantom . . . 64
4.11 Differences between DDopt and RefPlan on water phantom CT . . . 65
4.12 Dose for different number of treatment fields on water phantom CT . . . 66
4.13 Dose on CT, DVH and line doses for patient 1 . . . 68
4.14 Dose on CT, DVH, and line doses for patient 2 . . . 69
4.15 Differences between DDopt and RefPlan for both patients . . . 70
4.16 DVH and LETVH for LETopt . . . 71

List of Tables

3.1 Number of questions of the TBI survey 24
3.2 Parameters for the translational couch technique 34
3.3 Parameters for the validation of the beam-zone method 36
3.4 Parameters for the comparison of TBI techniques 39

4.1 Response rate for the different RBE topics of the survey 49
4.2 Comparison between RefPlan, DDopt and LETopt for patient 1 71
4.3 Comparison between RefPlan, DDopt and LETopt for patient 2 73
4.4 NTCP for patient 1 and patient 2 73

List of Abbreviations

AAPM	American association of physicists in medicine
appa	Anterior-posterior/posterior-anterior
CI	Conformity index
CT	Computed tomography
CTV	Clinical target volume
DDopt	Dirty dose optimized
DGMP	German society for medical physics
DRP	Dose reference point
DSP	Dose specification point
DVH	Dose-volume histogram
ESTRO	European society for therapeutic radiology and oncology
extSSD	Extended source-to-surface distance
GTV	Gross tumor volume
helT	Helical tomotherapy
HI	Homogeneity index
HLUT	Hounsfield unit look-up table
HU	Hounsfield unit
IMPT	Intensity modulated proton therapy
IMRT	Intensity modulated radiotherapy
ITV	Internal target volume
LET	Linear energy transfer
LETopt	Linear energy transfer optimized
LETVH	Linear energy transfer-volume histogram
MLC	Multi leaf collimator
MRI	Magnetic resonance imaging
NTCP	Normal tissue complication probability
OAR	Organ of risk

PBS	Pencil beam scanning
POI	Point of interest
PTCOG	Particle therapy co-operative group
PTV	Planning target volume
RBE	Relative biological effectiveness
RefPlan	Reference plan
ROI	Region of interest
SOBP	Spread-out Bragg peak
SSD	Source-to-surface distance
TBI	Total body irradiation
TLD	Thermoluminescent dosimeter
TPS	Treatment planning system
transC	Translational couch
vRBE	Variable relative biological effectiveness
VMAT	Volumetric modulated arc therapy

1 Introduction

Radiotherapy has been an important part of the treatment of malignant diseases for many decades [1]. The main goal of radiotherapy is the elimination of tumor cells by using ionizing irradiation. When radiation traverses through tissue, a variety of interactions takes place, in which the radiation transfers energy to the tissue, which damages existing cells. This transferred energy per mass is called dose and represents the most important quantity when describing the effect of irradiation. Thus, for optimal patient treatment, precise knowledge of the applied effective dose is crucial.

Nowadays, usually, the first step for creating a treatment plan is the acquisition of a computed tomography (CT) image of the patient followed by the contouring of all regions of interest (ROI), e.g., the target volume and organs at risk (OAR). This CT image including the corresponding contours can then be used for dose calculation and optimization using modern algorithms simulating the energy deposition of the radiation to achieve the desired dose distribution. In this way, a precise 3 dimensional (3D) estimate of the applied dose can be obtained.

Radiotherapy can be performed using different modalities. Most irradiations nowadays are performed using high-energy photons. One irradiation technique exclusively performed with photons is the so-called total body irradiation (TBI). TBI represents an important part of the treatment of malignant diseases of the hematopoietic system, e.g., leukemia. In addition to killing cancer cells, the aim of TBI is also to destroy the patient's immune system in preparation for a subsequent stem cell transplantation [2, 3]. Different studies showed that such prior conditioning using TBI decreases the probability of occurrence of transplantation-induced side effects like graft-versus-host diseases and increases overall survival [4–6]. Since the target cells of TBI are present in the entire body, the entire body represents the target volume for TBI.

Worldwide, there are numerous different techniques for applying TBI [7–16]. For many frequently used TBI techniques, even today, precise 3D dose calculations, as common for standard radiotherapy, are no clinical standard. Often, one of various table-based methods is used to determine the dose at individual reference points (usually 12) along the patient's central axis [13]. These dose points are then used to estimate the dose distribution throughout the entire body. However, as this approach provides no 3D dose distribution, direct dosimetric comparisons between different TBI techniques are complicated.

Another increasingly utilized modality for radiotherapy is the irradiation with

protons. There are two main differences between irradiating with protons and photons. First, protons deposit, in contrast to photons, most of their energy at the end of their range in a certain depth, and second, protons are biologically more effective in cell killing compared to photons. To account for this, the biological effective dose, defined as the product of the absorbed physical dose times the relative biological effectiveness (RBE), is used in proton therapy. By using this RBE concept, prescription and tolerance doses derived from many years of experience with photons can also be used in proton therapy. Currently, a constant RBE of 1.1 is clinically applied assuming that protons are under every circumstance 10% more effective in cell killing than photons.

Numerous in vitro, in vivo and retrospective patient studies [17–24] found, that the RBE depends on different biological and physical parameters, and shows a maximum towards the end of the proton track [25–27]. Thus, the exact applied biological effective dose at the distal edge of a clinical treatment field is, so far, uncertain. Because of the safety margins used in clinical practice, the distal edge is usually located in healthy tissue. Therefore, the application of photon-based tolerance doses together with a constant RBE introduces uncertainties within the normal tissue leading to an increased probability of side effect occurrence.

Compared to standard photon therapy, TBI and proton therapy, are specialized and therefore rather rare treatments, due to the limited number of patients per center for TBI and the limited number of centers for proton therapy, respectively. Therefore, the correlation between the applied effective dose and the achieved clinical outcome is still under investigation underlying the importance of an accurate estimate of the applied effective dose. Thus, the aim of this thesis is the improvement of the exact effective dose calculation for both, TBI and proton therapy.

After a brief introduction of the underlying concepts of radiotherapy (chapter 2), this thesis is divided into two different research projects: "Project photons: Total body irradiation" (chapter 3) and "Project protons: Variable relative biological effectiveness" (chapter 4). Both projects were structured in the same way. First, a survey asking for the current clinical practice and future requirements of TBI or RBE consideration in proton therapy was performed, and second, based on the results of these surveys, in silico patient studies were performed. For TBI, a novel Monte Carlo-based simulation workflow was developed, making the determination of 3D dose distributions for TBI techniques, for which no corresponding dose distributions were previously available, possible. For proton therapy, a novel concept, the dirty & clean dose concept, was introduced allowing for a targeted reduction of the fraction of the dose associated with high uncertainties due to an increased RBE. The results of both projects are summarized and concluded in the last chapter (chapter 5).

2 Theoretical background

In this chapter, theoretical concepts relevant to this thesis are presented. First, aspects of radiation physics important for radiotherapy are introduced, followed by basic principles of radiobiology to explain the effect of different irradiation types on tissue. Then, different irradiation techniques as well as clinically applied approaches for treatment planning are presented.

2.1 Radiation physics

As different types of ionizing irradiation like photons or protons are traversing through matter, they undergo different interactions in which they deposit energy. The absorbed energy $\mathrm{d}E$ per mass element $\mathrm{d}m$ is defined as the energy dose D

$$D = \frac{\mathrm{d}E}{\mathrm{d}m} \tag{2.1}$$

and is given in units of Gy. Depending on the way the energy is transferred, different irradiation types are defined as indirectly, or directly ionizing radiation [28].

Photon interactions with matter

Photons transfer their energy to secondary charged particles, e.g. electrons, which then deposit their energy to the matter. Therefore photons are defined as indirectly ionizing radiation. Photons lose their energy in a few large interactions and have therefore a relevant probability of passing through matter without undergoing any interaction which means that there is no defined range of photons in matter. The most important interactions for photons are the photoelectric effect, Rayleigh scattering, Compton scattering, and pair formation, while for clinical acceleration voltages of 6-25 MV (corresponds to photon energies of approximately 4-25 MeV) the Compton scattering is the dominant process [29]. If a narrow photon beam with N_0 incident photons traversed through matter, the number of photons $N(x)$ after traversing through a layer of material with a thickness of x and a mass attenuation of (μ/ρ) can be described with the concept of exponential attenuation:

$$N(x) = N_0 \exp\left(-\frac{\mu}{\rho}x\right) \ . \tag{2.2}$$

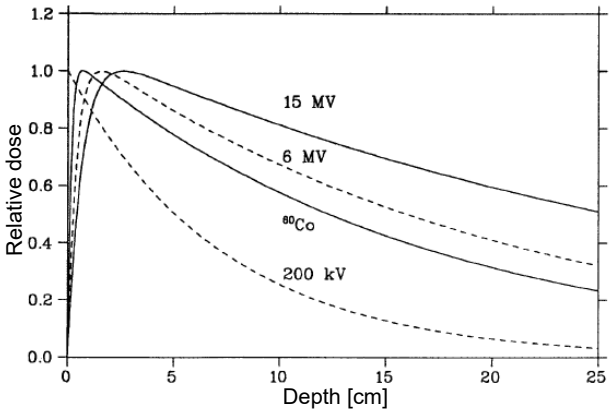

Figure 2.1: Relative depth dose curve for different linear accelerator photon energy sources and a ^{60}Co source in water. Adapted from [29].

Here, μ represents the attenuation coefficient, and ρ is the density of the material. Therefore, the depth dose curve of photons can be described with an exponential function. For the energy range used in radiotherapy, the depth dose curve first shows a build-up region and a dose maximum, before the typical exponential decrease (Fig. 2.1). When the photon beam enters the matter the primary photon fluence, defined as the number of particles per area, decreases while the fluence of secondary electrons increases. Therefore, the dose deposited by secondary electrons increases until an equilibrium of secondary electrons and thus the dose maximum of the build-up region is achieved [29].

Proton interactions with matter

Because of their high mass and their positive charge, proton interactions with matter differ relevantly from photon interactions. Protons are defined as directly ionizing particles and they transfer their energy by Coloumb scattering, nuclear interactions and radiative interactions emitting bremsstrahlung [29]. Therefore, the mean energy loss $\mathrm{d}E$ per unit path length $\mathrm{d}l$, also known as the total stopping power S, can be defined as [30]

$$S = -\frac{\mathrm{d}E}{\mathrm{d}l} = S_{\mathrm{el}} + S_{\mathrm{nuc}} + S_{\mathrm{rad}} \tag{2.3}$$

with S_{el} being the electronic stopping power, S_{nuc} the nuclear stopping power and S_{rad} the radiative stopping power. When protons traverse through matter, they usually undergo numerous interactions transferring only a small amount of energy in each individual interaction. Therefore, protons lose their energy almost gradually

along their track. This process can be approximated using the continuous slowing-down approximation (CSDA), which allows for the calculation of the proton range in material [31]. The proton range R as a function of the kinetic energy E can be described as

$$R(E) = \int_0^E \frac{1}{S(E)} dE \tag{2.4}$$

with S being the stopping power [29]. For clinically used incident proton energies (100 MeV - 200 MeV) the energy loss due to Coloumb scattering is predominate. Therefore, S_{nuc} and S_{rad} can be neglected [32]. S_{el} can be described by the Bethe-Bloch-formula [33–35]:

$$S_{\mathrm{el}} = k\frac{z^2}{\beta^2}\eta L(\beta) \approx k\frac{z^2}{\beta^2}\eta \left[\ln\left(2m_{\mathrm{e}}c^2\frac{\beta^2}{1-\beta^2}\right) - \beta^2 - \ln(I)\right] . \tag{2.5}$$

Here z is the projectile charge, β the velocity in units of the velocity of light in vacuum c, η the electronic density of the target material, m_{e} the mass of electrons, I the mean excitation energy of the target material, $L(\beta)$ the material stopping number function and k a constant factor defined as $k = 5.1 \times 10^{-25}$ MeV cm^2. Protons show a different depth dose curve compared to photons due to the difference in interactions. With decreasing velocity of the protons, the transferred energy per path length increases. Therefore, after an entrance plateau region with an almost constant slowly increasing dose deposition, the depth dose curve of protons shows the characteristic sharp dose maximum followed by a rapid dose decrease, which is called the dose fall-off region (Fig. 2.2). The depth dose curve of protons is called Bragg-peak curve, because of its characteristic maximum. The proton range and therefore the position of the dose maximum depends on the initial energy of the incident particles. To irradiate an entire tumor volume, single Bragg peaks with different energies can be superimposed creating a so-called spread-out Bragg peak (SOBP) (Fig. 2.3).

Linear energy transfer

The absorbed dose is the most important surrogate for the biological effect on the irradiated cells. In addition, the local dose structure around the proton track, and therefore the local ionization density, also influences the achieved biological effect on a cellular level. To describe the local dose structure the linear energy transfer (LET) was introduced [37]. The LET is defined as the energy transferred locally due to electronic interactions per unit path length dl minus the energy carried away by secondary particles with an energy higher than the energy cut-off Δ [30]. Therefore,

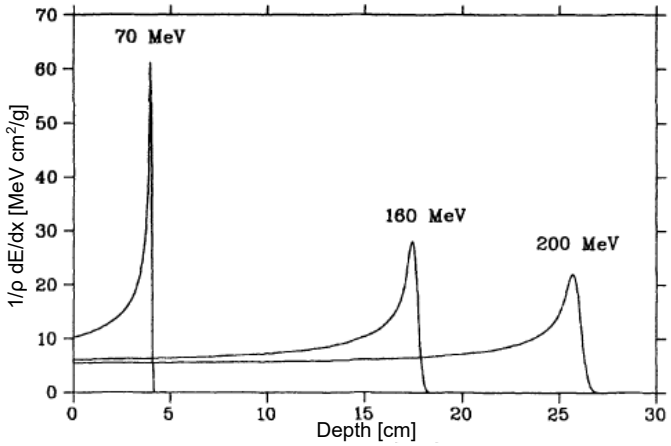

Figure 2.2: Depth dose curves, so-called Bragg peak curves, for protons with different initial energies in water. Adapted from [29].

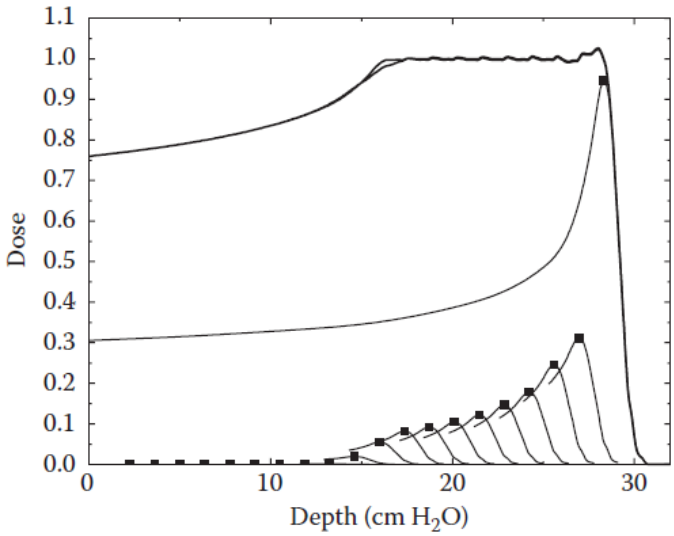

Figure 2.3: Proton spread-out Bragg peak (SOBP) created by superimposing appropriate weighted single Bragg peaks with different energies. Adapted from [36].

the LET is closely related to the stopping power and is defined as

$$\mathrm{LET}_{\Delta} = \frac{\mathrm{d}E_{\Delta}}{\mathrm{d}l} = S_{\mathrm{el}} - \frac{\mathrm{d}E_{\mathrm{ke},\Delta}}{\mathrm{d}l} \ . \tag{2.6}$$

Here LET_{Δ} represents the restricted LET, S_{el} represents the electronic stopping power, and $\mathrm{d}E_{\mathrm{ke},\Delta}$ is the mean sum of energy transferred to electrons with an energy higher than Δ. Including all secondary particles ($\Delta \to \infty$) leads to the unrestricted LET_{∞}, from now on denoted as LET, which equals S_{el}.

In a clinical environment, LET values in a voxel originate from protons with different energies as well as different secondary particles. Thus, two different voxel-wise averaging techniques were introduced. The first one is the so-called track-averaging resulting in the track-averaged LET:

$$\mathrm{LET}_{\mathrm{t}}(x) = \frac{\sum_z \int_0^{\infty} S_{\mathrm{el}}(E)\Phi(E,x)\mathrm{d}E}{\sum_z \int_0^{\infty} \Phi(E,x)\mathrm{d}E} \ . \tag{2.7}$$

Here, z denotes the charge of the different contributing particles, E denotes the kinetic energy of the primary charged particle, and Φ is the fluence at position x. The second method is the so-called dose-averaging leading to the dose-averaged LET:

$$\mathrm{LET}_{\mathrm{d}}(x) = \frac{\sum_x \int_0^{\infty} S_{\mathrm{el}}(E)D(E,x)\mathrm{d}E}{\sum_z \int_0^{\infty} D(E,x)\mathrm{d}E} \ . \tag{2.8}$$

Here $D(E,x)$ is the absorbed dose transferred by primary particles with kinetic energy E at position x [38]. The maximum of the LET along the beam path is not located at the same position as the maximum of the depth dose curve, but shortly behind (Fig. 2.4) [37], because the maximum of depth dose curve itself results from a combination of the increasing LET and the decreasing proton fluence [39].

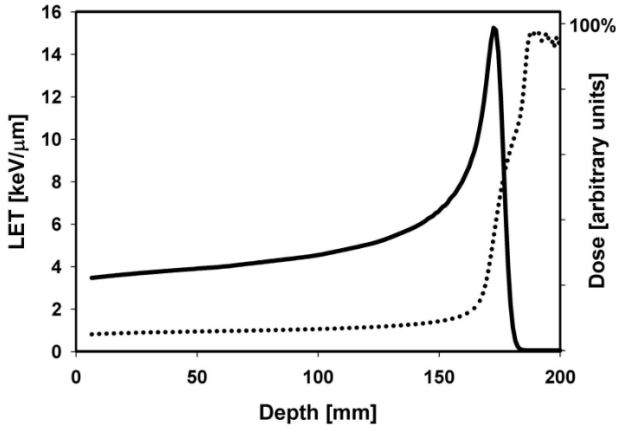

Figure 2.4: Depth dose curve (solid line, right axis scale) and total dose-averaged linear energy transfer LET (dotted line, left axis scale) for a proton beam with an initial energy of 160 MeV in water. Adapted from [26].

2.2 Radiation biology

The primary aim of radiotherapy is to eradicate tumor cells by inducing lethal damage of the DNA. Therefore, the most important endpoint for evaluating the biological effect of a radiation type is cell survival. Based on numerous performed in vitro analyses the so-called linear-quadratic model was introduced to describe the cell survival fraction SF in dependence of the absorbed dose D [40, 41].

$$\mathrm{SF}(D) = \exp(-\alpha D - \beta D^2) \tag{2.9}$$

α and β are free parameters of the model and can be determined by fitting eq. 2.9 to measured cell survival curves. The α/β ratio defines the curvature of the survival curve. α and β are cell type-specific parameters used to assess and describe the radiosensitivity of the regarded cells or tissue type [42]. The cell survival curves for protons are usually steeper than for photons indicating that for the same absorbed dose, protons are more effective in cell killing than photons. This higher biological effectiveness of protons originates from the higher LET and the associated more clustered DNA damages, which are more difficult to repair by the cells. To account for this difference in cell killing between protons and photons, the relative biological effectiveness (RBE) was introduced. The RBE is defined as the ratio of doses between a reference irradiation D_{x} and the irradiation type of interest, e.g., protons, D_{p} yielding the same biological effect [39]:

$$\mathrm{RBE}(\mathrm{endpoint}) = \frac{D_{\mathrm{x}}}{D_{\mathrm{p}}} \ . \tag{2.10}$$

In proton therapy, prescription doses for the target volume and tolerance doses for organs at risk (OAR) are usually given as the product of absorbed physical dose D times RBE, also called RBE-weighted dose

$$D_{\mathrm{RBE}} = D \times \mathrm{RBE} \ . \tag{2.11}$$

To indicate, that the RBE-weighted dose is used, the unit of D_{RBE} is usually noted as Gy(RBE). By applying the RBE concept, the well-established values for prescription and tolerance doses from many years of experience with photons can also be applied in proton therapy.

In clinical practice, protons are assumed to be 10% more effective in cell killing than photons, i.e., a constant RBE of 1.1 is used [39]. This value is based on several in vivo studies performed in the early years of proton therapy and was found as an averaged value over several different endpoints [43–46]. The clinically used value of 1.1 is a conservative assumption to ensure tumor control, since in the tumor also smaller values than 1.1 might occur. By definition, the RBE is not a constant but depends on the regarded endpoint. In vitro studies have shown that the RBE varies with different biological and physical parameters, like the LET, the radiosensitivity of the tissue (α/β), the regarded endpoint, and the dose per fraction [26, 27]. The RBE is highest at the distal edge of a clinical SOBP (Fig. 2.5). Because of the safety margins used in clinical practice, this maximum is often located in normal tissue, which can lead to unexpected side effects, especially for late-responding (low α/β) OARs located close to the target volume [47].

There are different phenomenological models for describing the RBE, most of them are based on several measured cell survival curves [49–51]. One of them is the model developed by Wedenberg et al [49] describing the RBE in dependence of the physical absorbed proton dose D, the LET, and the radiosensitivity of the tissue when irradiating with photons $(\alpha/\beta)_{\mathrm{phot}}$:

$$\begin{aligned} RBE(D, LET, (\alpha/\beta)_{\mathrm{phot}}) = & -\frac{1}{2D}\left(\frac{\alpha}{\beta}\right)_{\mathrm{phot}} + \\ & \frac{1}{D}\sqrt{\frac{1}{4}\left(\frac{\alpha}{\beta}\right)^2_{\mathrm{phot}} + \left(qLET + \left(\frac{\alpha}{\beta}\right)_{\mathrm{phot}}\right) D + D^2} \end{aligned} \tag{2.12}$$

Here, the constant q is a free parameter of the model and can be determined by fitting experimental in vitro data. When applying this model clinically, the dose-averaged LET is usually used to characterize the LET in voxel.

Due to the variability of the RBE, the 1.1-weighted dose at the distal edge of an SOBP cannot be considered as photon-like. Therefore, the use of dose limits for OAR based on photon data together with a constant RBE of 1.1 introduces uncertainties. Recent retrospective clinical studies could correlate the increase of

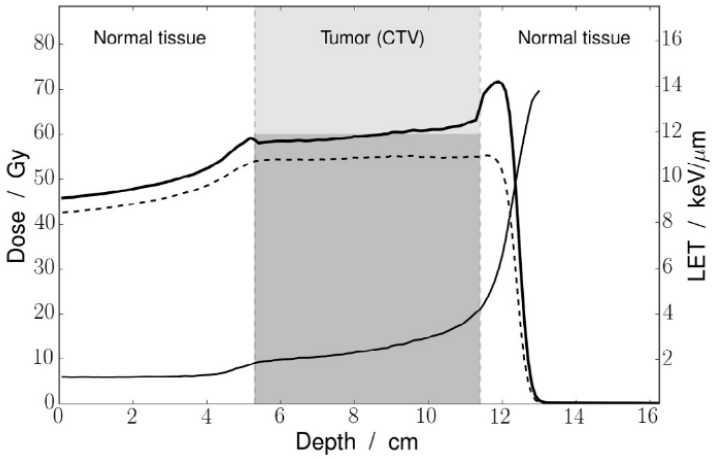

Figure 2.5: Absorbed physical dose (dashed line), dose-averaged linear energy transfer LET (solid line) and variable relative biological effectiveness (RBE)-weighted dose (bold line) using RBE values based on in vitro data [48] for a clinical spread-out Bragg peak [47]

the biologically effective dose at the distal edge of an SOBP to unexpected side effects showing the clinical relevance of the variability of the proton RBE [17–19, 52]. Moreover, the use of averaged LET values as a surrogate for variable RBE (vRBE)-related effects is currently under debate since different LET spectra in a voxel can lead to the same averaged LET value although the biological effect might differ [53].

2.3 Irradiation techniques

In order to treat patients with different ionizing radiation, the radiation must be generated, accelerated, and adapted to the size and shape of the volume to be treated. The methods for generating and shaping the required treatment fields differ depending on the modality, e.g., photons or protons, used for treatment.

Photon irradiation sources

For the irradiation with photons clinical linear accelerators, so-called linacs, are most commonly used. A linac accelerates electrons using an electric field. The accelerated electrons are then hitting a target creating the photons used for irradiation by being slowed down in the Coulomb field of the atomic nucleus of the target atoms and emitting high-energy bremsstrahlung. Therefore, the energy spectrum of the emitted photons depends on the voltage used for accelerating the electrons (Fig. 2.6). Most

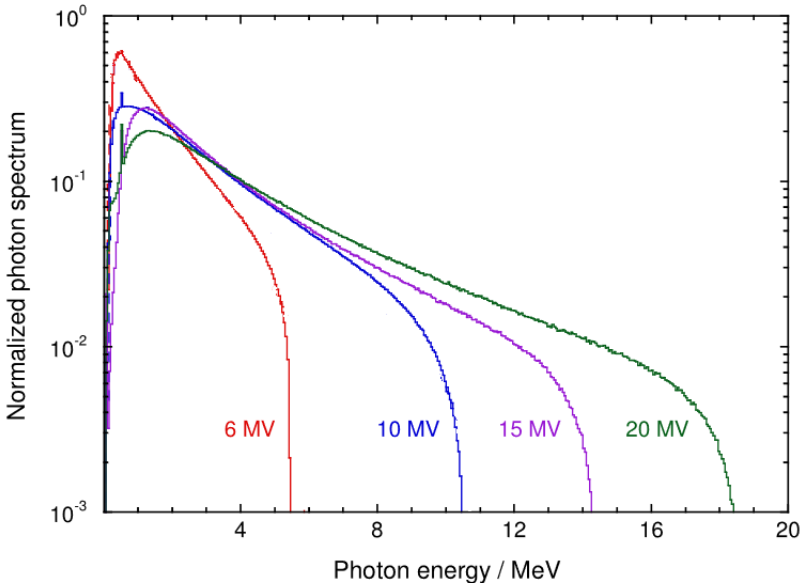

Figure 2.6: Photon spectra for acceleration voltages of 6 MV, 10 MV, 15 MV, and 20 MV of a clinical linear accelerator normalized to their integral. Adapted from [54]

clinical linacs also offer the opportunity to irradiate the patient with the accelerated electrons directly.

The components used for shaping the beam are located in the head of the linac (Fig. 2.7). The most important components are the primary collimator for collimating the, from the target emitted, primary photons, the flattening filter for creating a homogeneous lateral dose distribution, the x- and y-jaws to determine the field size, the multi leaf collimator (MLC) to adapt the field to the shape of the target volume and different monitor chambers to measure the delivered dose. For most clinical linacs, a maximum field size of 40 cm $\times$ 40 cm at a source-to-surface distance (SSD), i.e. the distance between the location of the radiation source and the surface of the subject to be irradiated (e.g., the surface of a phantom or the skin of a patient), of around 100 cm can be achieved. This maximum field size is usually sufficient to irradiate solid tumors. The dose rate mainly depends on the fluence of the accelerated electrons and the energy spectrum of the emitted photons mainly depends on the used voltage for acceleration as well as the used filter materials in the beam path. Therefore, the energy is usually specified in the unit of voltage. The most commonly used acceleration voltages are 6 MV, 10 MV, 12 MV, and 18 MV [55].

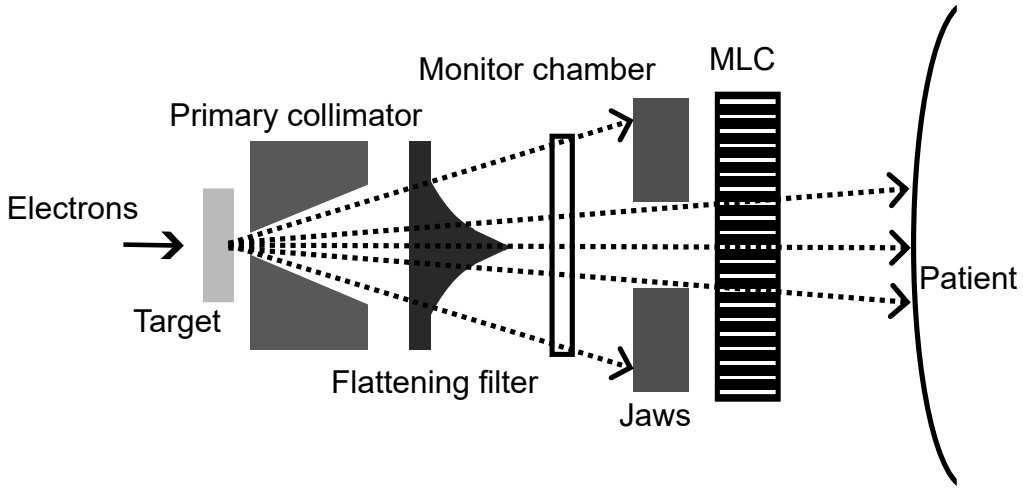

Figure 2.7: Schematic set-up of the head of a clinical linear accelerator. The dashed arrows indicate the photon beam. MLC: Multi leaf collimator.

Photon irradiation techniques

One commonly used irradiation technique when irradiating with photons is the so-called 3D conformal radiotherapy, in which the target volume is usually irradiated with 3-5 fields from different directions to ensure a homogeneous dose coverage of the target volume while sparing healthy tissue, especially OARs. A more advanced form of the 3D conformal radiotherapy is the so-called intensity modulated radiotherapy (IMRT) [56]. In this technique, the intensity and thus the local dose within a field is modulated by a continuous motion of the MLC. The so-called volumetric modulated arc therapy (VMAT) is a further development of the IMRT technique [57]. For this technique, the accelerator head rotates continuously in arcs around the patient, while the MLC simultaneously adapts correspondingly to ensure the desired local dose distribution. Another form of arc therapy is the so-called tomotherapy. During tomotherapy, the radiation is delivered in a modulated fan beam in a spiral rotation pattern which is created by moving the patient through the scanner [58].

Total body irradiation

One special treatment when irradiating with photons is the total body irradiation (TBI), which is often indicated as part of the treatment of malignant systemic diseases. For this treatment, the whole body represents the target volume [59, 60]. As mentioned above, the maximum field size is 40 cm $\times$ 40 cm with an SSD of 100 cm. Thus, irradiating with the conventional 3D conformal irradiation technique

is not possible, because the target volume (the whole body) is larger than the achievable field size. Therefore, different techniques to create large effective field sizes to homogeneously irradiate the entire body were developed. One of the first and still applied methods of total body irradiation was to greatly increase the distance between the photon source and the patient. To homogeneously irradiate the entire body of an adult patient, an SSD of around 4 m is required. Due to the irregular lateral body contour, better dose homogeneity can be achieved with anterior-posterior/posterior-anterior (appa) irradiation than with bilateral irradiation [61].For treatment rooms with sufficient space, a TBI can therefore be performed using the so-called extended SSD (extSSD) technique (Fig. 2.8A). For this technique, the patient stands at a distance of approximately 4 m from the irradiation source and is irradiated once with the face to the source (anterior-posterior) and once with the back to the source (posterior-anterior)[3, 61].

Since not all treatment rooms meet these spatial conditions, the so-called translational couch (transC) technique was developed (Fig. 2.8B). For this technique, the patient lies on a couch close to the floor with an SSD of approximately 2 m and is moved through the irradiation field. For this distance between the source and the patient, the field size is approximately 80 cm $\times$ 80 cm. Thus, the width of the field is sufficient to cover the body in lateral direction and therefore irradiate the patient laterally homogeneous. The translational motion of the couch creates a homogeneous field along the entire length of the patient. To perform an appa-irradiation the patient gets irradiated in the prone and supine position. To prevent an underdosage of the skin due to the build-up region of photon depth dose curves (Fig. 2.1), a lucite plate close to the patient is used as a beamspoiler to shift the beam maximum to the skin surface [13, 62].

Proton irradiation

For irradiation with protons, the protons have to be accelerated to energies of up to 250 MeV. This can be achieved either with a synchrotron or cyclotron. To cover the target volume homogeneously with dose, the beam must be shaped both laterally and in depth. Nowadays, this is usually achieved using pencil beam scanning (PBS). In PBS, a narrow proton beam is deflected using magnets to scan the entire target volume (Fig. 2.9). The generation of the SOBP is achieved by changing the energy of the primary protons. In this way, one ”energy layer” after the other can be scanned and irradiated. PBS offers the possibility to modulate the intensity of each spot individually. If this is exploited, PBS is often referred to as intensity modulated proton therapy (IMPT) [63].

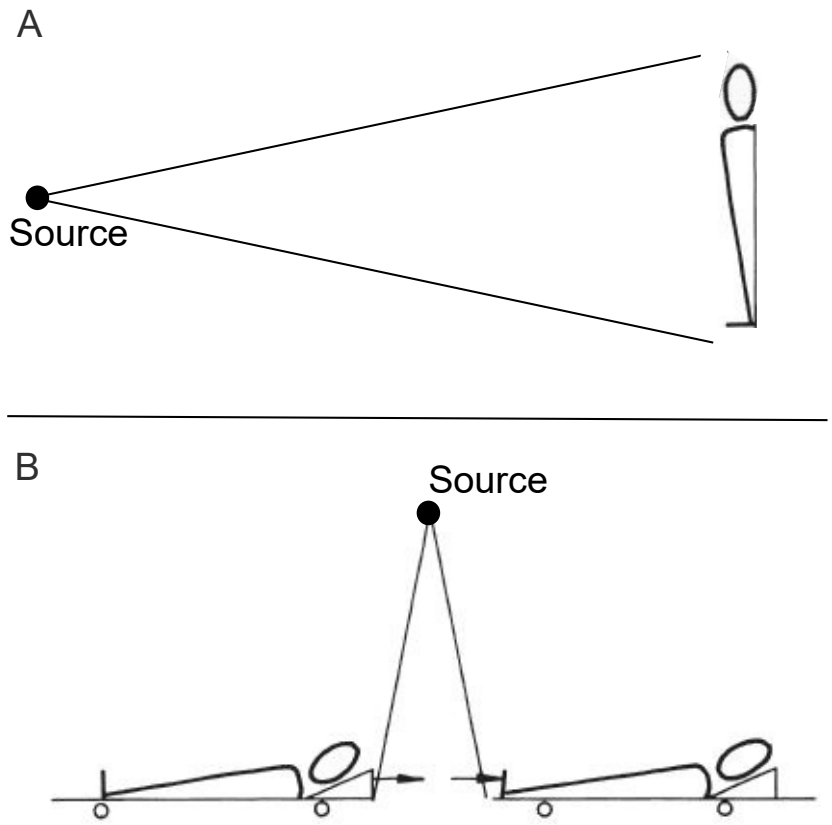

Figure 2.8: Extended source-to-surface distance (A) and translational couch technique for total body irradiation using anterior-posterior/posterior-anterior field orientations. Adapted from [59].

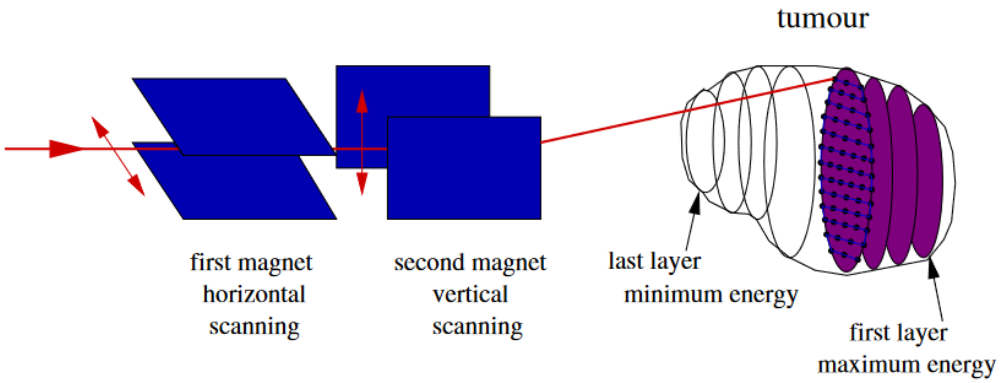

Figure 2.9: Schematic set-up of a proton pencil beam scanning system. Adapted from [64].

2.4 Treatment planning

Independent of the irradiation technique, a model of the patient is required for planning and calculating the dose. Usually, a patient CT is used for this. Each CT-voxel is assigned a CT number which is given in so-called Hounsfield Units (HU)-value and which represents the photon attenuation coefficient of the voxel material relative to that of water. For the use in proton therapy, the HU-value is converted to proton stopping power using Hounsfield Unit look-up tables (HLUT) [65, 66]. For every irradiation, the first step is usually the contouring of the target volumes and the organs at risk. When determining the target volume, usually the target volume concept [67, 68] is applied. According to this concept, the gross tumor volume (GTV) is the tumor volume visible in the CT or in other acquired medical images (e.g., magnetic resonance images (MRI)). The clinical target volume (CTV) is defined as an expansion of the GTV to account for possible tumor cells not visible in the medical images. By adding an internal margin to account for potential changes in the position, size, and shape of the tumor during the treatment process, the internal target volume (ITV) is created. For the planning target volume (PTV) another safety margin is applied to account for potential patient movement, positioning, and dose calculation uncertainties. To be able to spare OARs during the irradiation, the OARs are also contoured on the CT.

The process of creating a treatment plan represents a trade-off between a homogeneous prescription dose in the target volume and the lowest achievable dose in the OARs. Based on available clinical outcome data, dose limits for OARs were defined [69, 70], which should not be exceeded during irradiation of the patient to reduce the

possibility of side effects. Nowadays, especially for intensity modulated techniques, an inverse treatment planning method is used. For the target volume and the OARs, clinical goals considering the desired dose distribution in these regions of interest (ROI) are defined. These clinical goals usually include the prescribed dose for the target volume and dose limits for OARs. To achieve these clinical goals, different dose objectives, each associated with a penalty function, are defined during treatment planning. All of these dose objectives combined yield the composite objective function to be minimized during the optimization process. Since a fulfillment of all dose objectives at the same time is usually not possible, weights can be assigned to the individual objective functions. In this way, the planner can decide which objective should be prioritized by the optimizer.

To evaluate the resulting treatment plan after the optimization different parameters are calculated, most of them are based on the dose-volume histogram (DVH) [71]. The commonly used DVH is a cumulative DVH relating the absorbed dose to the irradiated volume of a regarded ROI and is therefore a 1D representation of the 3D dose distribution [72]. Clinical goals can then be defined as DVH parameters. Important parameters are D_{V} representing the dose received by $V\%$ of the volume of the considered ROI and V_{D} representing the volume receiving at least a dose of D.

Another possibility to evaluate treatment plans is the calculation of explicit normal tissue complication probability (NTCP) values for OARs based on DVH parameters using a model like, e.g., the relative seriality model [73, 74]. According to this model, the NTCP of an OAR with i voxels can be calculated using

$$\mathrm{NTCP} = \left(1 - \prod_{i=1}^{n} \left(1 - P(D_i)^s\right)^{V_i}\right)^{1/s}$$

$$\text{with } P(D_i) = 2^{-\exp\left(e\gamma\left(1 - \frac{D_i}{\mathrm{TD}_{50}}\right)\right)} \ . \tag{2.13}$$

Here, $P(D_i)$ represents the probability for complication when irradiating a relative volume V_i with dose D_i described by an estimation using Poisson statistics. TD_{50} describes the tolerance dose for the entire organ resulting in 50% complication probability, γ describes the slope of the sigmoid-shaped dose-response curve and s describes the seriality of an organ, whereby large values indicate a more serial structure while low values indicate a more parallel structure. For different organs and clinically relevant endpoints, model parameters were determined using clinical outcome data [74].

Treatment planning for translational TBI: Beam-zone method

In TBI the whole body, including all organs, represents the target volume. Therefore, usually, no dose sparing of OAR is performed. The lung is one of the most radiosensitive organs of the human body and limits therefore possible prescription doses. To allow for applying higher prescription doses to the rest of the body, the dose to the lung gets reduced during TBI often by using lead lung blocks. In contrast to standard radiotherapy, the lung is not treated as an OAR trying to keep its dose as low as possible, but rather as a target volume with a lower prescription dose.

Commonly used treatment planning systems (TPS) usually use several approximations of the dose calculation algorithm to lower the necessary computational time for the dose simulation. Therefore, clinical TPS are optimized for providing fast and accurate dose estimations for standard irradiation conditions and are only validated for standard SSD of approximately 1 m. Many complex measurements have to be performed to adjust the dose calculation algorithm and validate a clinical TPS for non-standard irradiation conditions.

Therefore, for the translational TBI irradiation technique a different treatment planning approach than for standard radiotherapy was established, the so-called beam-zone method [13]. The beam-zone method was introduced in 1985 and has been used unchanged since. The beam-zone method allows for a table-based calculation of the dose in a regarded point depending on the local thickness of the patient in beam direction and the so-called local effective field size, which defines the amount of tissue surrounding the regarded point.

When using the transC technique, the patient is moved with a constant velocity v through the treatment field. The dose D integrated over the whole translation time is inversely proportional to the velocity of the patient couch. Therefore, the most important dosimetric quantity in translational TBI is the velocity-dose product $(v \cdot D)$ for a given dose rate. The integrated dose at a specific point of interest (POI) and therefore also $v \cdot D$ is a composition of dose contributions from the attenuated primary photons and the scattered particles from surrounding tissue. The dose contribution by the attenuated primary photons depends on the local depth z in which the POI is located. When assuming that the POI is located in the midplane of the patient, then z equals $\Phi/2$ with Φ being the local thickness in beam direction of the patient.

The dose contribution of secondary particles depends on the amount of tissue surrounding the regarded POI, which can be characterized by the local effective field size A_{eff}. A_{eff} at a specific POI is defined as the size of a tissue-equivalent square shape phantom receiving the same dose at its center under TBI treatment conditions as the applied dose to the regarded POI. An increased A_{eff} corresponds to a higher proportion of scattered dose from surrounding material.

The influence of A_{eff} on $v \cdot D$ can be characterized and tabulated by performing

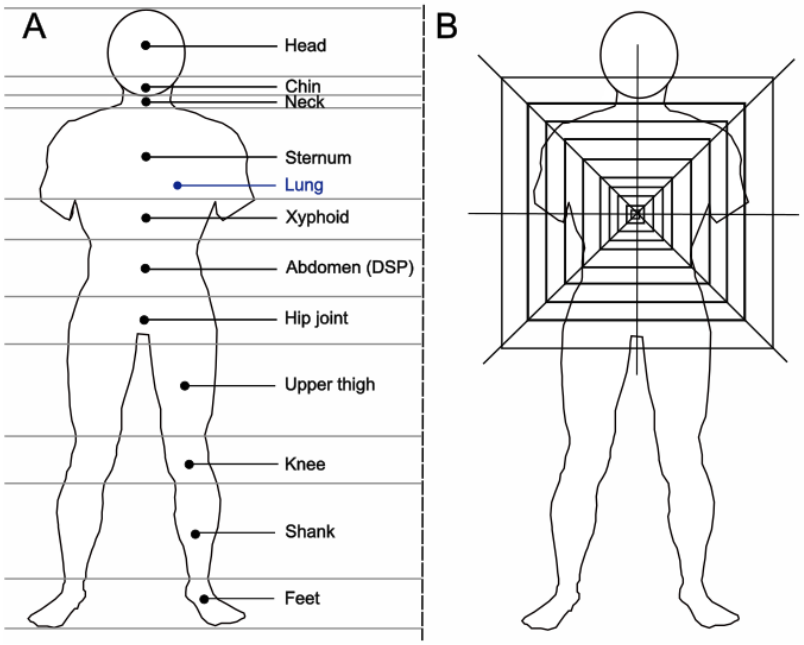

Figure 2.10: Dose reference points of the beam-zone method and beam-zone net used for determining the effective field size.

measurements of the integrated dose at the center of square-shaped phantoms with the same thickness Φ but different sizes at a known velocity v under transC conditions. The measured range of phantom sizes can then be divided into steps and thus into discrete effective field sizes in such a way that each step leads to an equal relative dose increase δ at the midpoint. These incremental field sizes are called beam-zones. Each beam-zone therefore defines an incremental phantom ring contributing the same dose δ to the central point. With the performed measurements using different square-shaped phantoms, the dimensions of individual beam-zones are determined and can then be used for creating a so-called beam-zone net. This beam-zone net is then used to calculate A_{eff} by overlaying it on a patient topogram centered on the POI (Fig. 2.10B) and counting the beam-zones covered by the body. To increase the accuracy of the dose estimation, not only completely covered beam-zones but also partial (up to eights) beam-zones are included. The number of beam-zones, including partial zones, is equivalent to A_{eff}.

To characterize the influence of Φ on $v \cdot D$ measurements using phantoms with the same size but different thickness are performed and tabulated. In this way, $v \cdot D$ can then be calculated for known A_{eff} and Φ using tables.

The applied dose during the translation depends on the used dose rate and velocity of the translating couch. For a given dose rate, the velocity is chosen in such a

way that at the so-called dose specification point (DSP), which is usually in the midplane of the patient near the umbilicus, the prescribed dose is applied. This velocity v_{pres} can be calculated with

$$v_{\text{pres}} = \frac{(v \cdot D)_{\text{rel,DSP}} (v \cdot D)_{\text{cali}}}{d_{\text{pres}}/2} \ . \tag{2.14}$$

Here, $(v \cdot D)_{\text{rel,DSP}}$ can be calculated with the beam-zone method and represents the velocity-dose product in the DSP relative to the calibration conditions, $(v \cdot D)_{\text{cali}}$ represents the measured $v \cdot D$ under calibration conditions (A_{eff} = 40 x 40 cm^2, Φ = 20 cm) and d_{pres} the prescribed dose per fraction.

To characterize the dose throughout the entire body, the beam-zone method is used to calculate the $v \cdot D$ relative to the DSP in eleven additional points along the entire body (2.10A), the so-called dose reference points (DRP). If dose deviations between the dose in the DRP and the DSP, which is similar to the prescribed dose, exceed the clinically acceptable value of $\pm$10%, A_{eff} or Φ can be artificially increased by adding (tissue-equivalent) bolus material to the body. Each DRP represents an anatomical region of the body and is located in the center of this anatomical region. When applying the beam-zone method for translational TBI treatment planning, only the dose at 12 different individual points along the body is calculated, and a homogeneous dose is assumed for the entire body depending on these 12 dose values [13]. Thus, no CT-based 3D dose calculation is performed. For other irradiation techniques including other TBI techniques, performing 3D dose calculations has long been clinical standard. Therefore, a dosimetric in silico comparison of translational TBI with other TBI techniques is not possible and a detailed knowledge of the applied dose distribution when performing translational TBI is, so far, lacking.

Dose calculation algorithms

For CT-based 3D photon dose calculations, different dose calculation algorithms exist. Often used algorithms are so-called kernel-based algorithms. These algorithms apply analytical models to describe the energy deposition instead of directly simulating the microscopic interactions of the radiation. As described above, there are two contributions to the dose: the dose deposited by the attenuated primary photon beam and the dose deposited by secondary particles. Therefore the dose can be described by the convolution of a primary attenuation function and the so-called kernel function describing the dose transferred to secondary particles. The dose deposited by primary photons is usually deposited close to the primary photon track, while the dose transferred to secondary particles is usually deposited further away from the primary photon track [75]. Examples of such algorithms are the convolution/superposition algorithm [76], the collapsed cone algorithm [76] and the pencil beam algorithm [77].

The most accurate dose algorithm is the Monte Carlo algorithm which is applicable for photon and proton irradiation [78]. Therefore, it is often considered as gold standard for dose calculation for both photons and protons. The Monte Carlo method allows for an explicit stochastic simulation of the track and microscopic interaction processes of each particle based on probability distributions. The probability of the different interaction processes is described by the corresponding cross-sections. If energy is transferred to secondary particles, their tracks and interactions are also explicitly simulated. According to the law of large numbers, the mean value of an experiment approaches the expected value the more often the experiment is performed. In terms of Monte Carlo simulations, this means that the simulation of a finite number of particles N is sufficient to approximate the actual dose value in a voxel. The statistical uncertainty of the simulation is proportional to $1/\sqrt{N}$ while at the same time, the computational time needed to perform the simulation is proportional to N. Therefore, precise Monte Carlo simulations are time-consuming.

3 Project photons: Total body irradiation

There are many different irradiation techniques for performing TBI leading to different approaches for treatment planning. For several techniques, like the extended SSD (extSSD) and translational couch (transC) technique, clinical TPS cannot be utilized because of the non-standard SSD used. Therefore, other treatment planning approaches have been established. These approaches are usually non-CT based and thus no 3D dose calculations on a patient CT are performed making dosimetrical comparisons between TBI techniques complicated. Instead, the dose at different dose reference points (DRP) is calculated and used to characterize the dose in the entire body. To find out, which TBI irradiation techniques are most common in Germany and which future requirements are urgently needed according to participating centers, a survey on the current clinical practice among German radiotherapy centers was performed. To offer the possibility for calculating 3D dose distributions for non-CT-based TBI techniques a novel Monte Carlo-based simulation workflow was introduced and used to validate the current treatment planning method for the transC technique as well as to dosimetrically compare different irradiation techniques.

3.1 Survey

Numerous different TBI techniques exist [7–16] and several surveys in different countries worldwide found a high heterogeneity in the performance and application of TBI [79–86]. The difference between centers includes, among others, the definition of the target volume, the dose limits for OARs, the prescription dose, and the fractionation scheme. Therefore, no standardization and commonly accepted planning and treatment approaches exist. To ensure the best possible treatment for patients, analyzing the achieved clinical outcome of the various TBI techniques is of major importance. To achieve this, similarities and differences between the various approaches used by centers in Germany have to be identified. Therefore, the first step towards formulating novel guidelines in Germany is a detailed overview of the current clinical practice. For this purpose, a German-wide survey on the actual applied approaches for TBI was performed.

3.1.1 Material and methods

In 2023, a questionnaire on the current clinical practice of TBI was created by the working group ”Large Field Irradiation Techniques” of the German Society

for Medical Physics (Deutsche Gesellschaft für Medizinphysik, DGMP). A copy of the questionnaire can be found in the appendix. The survey was designed as an online questionnaire using LimeSurvey (LimeSurvey GmbH) and was part of a larger questionnaire asking also for two other large field irradiation techniques (total skin and craniospinal irradiations). In this thesis, only the answers to the part covering TBI will be presented. The questionnaire was distributed using the newsletter of the DGMP (July and August 2023) and centers provided their answers between August and October 2023. After asking for personal information and if the center performs TBI, the main part of the survey asked for detailed information on the applied irradiation technique. The main part of the questionnaire was separated into different topics covering:

1. General Information (4 questions)
2. Irradiation unit (7 questions)
3. Irradiation technique (11 questions)
4. Treatment planning (11 questions)
5. Quality assurance (9 questions)
6. Future requirements (5 questions)

Some questions allowed the selection of more than one answer and individual questions could be skipped. Therefore, the number of centers answering a specific question differed. In addition, participants had the opportunity to leave comments to most of the questions. For analyzing the responses different strategies depending on the type of the question were applied. Closed questions (predefined answers) were analyzed quantitatively, while for open questions (free-text answers) a more qualitative approach was used trying to find similarities and differences, as well as considering the context of the given answers. Moreover, similar answers from different centers were grouped and then analyzed more quantitatively.

3.1.2 Results

75 centers answered at least one question of the questionnaire. In 72 centers the answers were provided by a medical physicist. However, most of them only answered the question if the center performs TBI. 40 centers stated to perform TBI. The number of centers providing answers to a specific question of the main part of the survey, asking for detailed information on the applied TBI techniques, varied strongly (Tab. 3.1). On average ($\pm$ standard deviations) questions of this main part of the questionnaire were answered by 17 ($\pm$ 4) centers.

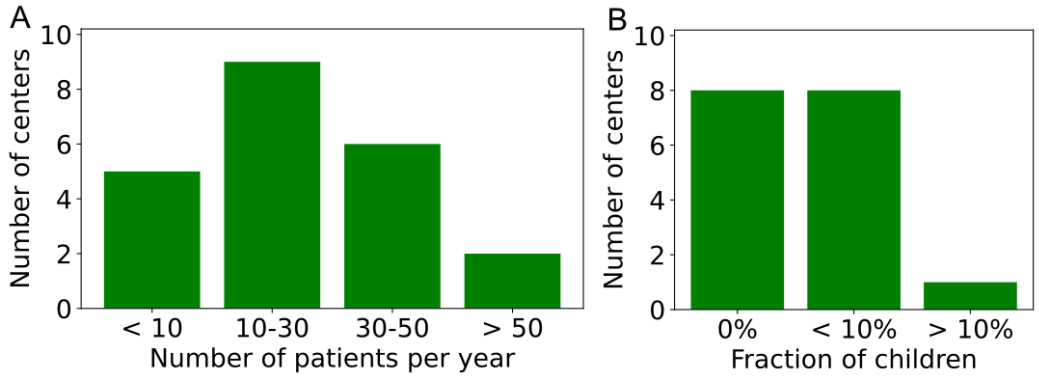

Figure 3.1: Number of patients per year (A) as well as the fraction of children (B) for centers performing total body irradiation.

Most centers (9) answering the regarded question stated to treat 10 to 30 TBI patients per year (Fig. 3.1A). Although almost all of them were adults (Fig. 3.1B), the treatment of children was generally not excluded. TBI was most often applied for leukemia patients (22 centers), followed by lymphoma patients (11 centers).

Only a few differences were found between the individual centers in terms of the irradiation unit and the energy used. 19 centers used the standard linac to perform the irradiation, while three centers used their tomotherapy irradiation unit. 15 centers used photons with an acceleration voltage of 6 MV and three centers stated to vary the used energy depending on the individual patient case applying sometimes also higher energies with acceleration voltages of up to 18 MV.

When asking for the used dose rate at the patient position the answers varied much between centers. Used dose rates ranged between 5 to 125 cGy/min, while the highest values were usually used when applying VMAT or tomotherapy techniques. Moreover, for these techniques, the dose rate is usually not constant while for translating couch and extended SSD techniques usually the same dose rate is applied for all patients over the entire body.

A high heterogeneity was found regarding the applied technique used to irradiate the entire body. In eight centers the applied technique for TBI was the irradiation with an extended SSD of up to 400 cm to create an effective field size large enough to cover the entire body (Fig. 3.2). Seven centers were using the translating couch technique performing the treatment planning using the beam-zone method [13]. A boost of the chest wall using electrons was performed by three centers, while 15 centers stated to never boost the chest wall, four of them being centers using the VMAT or tomotherapy technique for which no chest wall boost is necessary. All responding centers were usually using one technique for all patients.

The question asking for the utilized patient position was answered by 15 centers.

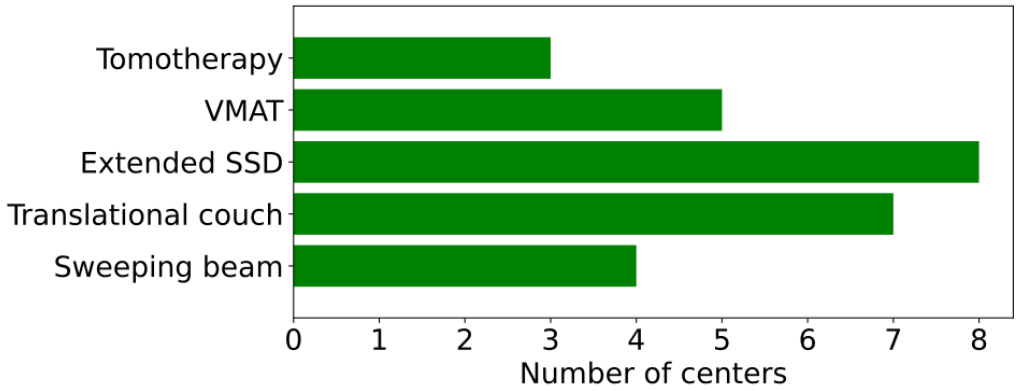

Figure 3.2: Number of centers using Tomotherapy, volumetric modulated arc therapy (VMAT), an extended source-to-surface distance (SSD), the translational couch technique or a sweeping beam for total body irradiation.

Table 3.1: Number of questions (No.Q) of the main part of the survey on the current clinical practice of total body irradiation and corresponding averaged (± standard deviation) number of centers (No.C) responding to the regarded questions.

Topic	**Closed**		**Open**		**Total**	
	No.Q	**No.C**	**No.Q**	**No.C**	**No.Q**	**No.C**
General Information	2	14 (±4)	2	16 (±3)	4	15 (±3)
Irradiation unit	3	15 (±0)	4	10 (±5)	7	12 (±5)
Irradiation technique	5	13 (±2)	6	12 (±3)	11	12 (±3)
Treatment planning	5	13 (±0)	9	11 (±2)	11	12 (±2)
Quality assurance	5	11 (±1)	4	8 (±3)	9	10 (±3)
Future requirements	-	-	5	11 (±3)	5	11 (±3)

Most of these centers (11 centers) performed their irradiation in appa field orientation by utilizing the prone and supine position. Two centers were irradiating their patients in a sitting position. The patient position was mostly assured only optically and with the help of the laser system in the irradiation room (7 centers). Five centers used radiochromic films and three applied photostimulable phosphor (PSP) plates, especially for ensuring the right position of the lung blocks. One whole treatment, including the positioning of the patient and the used equipment, took 30 minutes to one hour, while the irradiation itself was mostly below 15 minutes (7 centers) and never exceeded one hour.

Twelve centers gave a detailed description of their irradiation techniques. Eight of them utilized a technique described in the literature, e.g., five centers described the translating couch technique as in [13] and one was using a sweeping beam technique as in [87–89]. Two centers were using a rotatable table top on the standard linac couch for irradiation. These centers performed VMAT irradiations with 6 to 7 isocenters using overlapping 360° arcs with changing rotation direction as described in [89].

The other five centers giving a detailed description were performing a center-specific technique not following any TBI technique published in the literature. One center stated to apply all fractions with the extended SSD technique using an SSD of about 400 cm, a bilateral field orientation, and a patient couch at the wall of the treatment room for lower prescription doses. For higher prescription doses, one fraction was applied with an appa-irradiation using a patient couch on the floor, while all other fractions were applied with the same extended SSD technique as for lower prescription doses. For small children, this center used the standard treatment couch of the linac with an SSD of 120 cm irradiating several appa-fields. In another center, the patient lay on a carbon plate on the floor parallel to the movement direction of the gantry. For the irradiation, a generic rotation of the gantry was performed using a 40 cm $\times$ 40 cm field at the isocenter (SSD of approximately 100 cm). One other possibility for performing TBI was the irradiation in prone and supine position using three different gantry angles, one for the legs, one for the upper body, and one for the head having field junction at the upper thighs and the shoulders. The last center giving a detailed description of their technique used an arc technique irradiating the patient in prone and supine position and gantry angles between 300° and 70°.

Regarding the treatment planning process, an overall high heterogeneity was found in almost every aspect. The prescribed dose ranged between 2 and 12 Gy and all 16 centers answering this question stated to use at least two different prescription doses depending on the patient case. The prescription dose was defined as the dose to one specific point (e.g., the midpoint of the abdomen) by six centers and as the mean dose to the target volume by seven centers (Fig. 3.3A). All of these seven centers were calculating 3D dose distributions on a CT (Fig. 3.3B). Three centers used a

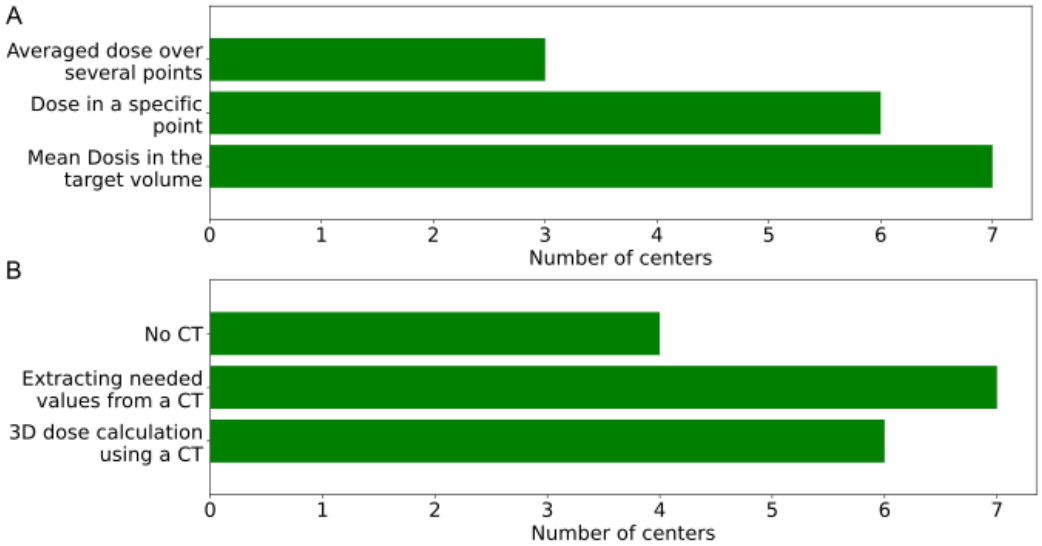

Figure 3.3: Different definitions of the prescribed dose used by the radiotherapy centers (A) and the number of centers using computed tomography (CT) images for treatment planning.

mean value averaged over several points along the patient. All centers performing VMAT or tomotherapy calculated 3D dose distributions on the patient CT, while most other centers (7 centers) used a patient CT for calculating needed quantities, e.g., the thickness of the patient at a specific point, without performing a 3D dose calculation. Four centers stated to never use a CT for treatment planning. The time needed for creating a treatment plan varied between 10 minutes for extended SSD techniques and up to one day for tomotherapy.

The only consent regarding the treatment planning process was found in the fractionation scheme and the dose reduction to the lung. All centers answering the regarded question (14 centers) applied 2 Gy per fraction and 2 fractions per day. Almost all centers (16 centers) reduced the dose to the lung, most of them to 8 Gy (5 centers) or 7 Gy (4 centers) using the lower value in the case of higher prescription doses. Some centers also reduce the dose to the kidneys (3 centers) and lenses (2 centers). Only one center stated to not spare any OAR. To achieve the desired lung dose reduction lung blocks were used by eight centers. Therefore, lung blocks were one commonly used equipment during irradiation. Besides these lung blocks, twelve centers also stated to use beam spoilers during irradiation for shifting the dose maximum to the skin surface.

Regarding the concept for machine failure, twelve centers stated to have two identical irradiation machines, which therefore can be used if one machine is not

working properly. Thus, there was no need for replanning in the case of machine problems. Three centers stated to use a different irradiation technique for performing TBI in the case of machine failure and therefore a replanning was necessary. Most centers followed the DGMP guidelines [90] (9 centers) or the AAPM report no. 17 [2] (6 centers) when performing TBI.

When asking for the advantages of the different techniques, centers stated to consider the more standard techniques like the irradiation with an extended SSD or the translating couch technique as robust, low-risk as well as easy to implement and perform. Stated disadvantages for these techniques were the strong dependence of the dose homogeneity on the patient thickness, the need for additional dose measurements since the irradiation conditions differ relevantly from standard radiotherapy due to the extended SSD, and the use of lungblocks, since they not only reduce the dose to the lung but also in surrounding tissue and therefore compromise dose homogeneity. Moreover, the lungblocks had to be manufactured individually for each patient. In contrast, for the more modern techniques, like VMAT and tomotherapy, no lungblocks are needed. Therefore, a reduction of the dose in the lung is possible without reducing the dose in the surrounding tissue. Moreover, a more homogeneous dose can be achieved independent of the patient thickness and no additional measurements need to be performed since the patients can be irradiated using a standard SSD. However, these techniques were considered less robust and more time-consuming. Furthermore, centers raised concern when using the modern techniques because of the segmented irradiation and the higher, not constant dose rates used. Since the target cells are present in the circulating blood, a segmented irradiation with high dose rates might lead to a decreased dose coverage of the target cells compared to techniques irradiating larger volumes of the body at the same time.

The most important future challenge considering TBI was the lack of standardization. The centers wish for more guidelines, especially considering the definition of the target volume, the prescription dose, and the dose limits of OARs. To be able to formulate guidelines in the future, centers proposed to perform retrospective patient studies combining and analyzing clinical outcome data of different centers.

3.1.3 Discussion

The survey revealed a high degree of heterogeneity in the use of TBI in Germany. Although TBI has been performed for a long time, there is no commonly used planning and treatment approach. Variations between centers can be found in almost every aspect of the irradiation process, e.g., in the prescribed dose, the definition of the target volume, the spared OARs, the dose limits for OARs, the used irradiation technique, the patient position, and the field orientation. The only areas of agreement were in the dose reduction to the lung and the fractionation

scheme, as all of the participating centers used 2 Gy per fraction and applied two fractions per day.

Surveys on the clinical practice of TBI in other countries like the Netherlands and Belgium [28], Canada [31], Australia and New Zealand [33], as well as Japan [29,30] also showed a high heterogeneity. The number of centers that were reported to perform TBI varies between 12 in Canada, 14 in Australia and New Zealand, 19 in the Netherlands and Belgium, and up to 186 in Japan. In the survey at hand, 40 centers reported to perform TBI, although the actual number might be even higher since not all radiotherapy centers in Germany responded to the questionnaire. Most of these centers treated around 10 – 30 patients per year which is in line with other countries. In Japan, most centers used the extended SSD technique followed by the translating couch technique similar to what was found here for Germany. In the other countries, almost all centers performed the extended SSD technique. Novel techniques such as VMAT and tomotherapy are much more frequently used in Germany than in all other mentioned countries. However, the surveys in the other mentioned countries were performed between 2017 and 2021, while the German-wide survey presented here was conducted in 2023. Thus, the number of centers applying modern techniques might have increased in the last years in Japan, Canada, Australia, New Zealand, Belgium, and the Netherlands. In Japan as well as Australia and New Zealand most centers stated to perform bilateral irradiation with the patient lying in the supine position, while in the Netherlands and Belgium, most centers performed an appa-irradiation with the patient in the lateral decubitus position. In Germany, most centers stated to use appa field orientations by utilizing the prone and supine position. Regarding the beam energies, most centers in Germany used an acceleration voltage of 6 MV, which is in line with the results from Australia and New Zealand. However, the most commonly used acceleration voltage in Japan was 10 MV, while in Belgium and the Netherlands, 10 MV and 15 MV were most common. All surveys showed that most centers apply 2 Gy per fraction and two fractions per day, thus matching the results found in Germany. In Belgium and the Netherlands, the prescription dose was usually defined as the dose to one specific point. Only two centers performed a 3D dose calculation on a patient CT. In Germany, the number of centers defining the prescription dose as the dose to a specific point almost equaled the number of centers defining the prescription dose as the mean dose to the target volume. Centers defining the prescription dose as the mean dose to the target volume were usually utilizing modern TBI techniques such as VMAT or tomotherapy and were therefore performing 3D dose calculations on a patient CT. Moreover, there was a consensus among almost all surveyed centers that the lung was the only OAR routinely protected during irradiation.

Although 69 centers answered the question asking whether TBI is performed, only a small ratio of these centers provided detailed answers about their TBI technique. Many questions were designed as open, allowing for detailed individual free-text

responses, since a high degree of variation in the techniques used was expected. At the same time, however, these open questions introduced the possibility of ambiguous responses and may have contributed to the low number of completed questionnaires. Moreover, the questionnaire was answered in almost all centers by medical physicists and therefore only represents the "physics" part of the treatment. For a complete picture, physicians and clinicians might be included in future studies and surveys.

Most centers considered the lack of standardization as the most important challenge for the future since the only existing guidelines [2, 90] are highly descriptive without specifying precise requirements for the irradiation and do not reflect the increasing use of modern irradiation techniques. Moreover, not all centers are following these guidelines. Thus, according to the participating centers, detailed guidelines for almost every aspect of the treatment planning process, including the prescribed dose, the target volume definition, the tolerance doses for OAR, and the used dose rate, are missing. To overcome this, centers suggested performing retrospective patient studies correlating these different aspects of the treatment process with relevant clinical endpoints, e.g., toxicities, survival, or the occurrence of graft-versus-host disease.

Furthermore, the question arises if one TBI technique is more favorable than another. Therefore, centers suggested performing dosimetrical comparisons between 3D dose distributions of different irradiation techniques and correlating these dose distributions with clinical outcome data to analyze the impact of the applied technique on the achieved clinical outcome. In this way, detailed dosimetric requirements for the applied TBI technique can be identified and considered when formulating novel guidelines. For statistically significant results a combing of the clinical data of different centers is necessary due to the high number of TBI techniques and the limited number of patients per center. Centers considered the performance of such retrospective studies correlating different aspects of the treatment process and used TBI techniques with clinical outcome data as the next important step towards standardization of TBI and therefore ensuring the best possible treatment for every patient.

3.2 In silico study

The performed survey showed that detailed retrospective patient studies correlating 3D dose distributions of different techniques with clinical outcome data are considered the most important future challenge in TBI. The most frequent TBI techniques in Germany are the translational couch technique and the extended SSD technique, for which 3D dose distributions are typically missing. Therefore, a Monte Carlo-based simulation workflow has been developed to provide 3D dose distributions for both techniques to allow a direct dosimetric comparison between these two techniques,

which are still the most commonly used in Germany, and other increasingly applied TBI techniques such as tomotherapy. This novel workflow was used to validate the beam-zone method (section 2.4), which is the treatment planning approach used by most German centers utilizing the translational couch technique. Furthermore, the workflow was used to compare the dose distribution of the translational couch (transC) and extended SSD (extSSD) techniques with the dose distribution of helical tomotherapy (helT) for an exemplary patient case.

3.2.1 Material and methods

To perform a 3D Monte Carlo dose calculations for the transC technique a whole-body patient CT was obtained using a resolution of 1.27 mm × 1.27 mm, and a slice thickness of 5 mm. Due to the limited scanning length of the clinical CT scanner, a headfirst and a feetfirst CT were obtained. Both CT data sets include the upper thigh allowing for the use of the bone structures visible in the CT to cut off and add together both CT sets for the simulation. On each CT slice, the outline of the body and the lung were contoured using the Eclipse TPS (Varian Medical Systems, Palo Alto, US). All centers stated in the questionnaire to use at least two different prescription doses for the body and lung. Therefore, two different dose scenarios were simulated to validate the beam-zone method by evaluating its accuracy for different dose regimes. For the first one, hereinafter referred to as low-dose set-up, a prescribed dose of 8 Gy to the body in four fractions over two days was assumed and the mean dose to the lung was restricted to 7 Gy (87.5% of the prescribed dose to the body). For the second scenario, hereinafter called high-dose scenario, a prescribed dose of 12 Gy to the body in six fractions over three days was assumed. For this prescription dose, the mean dose to the lung is usually restricted to 8 Gy (66.7% of the prescribed dose to the body). The low-dose scenario represents the dose regime actually prescribed for the regarded patient and therefore this scenario was used for the comparison with other irradiation techniques. For analyzing the dose homogeneity, the homogeneity index (HI) defined as $\mathrm{HI} = (D_2 - D_{98})/D_{50}$ was calculated, with D_X representing the dose in X% of the considered volume [91]. Lower values of HI indicate better homogeneity. For the calculation of the skin dose, the skin volume was defined as all voxels at the outer edge of the body contour and therefore assuming a skin thickness of the size of one voxel (1.27 mm).

A treatment plan was generated using the beam-zone method, which calculates the relative dose at 12 different DRPs along the patient. The accuracy of the beam-zone method was evaluated by comparing these values with the dose from the simulated 3D dose distributions at the same 12 anatomical points. The necessary whole-body topogram was created by summing up CT slices along the anterior-posterior direction. The, for the beam-zone method needed, patient thicknesses in anterior-posterior direction at all DRP were measured using the CT.

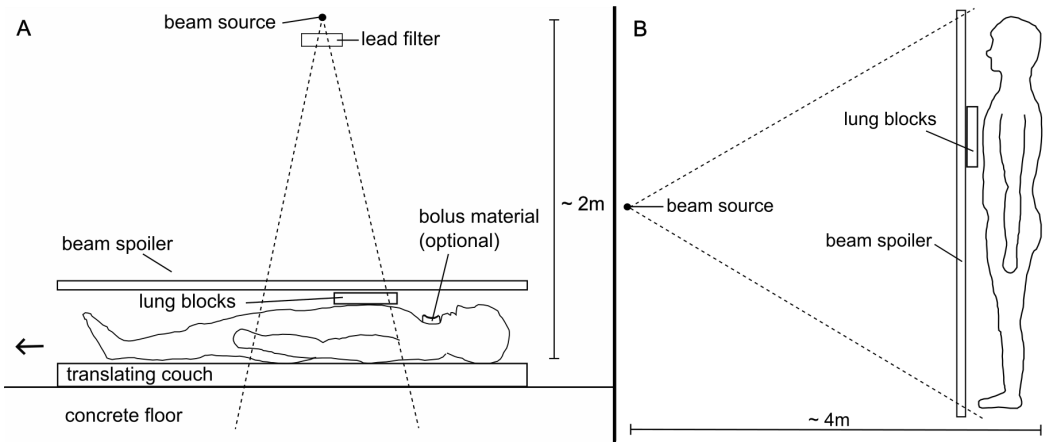

Figure 3.4: Schematic set-up for the simulation of the translational couch (transC) technique (A) and the extended source-surface-distance (extSSD) technique (B) for total body irradiation.

To calculate the 3D dose distribution for the transC technique, a Monte Carlo simulation of the set-up, as used in the university hospital Essen, was performed using TOPAS version 3.6.1 [92]. The set-up contained a 6 MV photon source, a 10 mm lead filter, a 1 cm lucite plate as beam spoiler for shifting the dose maximum to the skin surface, lung blocks for reducing the dose to the lung, (optional) water-equivalent bolus material, the patient (here represented by the CT), the aluminum patient couch, and the concrete floor (Fig. 3.4A). Phase space files provided by Varian (Varian Medical Systems, Palo Alto, US) obtained above the movable upper jaws and therefore representing the patient-independent part of the linac, served as the 6 MV beam source for the Monte Carlo simulation. For speeding up the patient simulations, new phase space files directly above the beamspoiler, and therefore closer to the patient, were created and used for all further simulations.

Prior to the patient simulations, water phantom simulations with and without the concrete treatment room floor were performed, to determine if the backscatter from the concrete floor had a relevant influence on the dose distribution, and therefore needed to be included in the patient simulations. For these analyses, the patient CT was replaced by a water phantom with a size of $40\times40\times20$ cm^3.

The lung blocks were added in the CT by using the outer contours of the lungs and overwriting the corresponding air voxels above the patient in the CT with a specific HU value. In the simulation, the material composition (H: 1.2% H, O: 38.5%, Al: 13.9%, P: 10.7%, Pb: 35.7%) and density (4.5 g/cm^3) of the lung blocks were assigned to this HU value. A lung block thickness of 11.4 mm and 33.0 mm were used for the low-dose and high-dose set-up, respectively.

Since the simulation of a continuous movement was not possible, the continuous

movement of the translating couch was approximated with a step-and-shoot approach. A step width of 0.5 cm was applied, simulating 10^7 particles originating from the phase space file above the beamspoiler in each step. The simulation was divided into 48 smaller simulations each containing 6 cm of the translation distance. These 48 simulations were performed twice, one time with the patient CT in supine and one time in prone position. Since the CT was obtained in supine position, a rotation of the CT of 180° in TOPAS was performed to create the prone position of the patient.

For the validation of the beam-zone method, the simulated dose distributions of the transC technique were normalized to the dose in the dose specification point DSP (midpoint in the abdomen) and divided into different anatomical regions, each represented by the DRP in its center (Fig. 2.10). To account for statistical fluctuations, a mean value considering 26 direct neighbor voxels of the DSP was calculated and used for normalization. DVHs of the different anatomical regions as well as the dose in the DRP were calculated. The anatomical regions were defined using the bone structures visible in the CT and the DRPs were defined as the central voxel of each region by measuring the size of the body included in the corresponding region. To evaluate the accuracy of the dose prediction by the beam-zone method, the simulated dose in each DRP $\mathrm{D_{DRP}}$ was compared with the planned dose in the same points of interest (POI) calculated with the beam-zone method $\mathrm{D_{plan}}$. For all anatomical regions the difference $\Delta_{\text{plan-DRP}} = D_{\text{plan}} - D_{\text{DRP}}$ was calculated and analyzed. For calculating the dose in the DRPs, similar to the approach for the DSP, a mean value including 26 direct neighbor voxels of each DRP was used. For regions with two DRPs, one on the right and one on the left side (upper thighs, knees, shanks, feet), the mean value of both DRPs was used for all analyses. To investigate the assumption of a homogeneous enough dose, so that one dose value in the center of a region is sufficient to characterize the whole dose distribution in the entire anatomical region, the difference $\Delta_{\text{50-DRP}}$ between the dose to 50% of the body volume included in each region $\mathrm{D_{50}}$ and the dose in the DRP $\mathrm{D_{DRP}}$ was calculated.

To create the 3D dose distributions for the extSSD technique, simulations similar to the simulations for the transC technique were performed. The CT was translated such that an SSD of 4 m was achieved. The set-up for the extSSD technique contained the same 6 MV photon source, the 1 cm lucite plate, the lead lung blocks, and the patient CT (Fig 2B). All simulations were also performed twice, one time with the patient-CT facing the beam source and one time with the back of the patient facing the source. For the comparison between the different irradiation techniques, all dose distributions were normalized to the D_{50} of the body for each technique.

For creating treatment plans using helT the Accuray planning station (HI-ART Version 5.1.6, Accuray, Sunnyvale, US) was used. Two separate treatment plans, one for the headfirst and one for the feetfirst CT, were created. In addition to the body

and lung contour, a PTV contour was created by extending the whole body contour with 2 cm tissue-equivalent material in all directions to account for uncertainties due to the positioning and movement of the patient. The PTV was used as the target volume during treatment plan optimization. Moreover, the lung was treated like an additional target volume during optimization using a lower prescribed dose. A fixed field width, defined as the full width at half the maximum of the longitudinal dose profile in isocenter plane [93], of 5.5054 cm and a pitch, defined as couch movement per gantry rotation [93], of 1.450 cm for one whole rotation was used. The dose was calculated with a resolution of 2.5×2.5×5 mm^3. For comparison with the other TBI techniques, the dose was interpolated to the same resolution as the CT using Python v3.9.13 and normalized to the D_{50} of the body.

3.2.2 Results

Validation of the beam-zone method

Since the water phantom simulations showed a mean (± standard deviation) relative error averaged over all voxels in the phantom between the simulated dose distribution with and without the concrete floor of 2.6% ± 1.7%, the floor was neglected in all patient simulations.

When looking at the treatment plan created with the beam-zone method, the dose in all DRP never exceeded clinically acceptable deviations of ±10% from the dose in the DSP, and therefore from the prescription dose. The lowest dose was found at the DSP representing the head region with a relative value of 91%. The highest dose was found in the DRP representing the feet. Here, a value of 109% was observed. At the neck, the thinnest region of the body, a deviation of 7% was found, even without any additional bolus material. Therefore, adding bolus material for artificially increasing the local thickness or effective field size was not necessary for the analyzed patient.

The transC dose distributions simulated for the validation of the beam-zone method showed that the D_{50} of the body excluding the lung as well as the lung contour equaled the corresponding body or lung prescription dose for both set-ups, respectively (Fig. 3.5, 3.6, Tab. 3.2). For the skin, a slight overdosage compared to the prescription dose was found for the low-dose as well as the high-dose set-up. When looking at the dose 95% of the body, the lung and the skin received, both set-ups showed comparable results. However, the low-dose set-up showed a higher homogeneity for all three regions of interest (ROI) (body, lung, skin), indicated by lower HI values.

Averaged over all different anatomical regions a mean value ± standard deviation of 0 percentage points (pp) ± 3pp [-1pp ± 4pp] for $\Delta_{50\text{-DRP}}$ was found for the low-dose [high-dose] set-up (Fig. 3.7, Tab. 3.3). The sternum and the head region

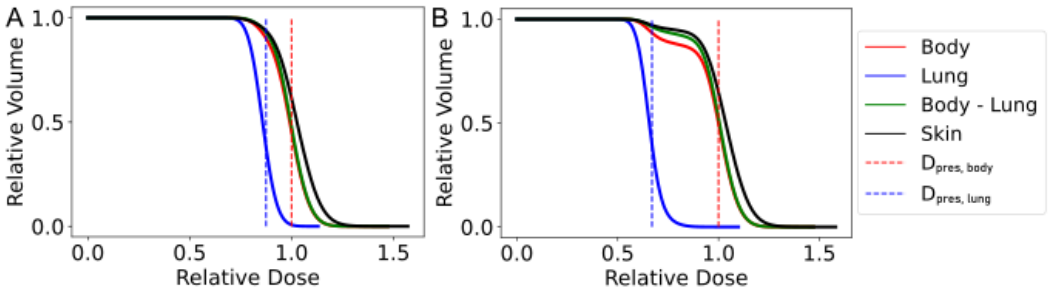

Figure 3.5: Dose-volume-histograms of the translational couch technique for the body (red), the lung (blue), the body excluding the lung volume (green) and the skin (black) for the low-dose (A) and high-dose (B) set-up. The vertical dashed lines indicate the prescribed dose D_{pres} to the body (red) and the lung (blue). All dose values are normalized to the dose in the dose specification point.

Table 3.2: Homogeneity index (HI), dose to 50% of the volume (D_{50}) and volume receiving at least 95% ($V_{D>95}$) of the corresponding prescribed dose for different region of interest (ROI) including the body, the body excluding the lung (body – lung), the lung and the skin. All values are given for the low-dose and high-dose set-up of the translating couch technique. The simulated dose distributions were normalized to the dose in the dose specification point.

Parameter	**ROI**	**Low-dose**	**High-dose**
HI	Body	0.35	0.55
	Body - Lung	0.34	0.53
	Lung	0.27	0.35
	Skin	0.4	0.57
D_{50}	Body	99%	100%
	Body - Lung	100%	100%
	Lung	86%	66%
	Skin	103%	104%
$V_{D>95}$	Body	70%	72%
	Body - Lung	73%	75%
	Lung	69%	66%
	Skin	80%	81%

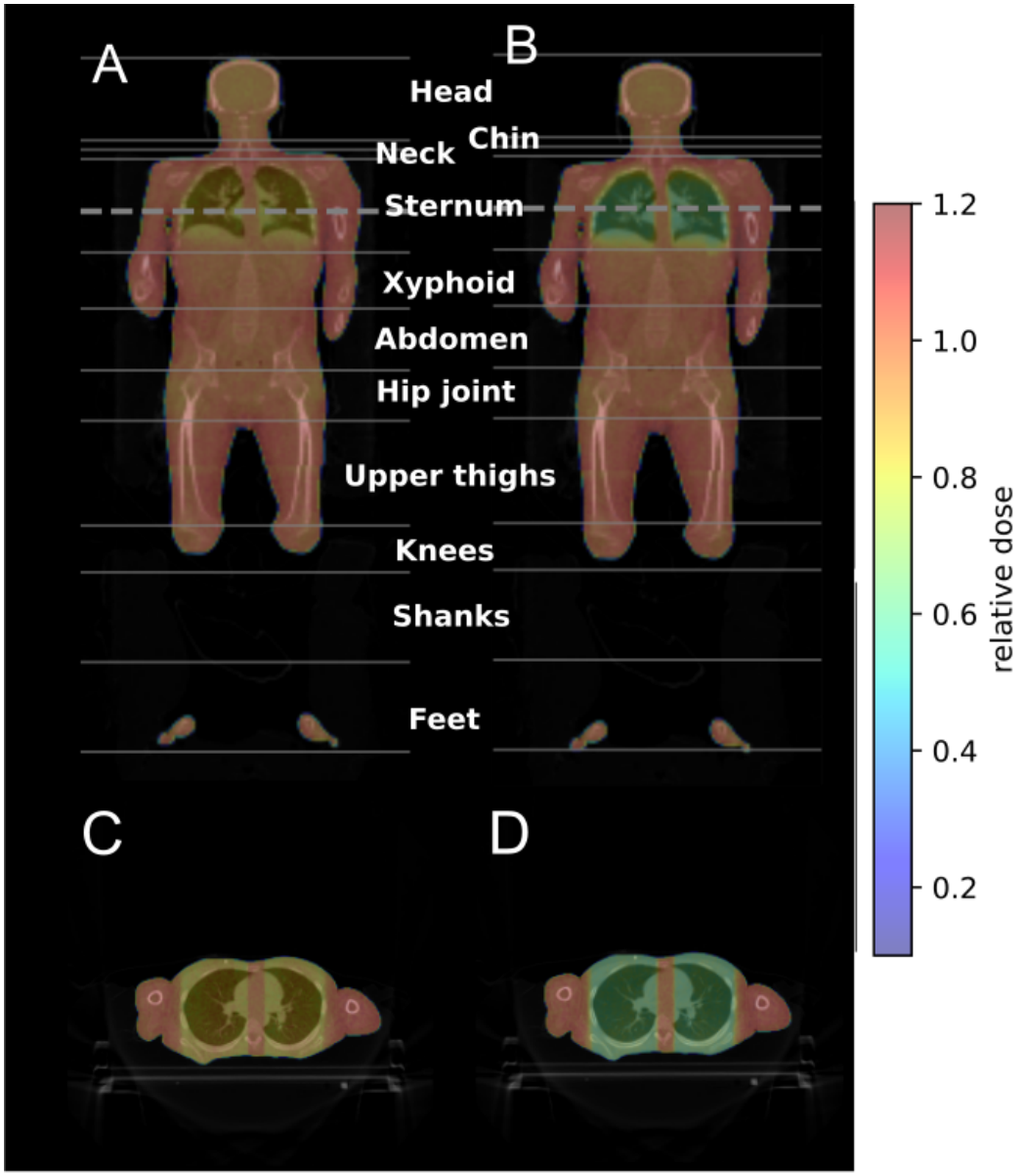

Figure 3.6: Simulated relative dose distribution on representative computed tomography (CT) slices for the low-dose set-up (A,C) and the high-dose set-up (B,D) of the translational couch technique. The grey lines indicate the different regions defined by the dose reference points of the beam-zone method. C and D show axial CT slices and dose along the dashed lines in A and B, respectively. All dose values are normalized to the dose in the dose specification point.

Table 3.3: Dose in the dose reference points predicted by the beam-zone method (D_{Plan}) and obtained with the Monte-Carlo simulation (D_{DRP}) as well as dose to 50% of volume in the different anatomical regions (D_{50}) for the low-dose and high-dose set-up of the translational couch technique. All dose values are normalized to the dose in the dose specification point.

Region	Parameter	Low-dose	High-dose
Head	D_{plan}	91%	91%
	D_{DRP}	89%	92%
	D_{50}	95%	96%
Chin	D_{plan}	98%	98%
	D_{DRP}	97%	101%
	D_{50}	99%	100%
Neck	D_{plan}	107%	107%
	D_{DRP}	107%	107%
	D_{50}	104%	105%
Sternum	D_{plan}	98%	98%
	D_{DRP}	98%	96%
	D_{50}	93%	83%
Xyphoid	D_{plan}	98%	98%
	D_{DRP}	98%	101%
	D_{50}	99%	100%
Abdomen	D_{plan}	100%	100%
	D_{DRP}	100%	100%
	D_{50}	100%	101%
Hip joint	D_{plan}	99%	99%
	D_{DRP}	99%	100%
	D_{50}	98%	99%
Upper thighs	D_{plan}	103%	103%
	D_{DRP}	103%	105%
	D_{50}	103%	104%
Knees	D_{plan}	102%	102%
	D_{DRP}	103%	104%
	D_{50}	102%	103%
Shanks	D_{plan}	108%	108%
	D_{DRP}	102%	104%
	D_{50}	105%	106%
Feet	D_{plan}	108%	108%
	D_{DRP}	106%	106%
	D_{50}	104%	105%

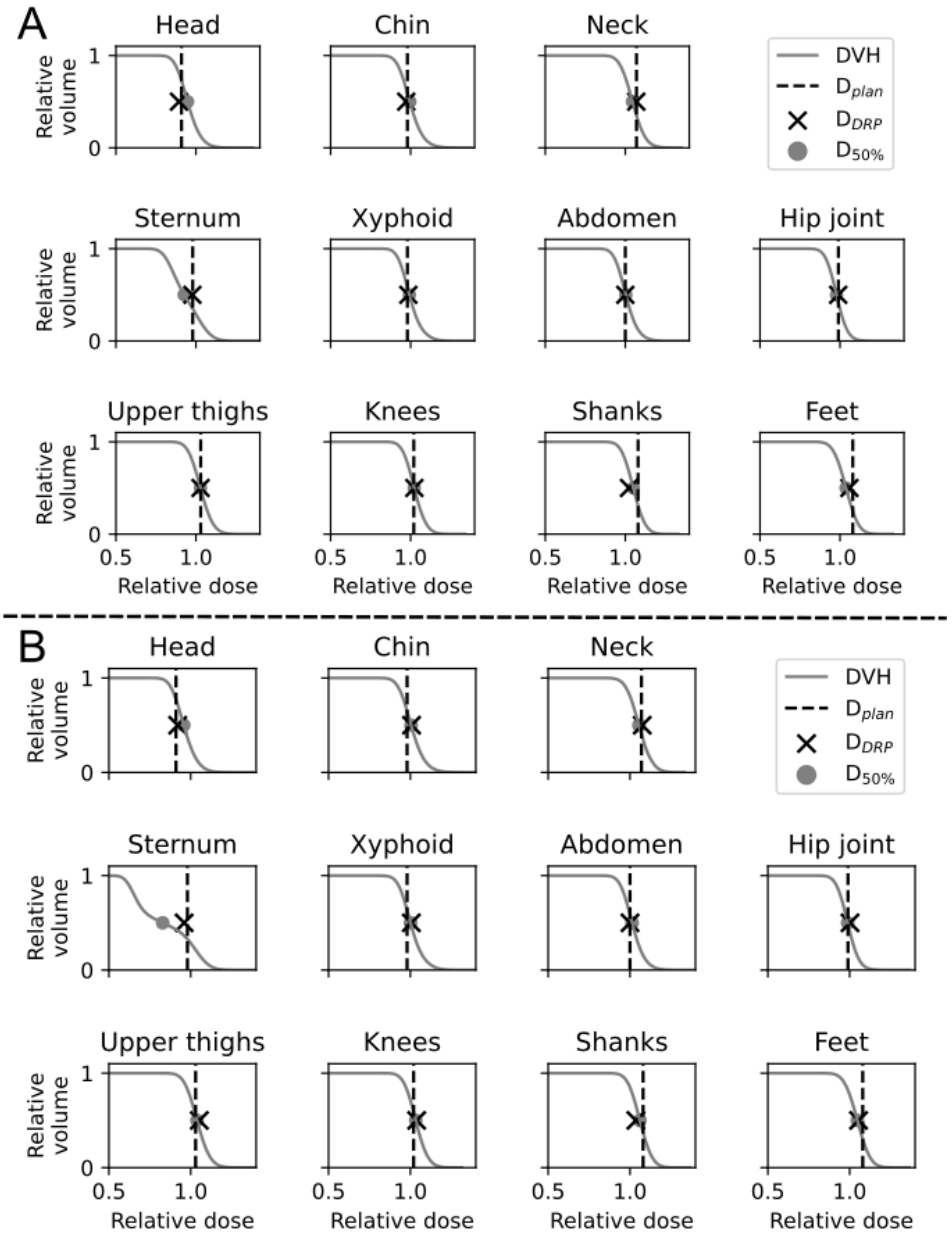

Figure 3.7: Dose-volume histograms (DVH) for the different body regions as defined by the beam-zone method for the low-dose (A) and the high-dose (B) set-up in grey. The black vertical dashed lines indicate the dose in the dose reference points predicted by the beam-zone method D_{Plan}, the black crosses indicate the dose in the dose reference points found in the simulations D_{DRP} and the grey circles mark the dose to at least 50% of the regarded volume in the simulation D_{50}. All dose values are normalized to the dose in the dose specification point

showed the highest values of $\Delta_{50\text{-DRP}}$. In the sternum region, the D_{DRP} was 5pp [13pp] higher than the D_{50} value for the low-dose [high-dose)] set-up, while in the head region, the D_{DRP} was 6pp [4pp] lower than the D_{50}. The different regions achieved on average a HI of 0.27 $\pm$ 0.05n [0.30 $\pm$ 0.12]. The highest HI, indicating low homogeneity, was found in the sternum region for both set-ups. When looking at the low-dose [high-dose] set-up, the sternum region yielded an HI of 0.41 [0.67]. When excluding the lung volume, the HI decreased to 0.39 [0.61]. When comparing the simulated dose in the DRP D_{DRP} with the predicted dose in the DRP by the beam-zone method D_{plan}, an averaged difference $\Delta_{plan\text{-}DRP}$ of 1pp $\pm$ 2pp [0pp $\pm$ 2pp] was found for the low-dose [high-dose] set-up. For both set-ups, this difference was highest in the shank region with a value of 6pp [5pp].

Dosimetrical comparison between different irradiation techniques

When comparing different TBI irradiation techniques, a comparable dose distribution over the entire body (Fig. 3.8, 3.9) as well as a comparable homogeneity for the body, the lung as well as the skin were found between transC and extSSD (Tab. 3.4).

When using the helT technique lower HI values, indicating higher homogeneity, were achieved for the body, the lung as well as the skin compared to the transC and extSSD techniques. Moreover, with helT, the HI value found for the skin was the same as for the rest of the body excluding the lung. For the other two techniques HI values of the skin were elevated, indicating lower homogeneity compared to the rest of the body. When looking at the D_{50}, all techniques achieved the corresponding prescription doses for the body and the lung. With the helT technique the D_{50} of the skin was found to be the same as for the rest of the body, while for transC and extSSD an overdosage of 104% of the skin was obtained. Furthermore, the volume receiving at least 95% of the corresponding prescription dose was relevantly higher for all ROI when using helT in comparison to transC and extSSD.

Table 3.4: Homogeneity index (HI), dose to 50% of the regarded volume (D_{50}) and volume receiving at least 95% ($V_{D>95}$) of the corresponding prescribed dose for different region of interest (ROI) including the body, the body excluding the lung (body – lung), the lung and the skin. All values are given for the translating couch (transC), the extended source-to-surface distance (extSSD), and the helical tomotherapy (helT) technique. All dose values are normalized to the dose to 50% of the body volume.

Parameter	**ROI**	**transC**	**extSSD**	**helT**
HI	Body	0.35	0.36	0.18
	Body - Lung	0.34	0.35	0.09
	Lung	0.27	0.22	0.16
	Skin	0.4	0.4	0.09
D_{50}	Body	100%	100%	100%
	Body - Lung	100%	100%	100%
	Lung	87%	86%	86%
	Skin	104%	104%	100%
$V_{D>95}$	Body	73%	74%	92%
	Body - Lung	77%	78%	96%
	Lung	73%	70%	87%
	Skin	82%	83%	98%

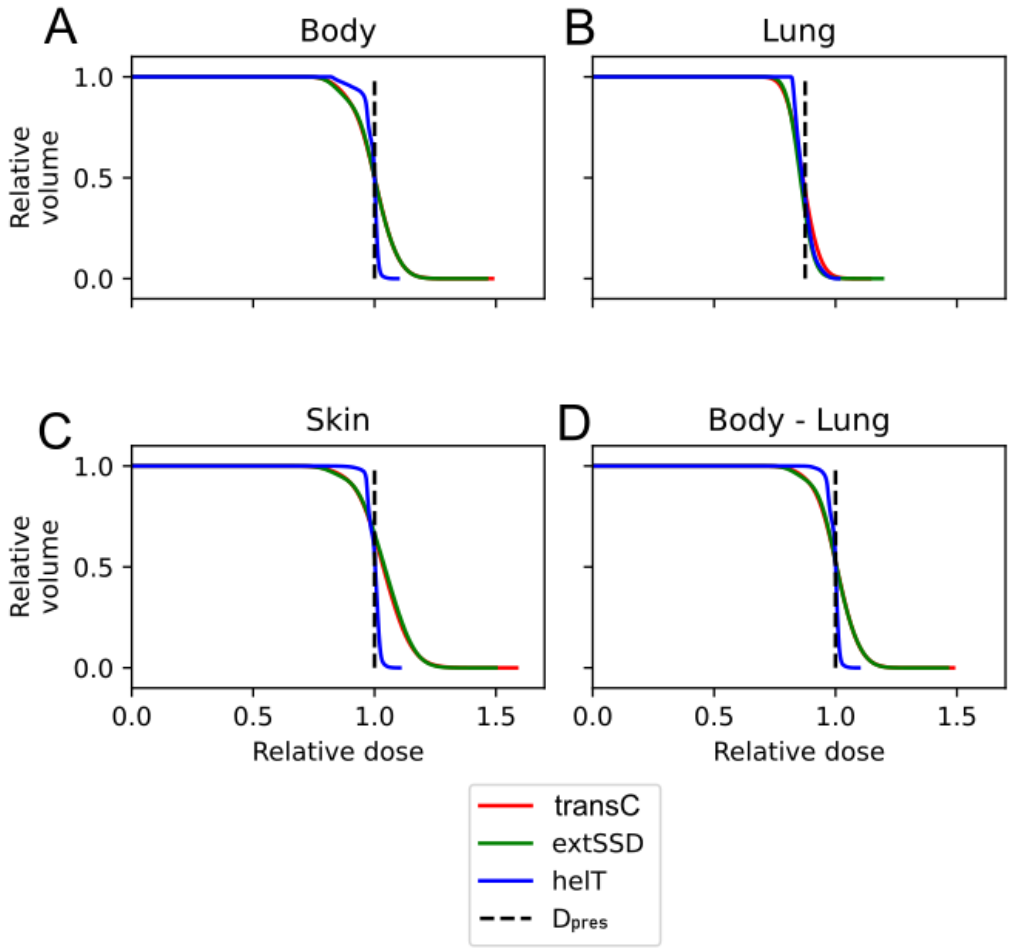

Figure 3.8: Dose-volume histograms (DVH) for the entire body (A), the lung (B), the skin (C), and the body excluding the lung volume (D). DVHs for the translating couch (transC) technique are shown in red, for the extended source-to-surface distance (extSSD) technique in green, and for the helical tomotherapy in blue (helT). The dashed lines indicate the prescription dose to the body (D_{pres} Body) and to the lung (D_{pres} Lung). All dose values are normalized to the dose to 50% of the body volume.

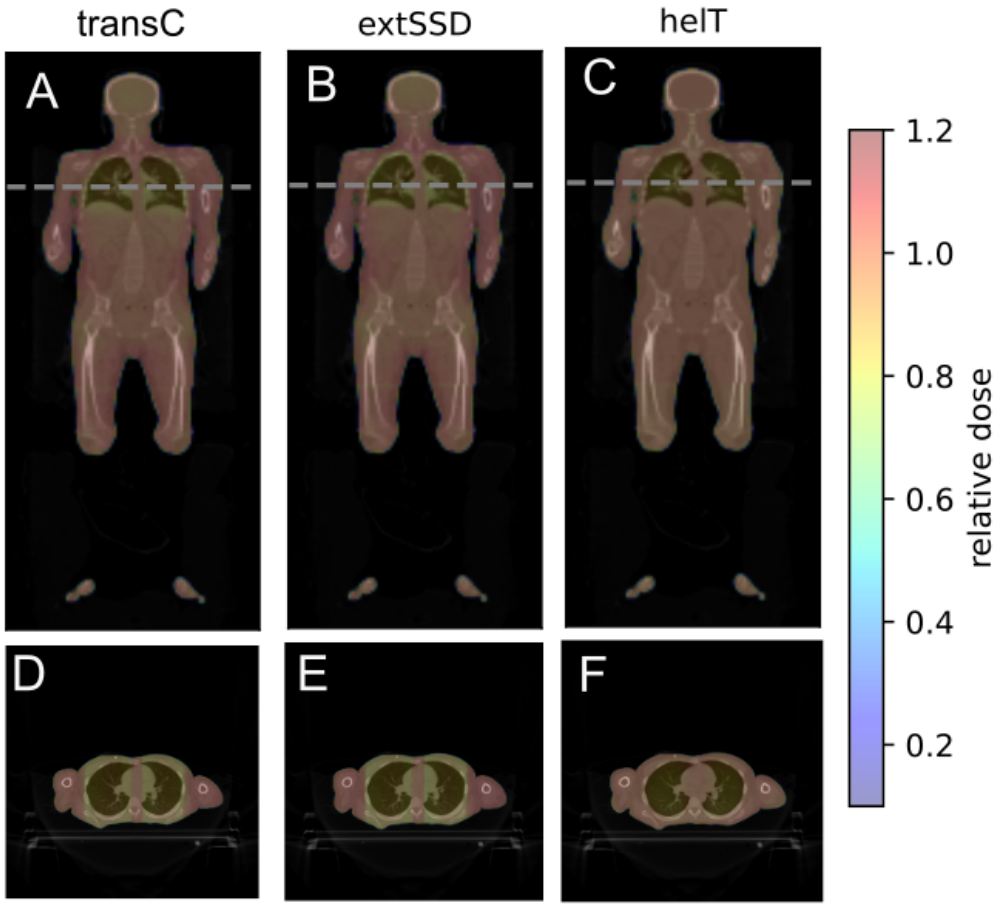

Figure 3.9: Relative dose distribution on representative CT slices for the translating couch (transC, A,D), extended source-to-surface distance (extSSD, B,E) and helical tomotherapy (helT, C,F) technique. The dashed lines in A,B,C indicate the location of the axial slices shown in D,E,F. All dose values are normalized to the dose to 50% of the body volume.

3.2.3 Discussion

There are two main sources of uncertainty when applying the beam-zone method [13]. The first one is the accuracy of the dose prediction in the DRP by the beam-zone method. To evaluate this source of uncertainty, the differences between the planned dose using the beam-zone method and the simulated dose in a DRP were calculated for all 12 DRPs. The second source of uncertainty is the assumption that the dose is homogeneous enough in the 12 different anatomical regions, such that the dose at the center, the DRP, is sufficient to characterize the dose in the entire region. To evaluate this, the differences between the simulated dose in the DRP and the D_{50} of each region were calculated. In all regions, besides the sternum region, both dose differences never exceeded a value of 6pp, which is in line with the clinically accepted dose variation of $\pm 10\%$ [2, 94]. Moreover, the homogeneity index of each region was calculated to further analyze the achieved homogeneity of the applied dose. The lowest homogeneity was observed in the sternum region. Since the lung blocks not only reduce the dose to the lung, but also to the tissue in beam direction in front of and behind the lung, dose inhomogeneities in the tissue surrounding the lung, and therefore in the sternum region, occur. This might lead to dose deviations in this anatomical region higher than the clinically acceptable value of 10%, especially for scenarios with a high difference between the lung and body prescription dose. Therefore, the use of the dose at the DRP may be insufficient to characterize the dose distribution in an anatomical region where radiation blocks are used to reduce the applied dose.

In the performed survey, centers considered the use of lung blocks as the major source of dose differences between different techniques, which has been confirmed by the performed patient study. Techniques that avoid using shielding material, such as helical tomotherapy (helT), allow for reducing the dose to the lung without introducing dose inhomogeneities in the surrounding tissue. Therefore, dose deviations between different TBI techniques might be particularly pronounced, when the prescribed dose for the lung differs substantially from the prescription dose for the rest of the body. To which extent this difference might be of clinical relevance, remains, due to the lack of published clinical outcome data, unknown. This lack of data was considered as one important challenge considering the application of TBI by centers participating in the survey. Analyzing clinical outcome data was considered an important step in determining the best possible treatment techniques for TBI. To achieve a more homogeneous dose in the sternum region, some centers use additional electron beams to boost the dose to the chest wall [12, 95], which might lead to more comparable dose distributions between irradiation techniques using lung blocks and techniques not utilizing them. However, according to the performed survey, this is only done by a minority of the participating centers.

Another difference between the translational couch (transC) and extended source-

to-surface distance (extSSD) technique compared to helT was found regarding the dose to the skin. With transC and extSSD a less homogeneous dose to the skin compared to helT was observed. Because of the two opposing beam directions and the beam spoiler used for transC and extSSD, the skin areas where the beam enters the body receive an elevated dose, leading to an overdosage of about 104% of the prescribed dose. At the same time, the lateral skin areas receive less dose, resulting in a more inhomogeneous dose to the skin compared to the rest of the body. For helT, the dose homogeneity of the skin is comparable to the dose homogeneity of the rest of the body and no overdosage of the skin was observed. Using a beam spoiler with a different thickness might reduce the skin dose maximum for transC and extSSD, but at the same time, this might lead to a higher dose further inside of the body because of the build-up region of the photon depth dose curve.

One important advantage of transC and extSSD is their high robustness against patient position and movement uncertainties because the field sizes used for these techniques are usually much larger than the patient. For helT, the outline of the patient contour was extended with a safety margin of 2 cm during treatment planning to account for these uncertainties at least to some extent.

When comparing the dose distribution of the transC and extSSD techniques, an overall high similarity was found. Therefore, the transC technique can be considered a good alternative to the extSSD technique for centers that cannot meet the necessary spatial conditions to perform extSDD irradiations.

One strategy proposed in the literature to calculate 3D dose distributions for TBI techniques for which usually no 3D dose distribution exists, is the use of the standard TPS [8, 96–98]. Normal TPS are not validated for SSD higher than approximately 100 cm. Therefore, before using the TPS for TBI dose calculation, extensive measurements have to be performed to validate the TPS for large SSDs. Moreover, clinical photon TPS are usually applying pencil beam, convolution, or AAA algorithms for TBI dose calculation, and therefore no Monte Carlo simulation, which is considered as gold standard for dose calculation, is performed. Lavallée et al [99], e.g., calculated the dose for the transC technique using a superposition-convolution algorithm. In their study, a volume of 81.3% of the body received at least 95% of the prescribed dose. The simulations performed in this thesis yielded a volume of 73% and 72% that receive at least 95% of the prescribed dose for the low-dose and high-dose set-up, respectively. This difference can be explained by the different dose algorithms used and the fact that no lung blocks were applied in the study by Lavallée et al.

Lavallée et al also optimized the velocity of the translating patient couch with the aim of achieving the prescription dose in all DRPs and compared the results with the dose distribution achieved with a constant velocity. A better homogeneity, especially in the head region, was observed. The volume receiving at least 95% of the prescribed dose in the head region was increased from 43.9% to 99.9%. In the

simulations performed in this thesis, the highest inhomogeneity was found in the sternum region, especially for the high-dose set-up, due to the use of lung blocks. Since the lung blocks would still be present when applying a variable velocity of the patient couch, the homogeneity in this critical region would not be improved. Nevertheless, using a variable velocity offers the possibility of adjusting the dose to one DRP without the need for additional water-equivalent bolus material to artificially increase the local thickness or effective field size.

In another study, performed by Umek et al [10], measurements of the dose using thermoluminescent dosimeters (TLD) during translational TBI were performed. The TLDs were positioned on the skin of the patient and the measured dose values were then used to calculate the dose at different points along the central axis of the patient, representing different anatomical regions. All anatomical regions showed deviations of less than 4% from the reference dose at the abdomen, which is in line with the results of the simulations performed in this thesis. The remaining deviations between the measured values by Umek et al and the simulated dose values found in the thesis at hand can be explained by the fact that Umek et al used a Co-60 source to perform TBI while here a 6 MV linac was used.

TBI is a specialized treatment and irradiation techniques vary widely between centers worldwide [28-35] and also within Germany, as shown by the survey. In recent years, modern treatment techniques such as VMAT and helical tomotherapy have been increasingly used for TBI, especially in Germany. These techniques involve CT-based treatment planning as a standard procedure providing 3D dose distributions for every patient. The use of a simulation workflow, as presented here, provides the possibility to create 3D dose distributions for other techniques, for which usually no 3D dose distribution exists. Moreover, the results of such simulations can be used to validate clinical TPS for greater SSD, without the need to perform extensive measurements. Comprehensive reporting procedures of the received dose are crucial for optimally treating TBI patients. With a simulation workflow, as proposed here, now 3D dose distributions can be calculated for almost every patient, from whom a whole-body CT was acquired. The majority of centers participating in the survey stated to acquire whole-body CT scans of their patients, even if no 3D dose calculations were performed (Fig. 3.3). Therefore, the simulation workflow introduced here allows for future studies analyzing and correlating dose distributions with clinical outcome data, which is, according to the survey, considered the most important step towards standardization of TBI.

3.3 Conclusion

The performed survey provides a detailed insight into the current clinical practice of different TBI techniques in Germany showing a high heterogeneity between centers.

More standard techniques, such as using an extended SSD or a translational couch for irradiation, were still most commonly used, but the number of centers using more advanced techniques, such as VMAT or tomotherapy seems to be increasing. To ensure the best possible treatment for every patient, the need for standardization and detailed guidelines covering all dosimetric aspects of the treatment process arises. Therefore, differences in the achievable 3D dose distributions of the various TBI techniques as well as in the choice of dosimetrical plan parameters (e.g., prescription dose, dose rate, tolerance doses for OARs) need to be identified and analyzed with respect to the resulting clinical outcome. Because of the limited number of TBI patients per center, the numerous different techniques, definitions of the target volume, dose schemes, and dose limits for OARs used, centers suggested performing (retrospective) patient studies and combining clinical outcome data from different centers as a basis for standardization and future guidelines.

To identify dosimetrical differences between the different TBI techniques, 3D dose distributions are needed for all used techniques. The novel simulation workflow introduced here, offers the opportunity to calculate Monte Carlo-based 3D dose distributions for the extended SSD and translational couch technique, the two most frequently used TBI techniques in Germany. The resulting ability to correlate clinical outcome data that have emerged over the past decades with accurate estimates of the applied dose for these TBI techniques marks an important step towards standardizing TBI treatment in the future.

4 Project protons: Variable relative biological effectiveness

The use of a constant relative biological effectiveness (RBE) in proton therapy introduces uncertainties that might lead to toxicities after proton irradiation. Since the RBE depends on different biological and physical parameters, it is not a constant but varies along the proton track leading to an increased biological effective dose at the distal edge of an SOBP. To better understand the current clinically applied approaches to account for RBE uncertainties as well as future requirements regarding the variable RBE, a survey was distributed among all proton therapy centers in Europe treating patients [100]. To incorporate the variable RBE into treatment planning in the future, the novel dirty & clean dose concept was introduced and its benefits and risks were analyzed performing in silico water phantom as well as patient studies [101].

4.1 Survey

There is a growing awareness of the uncertainties caused by possible RBE effects leading to the questions on how to effectively account for the variability of the proton RBE during treatment planning. So far, no commonly applied guidelines or strategies exist on the consideration of the RBE. A first step towards novel guidelines in Europe is a detailed insight into already applied RBE strategies. Therefore, a survey on the current clinical practice of RBE consideration in European proton therapy centers was performed.

4.1.1 Material and methods

To determine the current clinical situation, a survey on the current clinical practice on a variable proton RBE was designed and distributed to all proton therapy centers in Europe treating patients in 2020. A copy of the questionnaire can be found in the appendix. To identify all suitable proton therapy centers in Europe the European Society for Radiotherapy and Oncology (ESTRO) and the Particle Therapy Co-Operative Group (PTCOG) were consulted. 25 centers from 14 different European countries were identified in this way and asked to fill out the online questionnaire (Fig. 4.1). The survey consisted of eight different sections, each dealing with a different topic, and was implemented using SurveyMonkey (SurveyMonkey, San

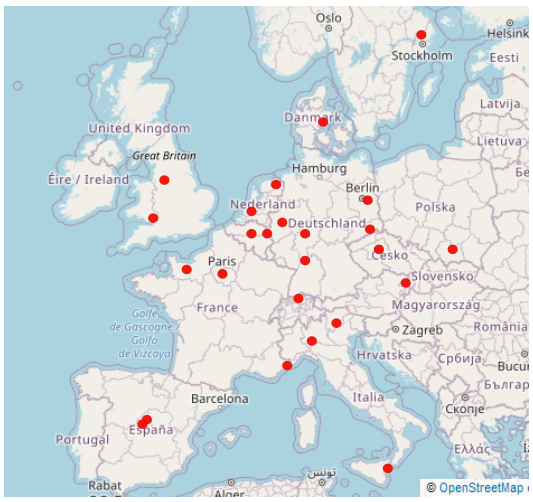

Figure 4.1: Map of Europe. The 25 proton therapy centers participating in the survey are indicated by the red dots. This map is made available under the Open Database License and any rights in individual contents of the database are licensed under the Database Contents License (both: http://opendatacommons.org/licenses/dbcl/1.0/). Adapted from [100].

Mateo, USA). The main part of the survey (sections 2-7) dealt with different aspects considering the proton RBE, while the first section asked for contact details of the center, and the last one offered the possibility for additional comments. Therefore, the different sections of the questionnaire were:

1. Contact information
2. Treatment field arrangement (9 questions)
3. Robust optimization (2 questions)
4. Variability of RBE in treatment planning (7 questions)
5. Estimation of LET and RBE for patient treatment (11 questions)
6. RBE consideration for patient follow-up (4 questions)
7. Future improvements (6 questions)
8. Additional comments

The main part of the survey (section 2-7) consisted of 39 questions. Of these, 24 questions had predefined options to answer (closed questions) and the other 15 questions were open questions, meaning the answers were provided in the form

of a free text. For some closed questions a selection of more than one answer was possible and single questions could be skipped. Therefore, the number of participants answering a specific question varied. Moreover, most questions offered the opportunity for additional comments. The closed questions were evaluated quantitatively, while open questions were evaluated more qualitatively. For this type of question, similarities and differences between participating centers were identified allowing for categorizing the responses and thus offering the possibility for performing more quantitative evaluations.

4.1.2 Results

All 25 proton therapy centers answered the questionnaire. In most centers (15 centers) the questions were answered by physicists, in nine by physicians, and in one by both together. The response rate differed for every question (Tab. 4.1). Open questions were on average answered by 54% of the centers while closed questions were answered by 98%. One participating center stated to only perform eye irradiation making several questions not appropriate. Therefore, this center was excluded in the following analysis. If not stated otherwise, 24 centers are considered as 100%.

The most commonly irradiated treatment sites (Fig. 4.2) were the base of skull (92%), the brain (92%), and head and neck tumors (88%). Other treatment sites were the prostate, the lung, and the craniospinal axis, which were irradiated by 42%, 50%, and 71% of the centers, respectively. Treatment sites like the esophagus, the liver, the breast, and the pancreas, were each treated by less than 38% of the centers.

All proton therapy centers followed current guidelines and used a constant RBE of 1.1 for prescription (Fig. 4.3A), while at the same time, all centers stated to perform some measures to actively counteract the uncertainties resulting from a variable RBE (Fig. 4.3B). Most common measures included the use of special beam arrangements, which was done by 96% of the centers, and the avoidance of beams stopping in or close to an OAR, which was performed by all centers (Fig. 4.4B). Thus, the possibility of a variable RBE (vRBE) was mostly (71%) considered for OARs (Fig. 4.4A). No center stated to consider a variable RBE for the target volume.

All centers considered some restrictions on the treatment field arrangement with the most frequent restriction being the choice of the incident beam direction. Beam angles leading to beams stopping inside or close to an OAR were, if possible, avoided by all centers. If this was not possible, the relative weight of the corresponding beams was reduced by nine centers, or the field range was extended to position the end of the proton track behind the OAR ('shoot-through') by four centers. When asking for the minimum number of beam orientations, centers stated to rarely irradiate with only one beam direction. Some treatment sites (base of skull, esophagus, pancreas,

Table 4.1: Number (No.) and response rate (RR) of closed and open questions for each topic, as well as the total number of questions with the corresponding response rate for each topic. RBE: Relative biological effectiveness. LET: Linear energy transfer. Adapted from [100].

Topic	**Closed**		**Open**		**Total**	
	No.	**RR**	**No.**	**RR**	**No.**	**RR**
Treatment field arrangement	7	98.3%	2	72.0%	9	92.4%
Robust optimization	2	96.0%	0	-	2	96.0%
Variability of RBE in Treatment planning	6	96.7%	1	12.0%	7	84.6%
Estimation of LET and RBE for patient treatment	6	99.3%	5	42.4%	11	73.5%
RBE consideration for patient follow-up	3	100.0%	1	33.3%	4	50.0%
Future improvements	0	-	6	68.0%	6	68.0%
Total	24	98.0%	15	54.0%	39	79.5%

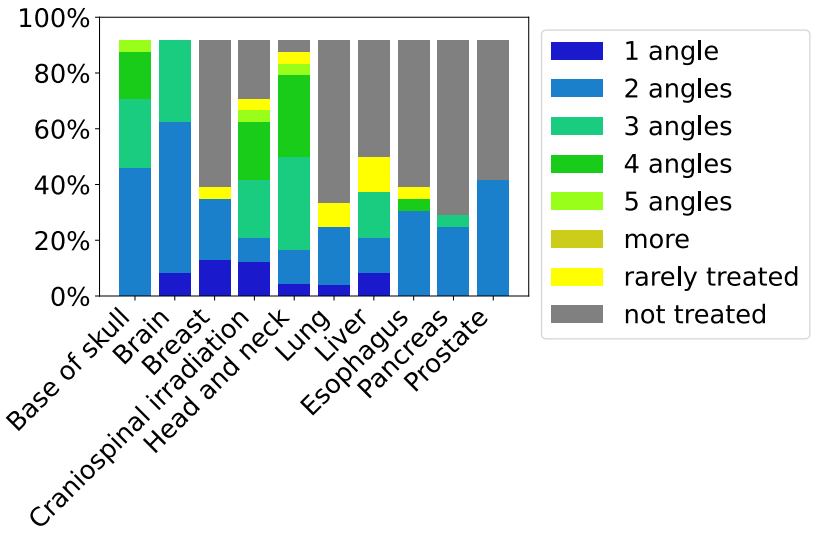

Figure 4.2: Percentage of centers applying a minimum number of treatment field orientations for different treatment sites. 22 centers answered this question. Adapted from [100].

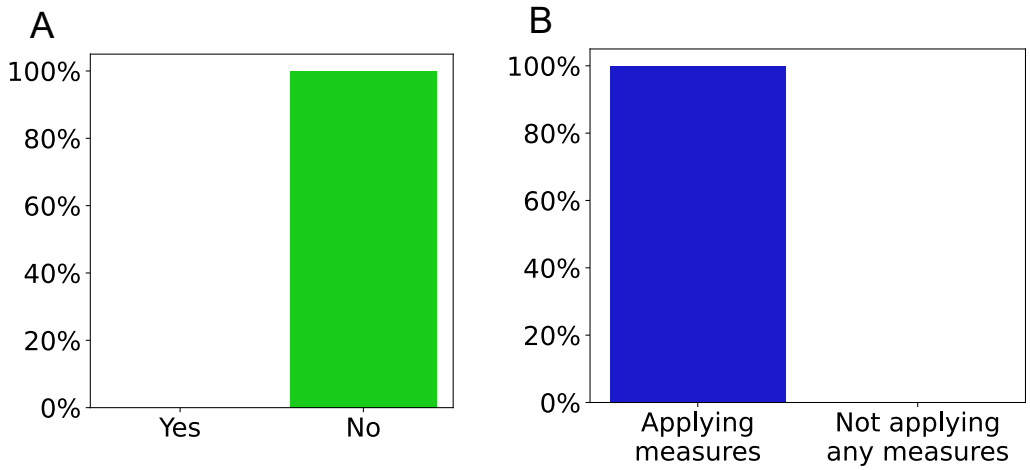

Figure 4.3: Responses to the questions: Do you prescribe anything else than a fixed relative biological effectiveness (RBE) of 1.1 for patient treatment? (A) and the number of centers stating to perform any measures to counteract a potentially variable RBE (B). Adapted from [100].

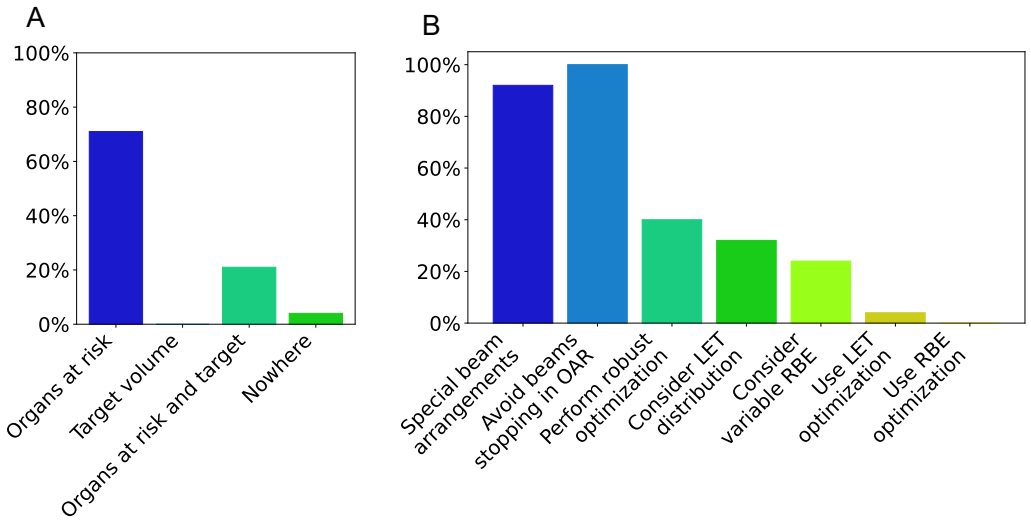

Figure 4.4: Sites for which the centers stated to actively consider a variable relative biological effectiveness (RBE) (A) as well as measures applied to counteract a variable RBE (B). OAR: Organ at risk. LET: Linear energy transfer. Adapted from [100].

prostate) were always irradiated with at least two beam orientations. Moreover, centers (75%) applied restrictions on the minimum angle between two beams. The ten centers precisely stating their restriction, applied a minimum angle of at least 10° (2 centers), 30° (6 centers), or even higher (2 centers). Moreover, nearly all centers (88%) utilized robust optimization for treatment planning considering robustness for target coverage (83%), for selected OARs (50%), and for all OARs (17%). Three centers stated to never use robust optimization.

Although the majority of centers (88%) performed at least some patient-specific calculation of LET or RBE, the results of these calculations were rarely used to support patient treatment. Mostly the calculations were performed for research purposes. So far, twelve centers had performed calculations of vRBE-related quantities to support treatment planning at least once. In terms of clinical treatment, the LET distribution was most commonly calculated (42%) followed by the vRBE distribution (25%, Fig. 4.5A). Eleven centers performed these calculations for retrospective analyses, ten centers for plan evaluation, also ten for clinical research, and three during treatment planning. The frequency of performing the calculation of vRBE-related quantities depends on the treatment site and was most frequently performed for brain (33%) and head and neck tumor patients (17%). The centers stated to use different software to perform these calculations. Most centers (38%) used a research version of the TPS RayStation (RaySearch Laboratories AB,

Stockholm, Sweden), while others used different research Monte-Carlo simulation or in-house software frameworks (Fig. 4.5B). The calculations were usually initiated by physicists followed by the treating physician and in most centers performed by physicists or research staff. The RBE was considered during patient follow-up in 58% of the centers, mostly (42%) to better understand the radiation response of the patient. Therefore, eight centers stated to perform the calculations, to investigate a possible correlation between the vRBE distribution or other vRBE-related quantities and the occurrence of side effects.

The part of the survey asking for future improvements consisted of only open questions and had a response rate of 68%, which was higher than the average response rate for open questions of the other topics (Tab. 4.1). The most frequent and urgent request was for more clinical evidence of possible side effects due to a variable RBE. The centers wished for more published retrospective and prospective studies with large patient cohorts examining the correlation of vRBE and the probability of toxicities. To be able to perform such studies, centers asked vendors to develop and implement LET and RBE visualization tools in their clinical TPS to visualize and store these quantities for all patients regularly. Nine centers would like to apply LET and RBE visualization not only for research purposes but also to support treatment planning, e.g., during plan approval. Moreover, seven centers indicated that they would like vendors to also develop vRBE-related optimization tools.

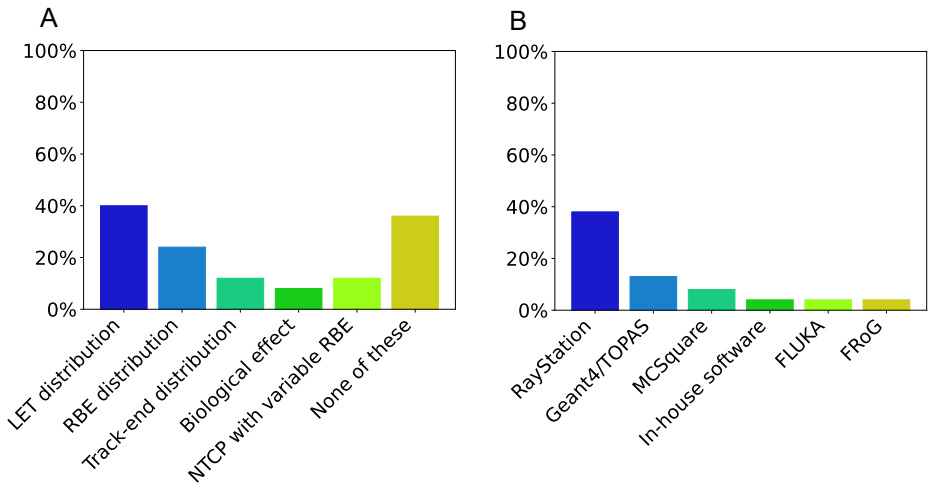

Figure 4.5: Number of centers calculating different quantities for clinical treatment (A) and the applied software to perform these calculations (B). LET: linear energy transfer, RBE: relative biological effectiveness, NTCP: normal tissue complication probability, Geant4/TOPAS/MCSquare/FLUKA: Tools for Monte Carlo simulations of particles through matter, FRoG: Fast dose Recalculation on GPU. [100].

4.1.3 Discussion

Many in vitro, in vivo, and recent retrospective patient studies [17–24] have shown, that the proton RBE varies along the proton track leading to an increased biological dose at the distal edge of an SOBP. Therefore, the use of a constant RBE of 1.1 during treatment planning, especially together with tolerance doses for OARs based on photon data, introduces uncertainties that might lead to unexpected side effects. So far it was not known, if and to which extent the variability of the RBE is already considered during daily clinical practice. Therefore, in this thesis, a questionnaire was distributed among all 25 proton therapy centers in Europe treating patients to gain a detailed insight into the actual clinical practice considering the proton RBE. All 25 proton therapy centers answered the questionnaire underlining the high relevance and importance of the RBE-topic.

Current guidelines [102] are still suggesting to prescribe a constant RBE of 1.1. All participating centers indicated to follow these guidelines and therefore adopt a constant RBE for dose prescription. At the same time, however, all centers indicated to apply different measures trying to reduce variable RBE (vRBE)-related uncertainties without contradicting these guidelines. Thereby, centers revert to well-known measures, which have been used in proton therapy for many years, since they not only reduce possible vRBE-related uncertainties but also range uncertainties. Such measures were, e.g., the avoidance of angles leading to beams stopping inside

or close to an OAR, the avoidance of acute angles between incident beams, the use of more fields to reduce the relative weight of critical incident angles or extending the field range to position the end of the proton track beyond an OAR.

Whether these measures are sufficient to account for the variability of the RBE is still under investigation. Some studies [103, 104] found measures as currently applied by European proton therapy centers to be effective in reducing vRBE-weighted dose values in critical OARs, while another study [103] showed that a higher number of treatment fields may in some cases not be sufficient to reduce vRBE-related uncertainties. Moreover, extending the proton range to place the end of the beam beyond an OAR can lead to an increased volume receiving a high vRBE-weighted dose without relevantly reducing vRBE-weighted dose hot spots [104]. Therefore, the efficiency of the different clinically applied measures depends strongly on the individual patient case. Thus, these measures cannot be considered as an universal approach to reduce vRBE-related uncertainties for all patients. Moreover, these measures can severely limit the possible degrees of freedom of proton therapy reducing the actual benefits of proton therapy compared to conventional radiotherapy using photons. The most important advantage of proton therapy is the sharp dose gradient at the distal edge, but as long as the biological effect at the distal edge is not correctly characterized and considered during plan optimization, the potential of proton therapy cannot be fully exploited.

When looking at the RBE values found in vitro and in vivo, much more vRBE-related side effects would have been expected than actually reported in the literature leading to a debate on the clinical relevance of the vRBE-effect. One possible reason for this fewer than expected patient side effects might be the so-called smear-out effect [25]. The prescription dose is usually applied in several fractions. Therefore, because of possible set-up and range variations during the entire course of irradiation, the distal edge of the SOBP is not located at the same position in every fraction leading to a smear-out of possible high biological doses. With increasing precision in proton therapy through the reduction of range and set-up uncertainty, the smear-out effect of the RBE might get smaller, and more pronounced RBE effects might be found in the future. Moreover, the results of the survey may provide another explanation. The fact, that centers are already applying different measures to counter RBE uncertainties might influence clinical outcome leading to a lower occurrence of toxicities as expected from preclinical studies underlining the clinical relevance of vRBE-related uncertainties. Therefore, considering RBE uncertainties during treatment planning is essential to provide the best possible treatment for patients, but so far a clinically acceptable standard approach for incorporating RBE uncertainties into treatment planning is still lacking.

The clinical relevance of RBE uncertainties is also supported by the published results of retrospective patient studies especially in brain tumor patients correlating vRBE-related quantities with image changes found in follow-up MRI [17–20]. Because

of the close proximity of radiosensitive OARs to the target volume in brain tumor patients, areas with high dose and high LET in or close to these OARs occur more frequently. Therefore, the risk for clinical side effects due to a vRBE is particularly high for these entities and most evidence for a clinically relevant vRBE effect was found for these anatomical regions. As shown by the survey performed in this thesis and also by a currently published study [105], brain tumors as well as head and neck tumors are the most commonly treated entities for proton therapy in Europe. Accordingly, the entities most likely to benefit from considering a vRBE during treatment planning, also represent the entities most commonly treated with proton therapy making it even more important to find suitable tools for effectively reducing vRBE-related uncertainties in a clinical environment.

The current strategy in clinics is to maintain target dose prescription using a constant RBE of 1.1 to ensure tumor control while decreasing the impact of a vRBE in OARs. This strategy is in line with a recent AAPM report [106] as well as current research works [22, 107–109]. Therefore, novel tools should focus on a targeted optimization of the part of the dose, whose biological effect is currently uncertain, while ensuring target dose coverage for the 1.1-weighted dose. In this way, uncertainties due to a vRBE can be reduced without compromising tumor control.

The question on how to proceed regarding the proton RBE was of great concern to all participating centers. This was highlighted by the high number of centers answering the open questions of the last part of the survey asking for future needs and requirements. Almost all centers stated, that more clinical data in the form of retrospective and prospective studies is needed to change current guidelines of prescribing a constant RBE. Most centers were not able to produce such data since no visualization tools of vRBE-related quantities implemented in their clinical TPS existed. Therefore, the centers requested vendors to provide such tools. This would enable centers to score and store vRBE-related quantities as a standard procedure for all patients as suggested by recently published recommendations for consistent toxicity scoring and follow-up in adult brain tumor patients, in which the analysis of follow-up image changes is considered as minimum of care [110]. Moreover, for comparability of clinical data, centers requested to harmonize the calculation and reporting of vRBE-related quantities, which would allow for consistent multicentric analysis of toxicity caused by an increased RBE [111].

Due to the specialized treatment, several questions were inadequate for the one center treating only eye tumors and thus it was excluded from the performed analysis. Answers by this center indicated that the vRBE effect is considered less important for ocular irradiation since no high-risk organ is close to the target volume. Nevertheless, the center also stated that an ocular TPS including the possibility of calculating vRBE-related quantities would be of interest and patients might benefit from using such tools.

The performed survey in this thesis provides a detailed insight on the consid-

eration of a variable RBE in current clinical practice. All centers were aware of potential risks when not considering the vRBE or vRBE-related quantities during treatment planning and were therefore applying some sort of measures to counteract potential risks. Moreover, all centers agreed on the importance of visualization and optimization tools of vRBE-related quantities to optimally exploit the potential of proton therapy and provide the best possible treatment for patients.

4.2 In silico study

The performed survey underlined the urgent need for visualization and optimization tools of vRBE-related quantities implemented in clinically used TPS. The novel dirty & clean dose concept, introduced here, represents a visualization and optimization tool of the part of the dose having the highest uncertainties due to a variable proton RBE. The novel concept was implemented into the research version of a clinically used TPS making a future use as a standard procedure during treatment planning for all patients possible. According to the survey, the current clinical strategy was the reduction of RBE-related uncertainties in critical OAR while maintaining target dose distribution to ensure tumor control. To enable this approach also with the novel dirty & clean dose concept, water phantom studies were performed to find suitable optimization parameter ranges. These parameter ranges were then used for in silico patient studies to assess the benefits and risks of the novel concept. Since cranial tumors are most commonly treated with proton therapy, patients undergoing cranial proton therapy were chosen for the in silico patient study.

4.2.1 Material and methods

The dirty & clean dose concept is a novel concept to incorporate RBE uncertainties into treatment planning. The idea is to divide the 1.1-weighted dose distribution into two parts by a defined LET threshold $\mathrm{LET}_{\mathrm{thres}}$. The dirty dose contains the sum of all dose contributions by individual protons with an LET above $\mathrm{LET}_{\mathrm{thres}}$. The remaining low-LET dose contributions represent the clean dose. Therefore, the sum of the clean and the dirty dose equals the 1.1-weighted dose. The separation of the total dose is done by a binary filter considering the actual LET value of each proton. Thus, no voxel-wise averaging of the LET spectrum is performed. The ratio between clean and dirty dose depends on the chosen $\mathrm{LET}_{\mathrm{thres}}$. The dirty dose as well as the clean dose represent just another dose distribution. Therefore, all objectives usable for standard dose optimization, e.g., max dose, min dose, and uniform dose, can also be applied on the clean and dirty dose distribution. In contrast to standard dose optimization, two parameters are needed when applying dirty dose optimization with the first one being $\mathrm{LET}_{\mathrm{thres}}$. This parameter defines the part of the dose to be considered as dirty and thus gets optimized. The second parameter is the dirty

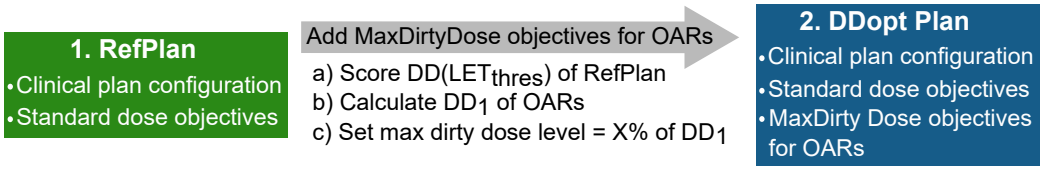

Figure 4.6: Two-step planning approach for creating the dirty dose optimized (DDopt) treatment plans by adding for each organ at risk (OAR) a MaxDirtyDose objective to the reference plan (RefPlan). DD: Dirty dose, LET_{thres}: Linear energy transfer threshold, DD_1: Dirty dose that 1% of the volume receives. Adapted from [101].

dose level parameter defining the dose objective used on the dirty dose distribution. For example, when using the MaxDirtyDose objective, the following two parameters are needed:

a) LET threshold: only protons with an LET higher than this value contribute to the dirty dose

b) max dirty dose level: maximum allowed dirty dose value in a voxel, dirty dose in a voxel exceeding this value gets penalized during optimization.

The standard dose optimization was extended by adding max dirty dose objectives for dose-limiting OARs close to the target volume penalizing dose contributions from high-LET protons (above LET_{thres}) that exceeded the defined max dirty dose level. Thus, the max dirty dose objective acts similarly to the standard max dose objective just on a different dose distribution, the dirty dose distribution. To score and optimize dirty and clean dose distributions, a binary filter of the standard dose scorer was implemented in a research version of the TPS RayStation 11B-IonPG (RaySearch Laboratories AB, Stockholm, Sweden). When a particle traverses a voxel, the actual LET value of this particle is calculated. If the LET of this particle is higher than LET_{thres}, the deposited dose is added to the dirty dose, otherwise the dose is added to the clean dose. Thus, the separation in dirty and clean dose is performed during the simulation of the particle transport. For the optimization of the dirty or the clean dose, a quadratic penalty function, as used for standard dose optimization, is applied.

To study the benefits and risks of the optimization of different dirty dose distributions in a water phantom as well as in patients undergoing cranial proton therapy, a two-step planning approach was applied (Fig. 4.6). First, a clinically acceptable reference plan (RefPlan) was created fulfilling all clinical goals for target dose coverage and OAR sparing using only standard 1.1-weighted dose objectives and therefore representing the optimal 1.1-weighted dose distribution. Second, dirty dose optimized (DDopt) treatment plans were created by maintaining all clinical plan

configurations, e.g., number and orientations of all treatment fields, and standard 1.1-weighted dose objectives of the RefPlan and adding one additional MaxDirtyDose objective for each critical OAR. The max dirty dose level for optimization was chosen as a percentage of the near-maximum dirty dose DD_1, defined as the dirty dose that 1% of the volume of interest received, to account for the dependence of the dirty dose on LET_{thres}. Thus, first, the DD_1 of the regarded OAR in the RefPlan was calculated. Then, the max dirty dose level for the DDopt plan was chosen relative to this DD_1 value, e.g., 50% of DD_1.

To visualize and optimize the dirty and clean dose distributions and to study the influence of the chosen LET_{thres} on the resulting distributions of the DDopt plans, in silico analyses with different field configurations and water phantoms were performed. First, a water phantom with a 5×5×5 cm^3 target volume was studied (Fig. 4.7A). A treatment plan irradiating the target volume homogeneously with one field applying a prescribed 1.1-weighted dose of 60 Gy(RBE) and 2 Gy(RBE) per fraction was created. For this treatment plan, dirty dose distributions using different LET_{thres} values were scored and compared with the 1.1-weighted dose distribution, the LET_d distributions as well as the vRBE-weighted dose distribution using the Wedenberg RBE model [49] with $\alpha/\beta = 2$ Gy and the voxel-wise proton dose per fraction. For optimization and further analysis, a 5×5×2.5 cm^3 OAR was added adjacent to the target volume of the water phantom (Fig. 4.7C) assuming a tolerance dose of 54 Gy(RBE). This phantom consisting of one target volume and one OAR was then used to find suitable ranges for the parameters of the max dirty dose objective (LET_{thres} and the max dirty dose level) in which a reduction of the vRBE-weighted dose in the OAR was achieved while maintaining the 1.1-weighted dose distribution in the target volume. A treatment plan with two orthogonal proton fields using only standard 1.1-weighted dose objectives and fulfilling clinical goals for target coverage and OAR sparing was created and served as RefPlan. The two-step planning approach was used to create different DDopt treatment plans with different LET_{thres} and max dirty dose level combinations. In total, 28 DDopt plans were created using LET_{thres} values between 1 keV/µm and 4 keV/µm. With this analysis, suitable parameter ranges were identified and afterward applied for two cranial patient cases. To identify potential benefits and risks of the dirty dose optimization, the LET_d and the vRBE-weighted dose distribution using the Wedenberg RBE model [49] with $\alpha/\beta = 10$ Gy in the target volume and 2 Gy otherwise using the voxel-wise proton dose per fraction were calculated. The LET_d was defined as the dose-averaged LET considering all protons in the local medium normalized to unity density [111]. To analyze the influence of the number of fields on the resulting DDopt plans, different plans keeping the parameters of the max dirty dose objective constant (LET_{thres} = 2 keV/µm and max dirty dose level = 70% of DD_1 of the RefPlan) and changing the number of treatment fields using one (Fig. 4.7B), two (Fig. 4.7C) and three (Fig. 4.7D) treatment fields, were created.

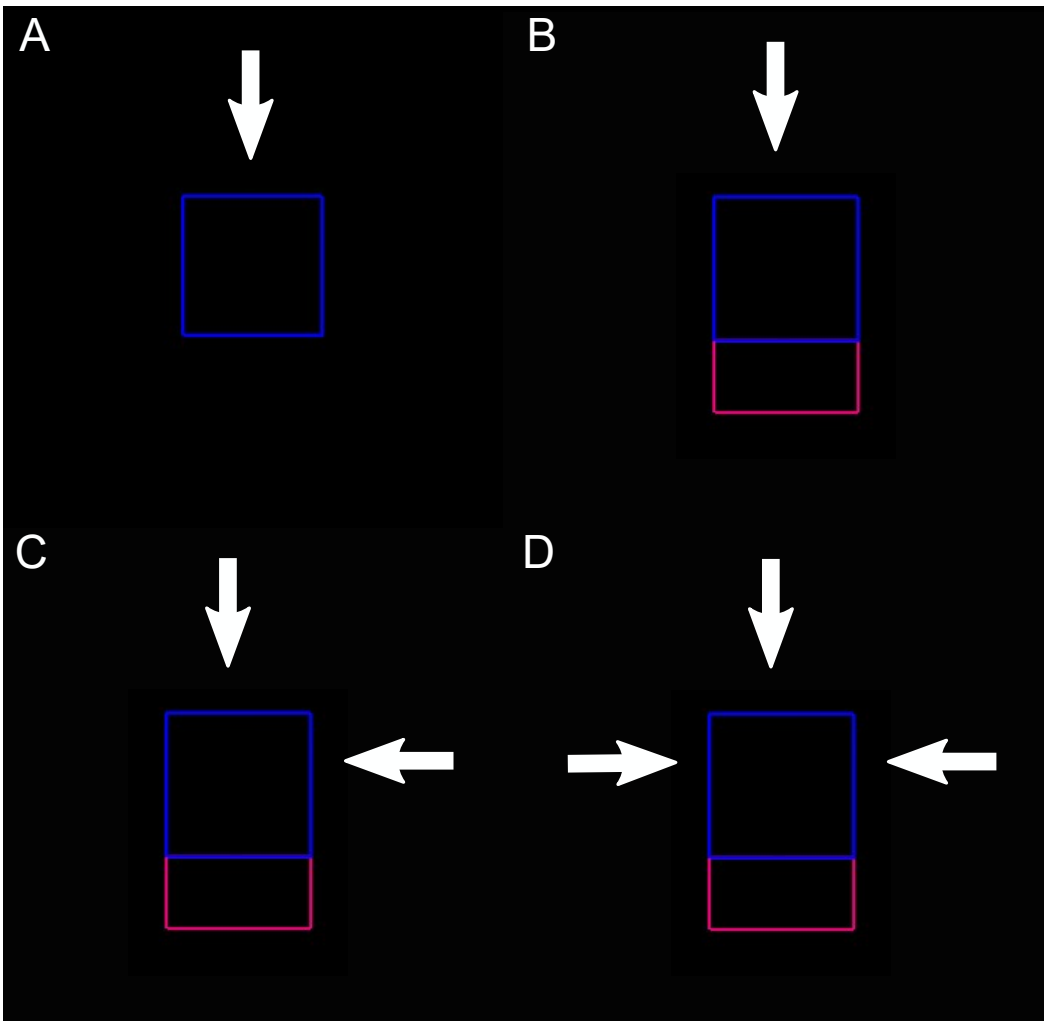

Figure 4.7: Computed tomography (CT) slices of the water phantom (25×25× cm^3) with target volume (blue, 5×5×5 cm^3) and organ at risk (magenta, 5×5×2.5 cm^3) used for visualization (A) and optimization (B,C,D) of dirty dose. The arrows indicate the beam orientations. The entire CT consists of water. Adapted from [101].

Two typical proton therapy patient cases were selected to analyze potential benefits and risks when applying dirty dose optimization. Both patients were cranial tumor patients enrolled in a prospective registry study ("ProReg", German Clinical Trial Register: DRKS00004384) covered by the ethics approval and had provided written informed consent. The first patient was diagnosed with a meningioma and prescribed a dose of 54 Gy(RBE) in 30 fractions. From hereafter this patient will be referred to as patient 1. The second patient, from hereafter called patient 2, was diagnosed with a chondrosarcoma receiving a prescribed dose of 69.3 Gy(RBE) to the smaller CTV2 and 54.45 Gy(RBE) to the CTV1 in 33 fractions using the simultaneous integrated boost strategy. For both patients, clinically acceptable multi-field optimized PTV-based treatment plans were created using IMPT and served as the RefPlan. These RefPlans only included objectives optimizing the 1.1-weighted dose and represented therefore the optimal 1.1-weighted dose distribution. The two-step planning approach was used to create the DDopt plans. For both patients, dose-limiting OARs near the target volume were the brainstem, the chiasm, and the right and left optical nerve. For each of these OARs, a MaxDirtyDose objective was added to the 1.1-weighted dose objectives of the RefPlan. The parameter combinations yielding the best results in the prior water phantom studies were used to create a set of different DDopt plans. A total of 18 DDopt plans, nine for each patient, were created using different LET_{thres} and max dirty dose level values. The max dirty dose level was, like in the water phantom studies, given relative to the DD_1 in the regarded OAR of the corresponding RefPlan. To evaluate the resulting DDopt plans, the 1.1-weighted dose distribution $D_{1.1}$, the LET_d distribution, and the vRBE-weighted dose distribution using the Wedenberg RBE model [49] D_{wed} were calculated. If not stated otherwise, when applying the Wedenberg RBE model, $\alpha/\beta = 10$ Gy was assumed for the target volume and $\alpha/\beta = 2$ Gy elsewhere as well as the voxel-wise proton dose per fraction. NTCP values based on $D_{1.1}$ ($NTCP_{1.1}$) and D_{wed} ($NTCP_{wed}$) were evaluated and analyzed. For NTCP calculation the relative seriality model for brainstem necrosis (model parameters: $s = 1$, $\gamma = 2.4$, $TD_{50} = 65.1$ Gy(RBE)) and blindness ($s = 1$, $\gamma = 2.5$, $TD_{50} = 65.0$ Gy(RBE)) were applied [73, 74]. To estimate the influence of the uncertainty in biological parameters, the $NTCP_{wed}$ calculations were repeated assuming $\alpha/\beta = 3$ Gy for healthy tissue including the critical OARs. The impact of the dirty dose optimization on the dose in the target volume was analyzed by evaluating the target dose coverage defined as the dose to 95% of the target volume D_{95}, the homogeneity index $HI = D_2/D_{98}$ as defined in the used TPS, with D_2 and D_{98} being the dose to 2% and 98% of the target volume, respectively, and the conformity index $CI = V_{95\%\text{-isodose}}/V_{\text{target volume}}$ as defined in the used TPS, with $V_{95\%\text{-isodose}}$ being the volume covered by the 95%-isodose and $V_{\text{target volume}}$ being the volume of the target volume. Higher values of HI and CI indicate better homogeneity and conformity, respectively. To compare the results of dirty dose optimization with other optimizing strategies LET-optimized

(LETopt) treatment plans reducing LET_d values in all critical OAR higher than 2.5 keV/µm in voxels receiving a dose of at least 40 Gy(RBE) were created. For all calculations, a dose and LET_d grid size of 2×2×2 mm^3 and a statistical Monte Carlo uncertainty of 0.5% was used.

4.2.2 Results

Water phantom study

The calculation of different dirty dose distributions with LET_{thres} values between 1 keV/µm and 5 keV/µm for an SOBP in the water phantom with one target volume using one treatment field showed a strong dependency of the dirty dose distribution on LET_{thres} (Fig. 4.8). For $LET_{thres} > 1$ keV/µm, the peak of the dirty dose distribution was located close to the peak of the D_{wed} distribution. Moreover, the smaller LET_{thres} the more the dirty dose distribution converged to the 1.1-weighted dose distribution.

The two-field reference plan for the water phantom with an OAR close to the target volume (Fig. 4.7C) showed increasing dirty dose at the distal edges of each beam leading to a maximum of the dirty dose distribution at the overlapping distal edges of both beams (Fig. 4.9). At the same time, this increase of the dirty dose led to a decrease of the clean dose at the distal edges of the fields. All DDopt plans showed a reduced near-maximum dose-averaged LET (LET_1) and Wedenberg dose $D_{wed,1}$ in the OAR compared to the RefPlan (Fig. 4.10). The achieved reduction depends on the chosen parameter combinations for the dirty dose optimization. For low LET_{thres} values of about 1 keV/µm, most dose contributions were considered as dirty and therefore got optimized when applying dirty dose optimization. Thus, the lower LET_{thres}, the more similar the dirty dose objective and the standard dose objective acted. This is, the lower LET_{thres}, the more the dirty dose optimization tended to optimize the absorbed dose (Fig. 4.10A) rather than the LET (Fig. 4.10C). For high LET_{thres} values only a small part of the dose was considered as dirty and therefore also considered during dirty dose optimization, which led to a smaller achieved reduction of $D_{wed,1}$ in the OAR. Moreover, some parameter combinations led to a slight increase of the 1.1-weighted dose in the OAR of maximal 0.1 Gy, even though a reduction of $D_{wed,1}$ was still achieved. Especially the parameter combinations achieving the highest reduction of $D_{wed,1}$ in the OAR led to a local increase of the absorbed dose of up to 25% compared to the RefPlan in areas outside of the OAR, where no dirty dose objective was applied (Fig. 4.11A,B). However, there was a range of parameter values (LET_{thres}: 2 keV/µm - 3.5 keV/µm, max dirty dose level: 60% - 70% of $DD_{1,RefPlan}$) for which a reduction of $D_{wed,1}$ was achieved without a relevant change of the 1.1-weighted dose distribution compared to the RefPlan (Fig. 4.11C, D). For these parameter combinations the reduction of $D_{wed,1}$

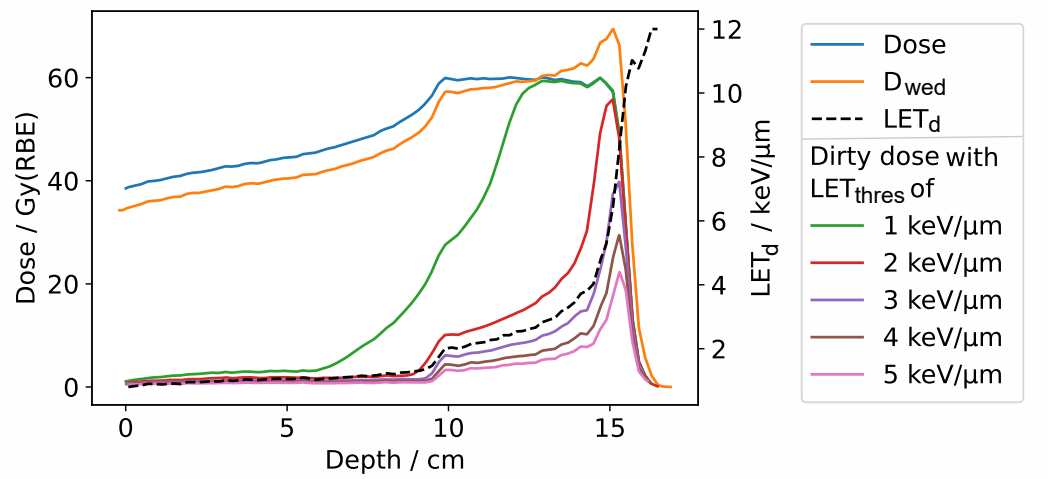

Figure 4.8: Line doses of the 1.1-weighted dose (Dose), Wedenberg dose (D_{wed}), and dirty dose distributions for different linear energy transfer threshold values (LET_{thres}) as well as dose-averaged LET_d in a clinical spread-out Bragg peak homogeneously irradiating a target volume in a water phantom (Fig. 4.7A). Adapted from [101].

was mainly achieved by changing the LET distribution in the OAR and not the 1.1-weighted dose.

When comparing the DDopt plans with different numbers of treatment fields (Fig. 4.7B,C,D), the amount of dose considered as dirty decreased with increasing number of treatment fields (Fig. 4.12). A reduction of DD_1 in the OAR of 11.1 Gy(RBE), 11.8 Gy(RBE), and 10.8 Gy(RBE) was achieved when using one, two, or three treatment fields, respectively. The dirty dose in normal tissue areas outside of the OAR was slightly increased by 0.2 Gy(RBE) and 1.3 Gy(RBE) for two and three treatment fields, respectively, when applying dirty dose optimization. In contrast, when using one treatment field, DD_1 was slightly decreased by 0.1 Gy(RBE) compared to the RefPlan. For this treatment plan, the reduction of DD_1 was achieved by redistributing the dirty dose within the OAR itself resulting in an increased mean dirty dose in the OAR by 4.7 Gy(RBE). For the other treatment plans, the mean dirty dose in the OAR was reduced by 1.2 Gy(RBE) and 1.8 Gy(RBE) for the two and three field treatment plans, respectively.

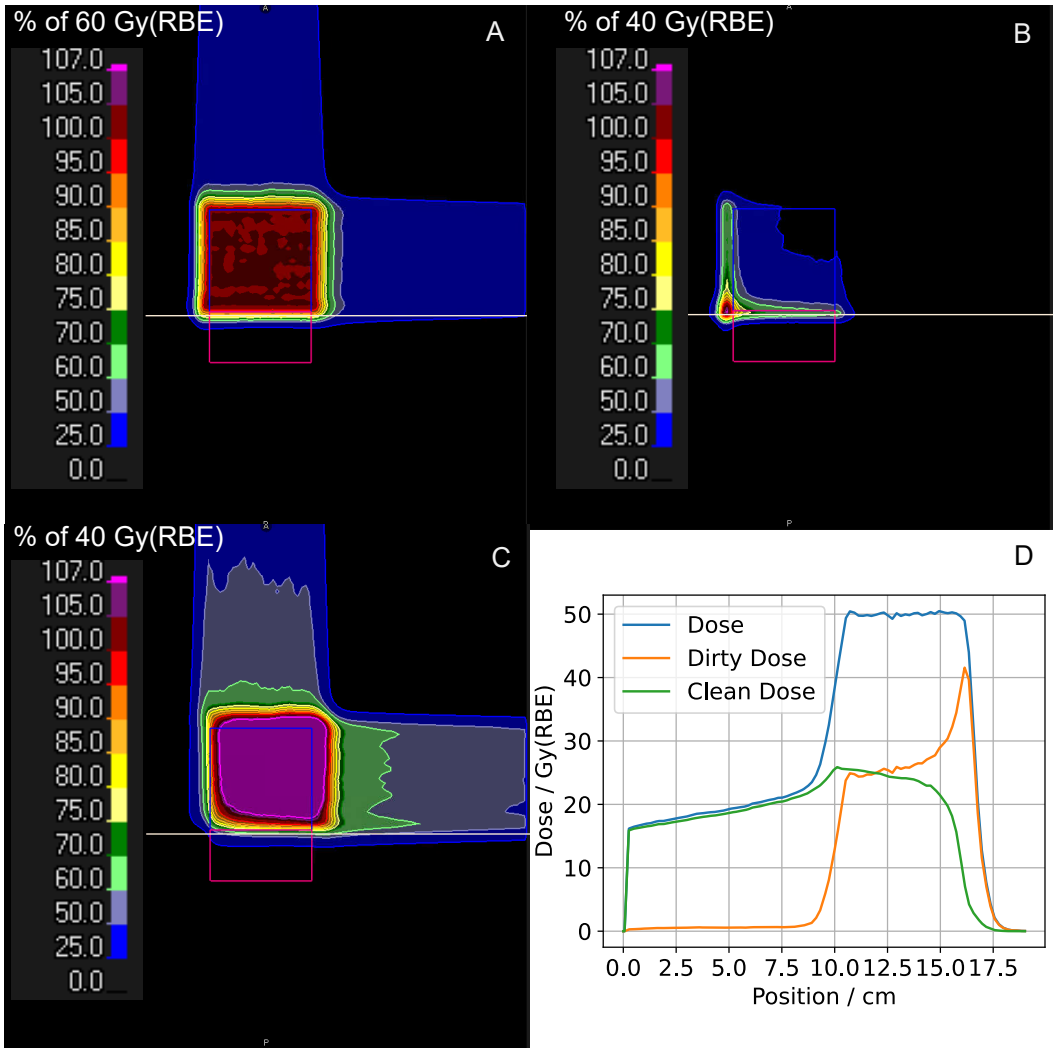

Figure 4.9: Representative computed tomography (CT) slice of the water phantom. The target volume is shown in blue and the organ at risk (OAR) in magenta. The 1.1-weighted dose distribution (A), the dirty dose distribution with a linear energy transfer threshold of 2.5 keV/µm (B), the clean dose (C) as well as corresponding line doses (D) along the horizontal grey line in the CT slice are shown [101].

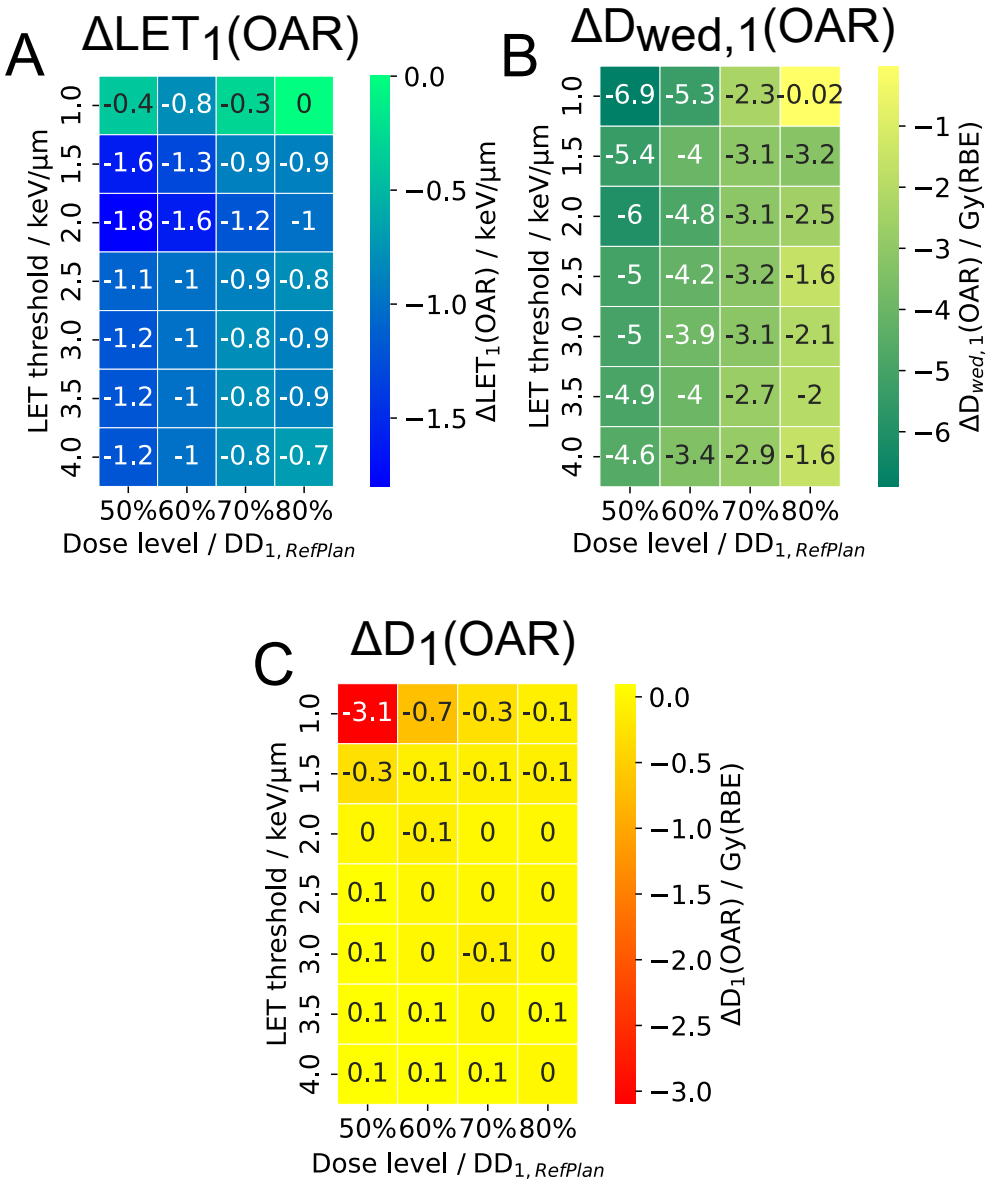

Figure 4.10: Differences in the near-maximum dose-averaged linear energy transfer LET_1 (A), variable relative biological effectiveness-weighted dose $D_{wed,1}$ (B) and 1.1-weighted dose D_1 in the OAR between the dirty dose optimized plans and the corresponding reference plan for different combinations of linear energy transfer (LET) threshold and max dirty dose level used for dirty dose (DD) plan optimization. Adapted from [101].

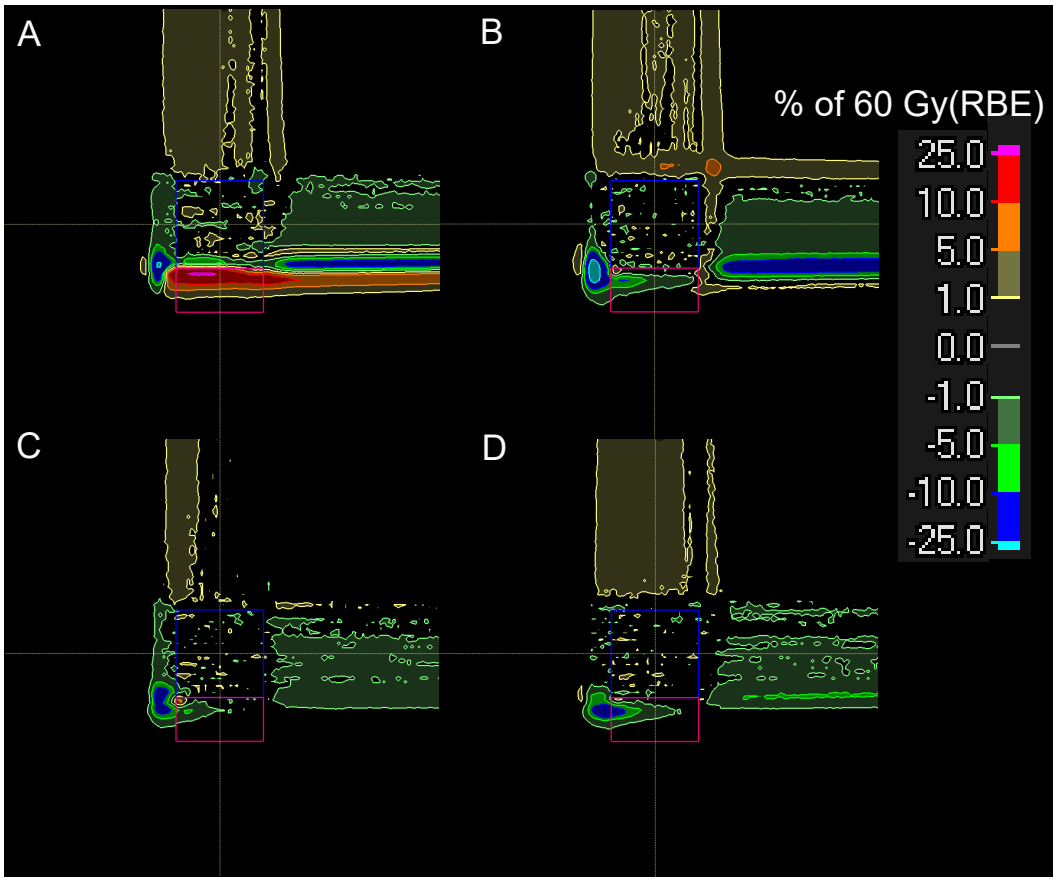

Figure 4.11: Differences in 1.1-weighted dose between the reference plan and four dirty dose (DD) optimized plans using different optimization parameter combinations (linear energy transfer threshold, max dirty dose level in the OAR relative to near maximum dirty dose DD_1 in the OAR of the reference plan). A: (1 keV/µm, 50%×DD_1); B: (2 keV/µm, 50%×DD_1); C: (2 keV/µm, 70%×DD_1); D: (2.5 keV/µm, 70%×DD_1). Contours of the target volume and the OAR in blue and magenta, respectively [101].

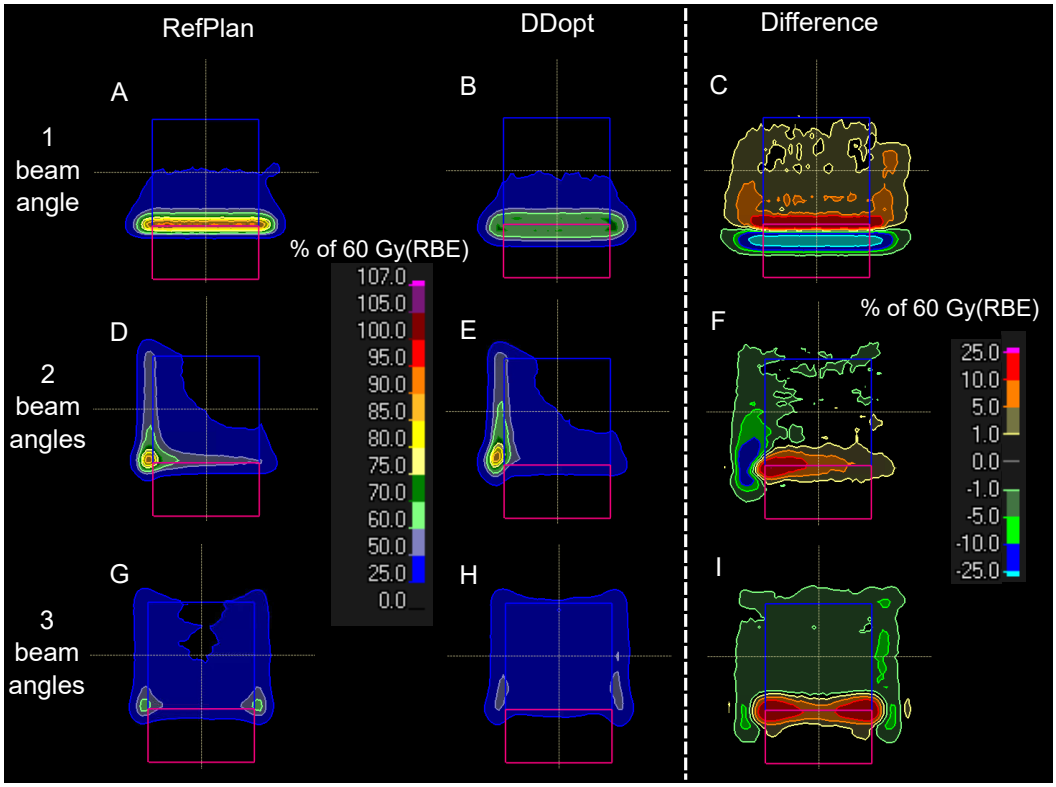

Figure 4.12: Dirty dose (DD) distributions for reference plans (RefPlan, A,D,G) and dirty dose optimized plans (DDopt, B,E,H) for one (A,B), two (D,E) and three (G,H) treatment fields as well as the difference between the DD of the RefPlans and the DDopt plans (C,F,I). The linear energy transfer threshold was set to 2 keV/µm and the max dirty dose level to 70% of the near-maximum dirty dose DD_1 of the RefPlan. Contours of the target volume and the OAR in blue and magenta, respectively [101].

In silico patient study

For the patient analysis, LET_{thres} values of 1.5 keV/µm, 2 keV/µm and 2.5 keV/µm were used together with max dirty dose level levels of 40%, 50% and 60% of the DD_1 in the OARs of the corresponding RefPlan. Scoring the dirty dose in addition to the 1.1-weighted dose took about 40% more computational time than scoring only the 1.1-weighted dose. Furthermore, the computational time for the optimization of DDopt plans was about 30% higher than for the RefPlans. All DDopt plans showed a decrease of the dirty dose while increasing the photon-like clean dose in the OAR (Fig. 4.13, 4.14). For all tested dirty dose optimization parameter combinations, lower LET_d values and therefore also lower $D_{wed,1}$ in critical OAR were achieved, while the D_1 of the 1.1-weighted dose in the OAR was slightly increased (Fig. 4.15). The only exceptions were the DDopt plans with the highest tested max dirty dose level (60% of the DD_1 of the corresponding RefPlan) of patient 2. For these plans, dirty dose optimization did not lead to a reduction of $D_{wed,1}$. The patient analysis showed a more pronounced dependency of the $D_{wed,1}$ reduction on the chosen max dirty dose level than on LET_{thres}.

When looking at the target volume, all DDopt plans showed the same HI and CI as the corresponding RefPlan. The mean difference (± standard deviation) of the D_{95} in CTV between the DDopt plans and the corresponding RefPlan was 0.04 (± 0.10) Gy(RBE), 0.06 (± 0.01) Gy(RBE) and 0.02 (± 0.37) Gy(RBE) for the CTV of patient 1, the CTV1 and CTV2 of patient 2, respectively. However, DDopt plans showed a slightly increased 1.1-weighted D_1 in the OAR (Fig. 4.15C, 4.15G) and D_{mean} in healthy brain tissue (Fig. 4.15D, 4.15H). The increase of D_1 in the OAR compared to the RefPlan was 0.47 (± 0.65) Gy(RBE) and 0.08 (± 0.28) Gy(RBE) for patient 1 and 2, respectively. This increase of the 1.1-weighted dose led to a maximum increase of the $NTCP_{1.1}$ of 1 pp. The averaged increase of D_{mean} in healthy brain tissue was 0.81 (± 0.21) Gy(RBE) and 0.53 (± 0.20) Gy(RBE) for patient 1 and 2, respectively.

When comparing dirty dose optimization with LET optimization, the LETopt plan showed an overall higher reduction in LET_d as well as D_{wed} in critical OAR, including the near-maximum values LET_1 and $D_{wed,1}$ for patient 1 (Fig. 4.16, Tab. 4.2). At the same time, LETopt showed a stronger influence on the dose distribution of the target volume than DDopt by decreasing the dose to 95% of the target volume, the HI, and the CI. Moreover, LETopt showed a higher increase in the mean dose to healthy brain tissue than DDopt for patient 1. For patient 2 comparable results between DDopt and LETopt were found for both, the dose in healthy tissue including the OARs as well as the dose in the target volume (Fig. 4.16, Tab. 4.3).

The achieved reduction of D_{wed} when using dirty dose optimization led to a reduced $NTCP_{wed}$ in all OAR compared to the corresponding RefPlan (Tab. 4.4). The

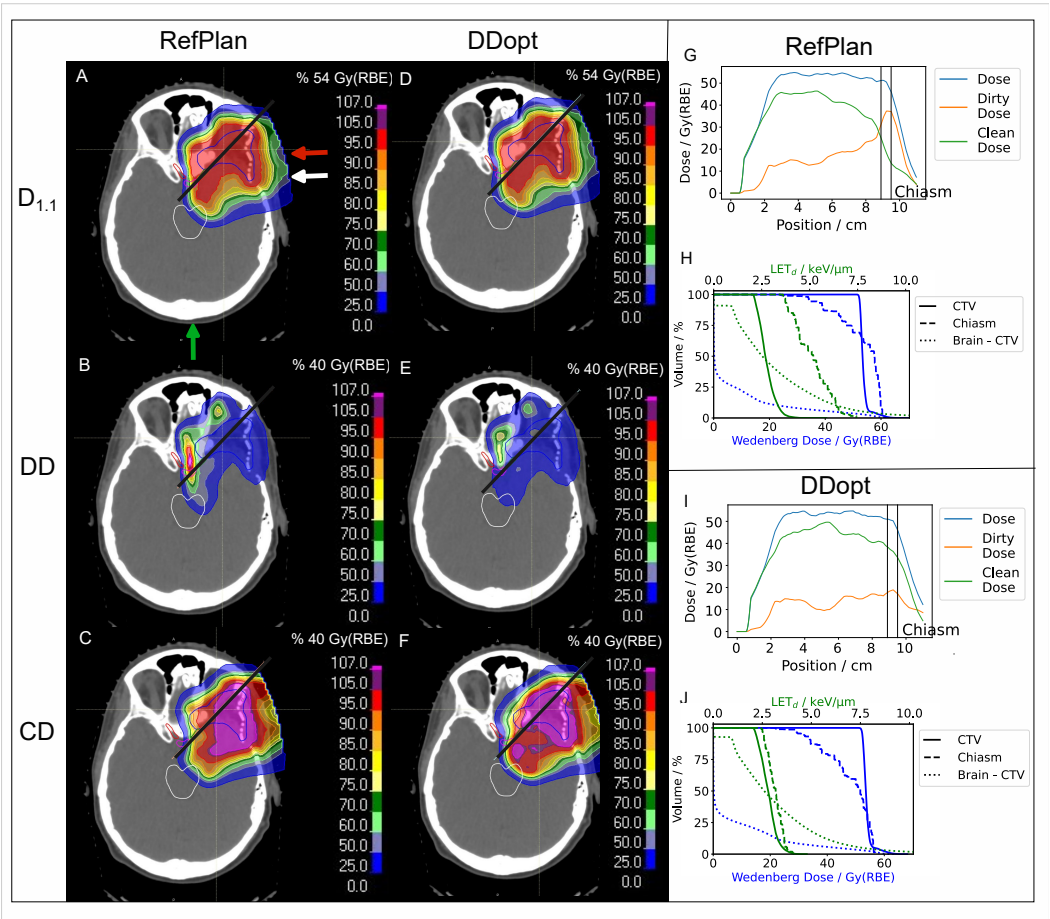

Figure 4.13: Representative computed tomography (CT) slice for patient 1 showing the clinical target volume CTV (blue), brainstem (white), chiasm (magenta), right (green) and left (red) optical nerve. The 1.1-weighted dose ($D_{1.1}$), dirty dose (DD), and clean dose (CD) for the reference plan RefPlan (A, B, C) and the dirty dose optimized plan DDopt (D, E, F) with linear energy transfer (LET) threshold = 2 keV/µm and max dirty dose level = 50% are shown. Corresponding line dose profiles (along the indicated straight black lines) for the RefPlan (G) and DDopt plan (I) as well as dose volume histograms (DVH) using the Wedenberg relative biological effectiveness model (blue) and LET volume histograms (green) for the reference plan (H) and the dirty dose optimized plan (J). Arrows indicate coplanar (white) and non-coplanar (red) beams as well as beams passing through the skull cap (green) [101].

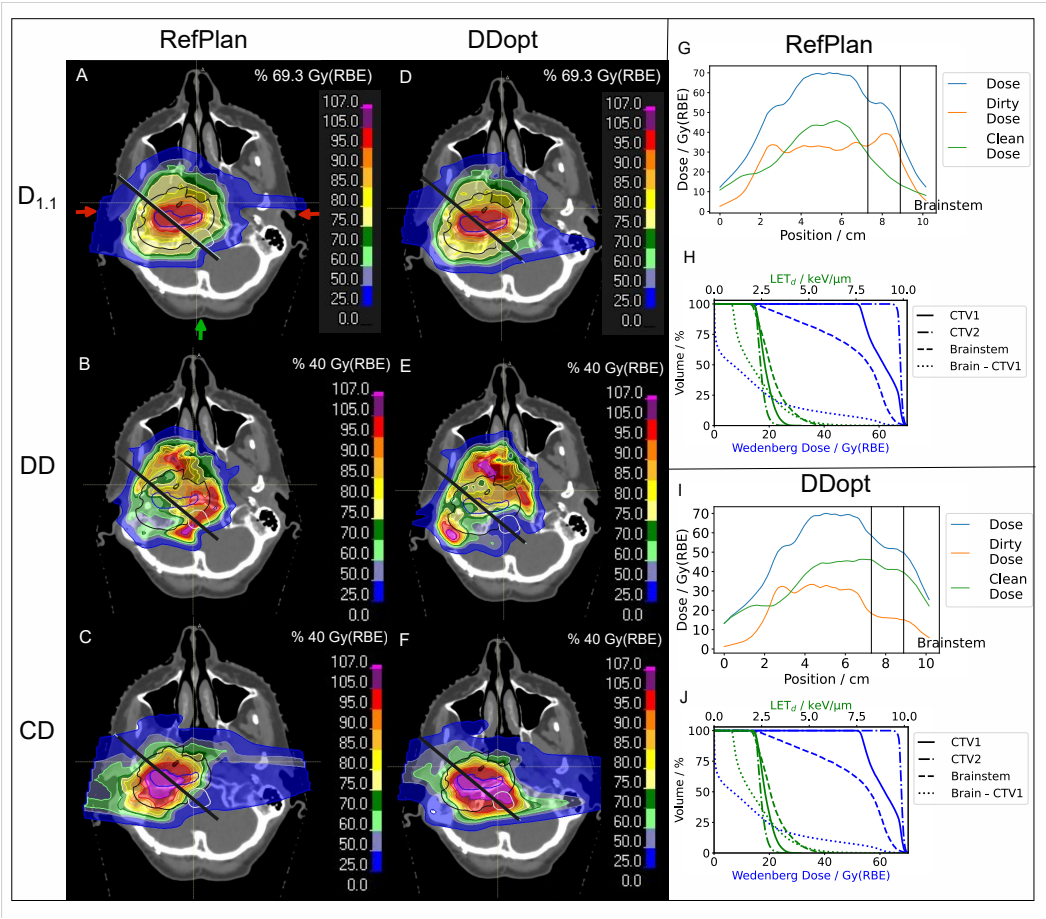

Figure 4.14: Representative computed tomography (CT) slice for patient 2 showing the clinical target volume CTV1 (blue), CTV2 (dark blue), and brainstem (white). The 1.1-weighted dose ($D_{1.1}$), dirty dose (DD), and clean dose (CD) for the reference plan RefPlan (A, B, C) and the dirty dose optimized plan DDopt (D, E, F) with linear energy transfer (LET) threshold = 2 keV/µm and max dirty dose level = 50% are shown. Corresponding line dose profiles (along the indicated straight black lines) for the RefPlan (G) and DDopt plan (I) as well as dose volume histograms (DVH) using the Wedenberg relative biological effectiveness model (blue) and LET volume histograms (green) for the reference plan (H) and the dirty dose optimized plan (J). Arrows indicate coplanar (white) and non-coplanar (red) beams as well as beams passing through the skull cap (green) [101]

.

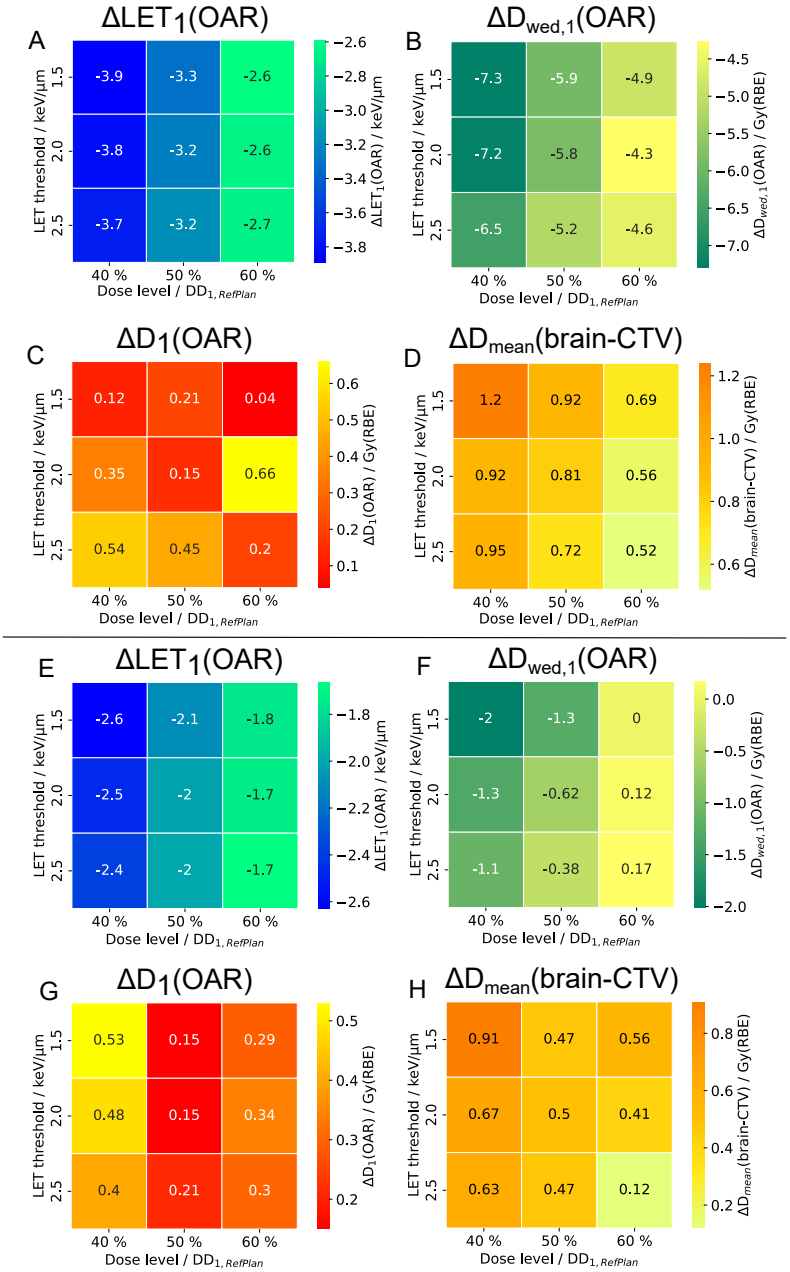

Figure 4.15: Differences between each dirty dose optimized plan and the corresponding reference plan for patient 1 in the chiasm (A-D) and patient 2 in the brainstem (E-F): near-maximum dose-averaged linear energy transfer (LET), $LET_{d,1}$ (A), near-maximum variable relative biological effectiveness (RBE)-weighted dose using the Wedenberg RBE model, $D_{wed,1}$ (B), near-maximum absorbed dose, D_1, (C). Differences in mean dose in the healthy brain tissue, D_{mean} (D) [101].

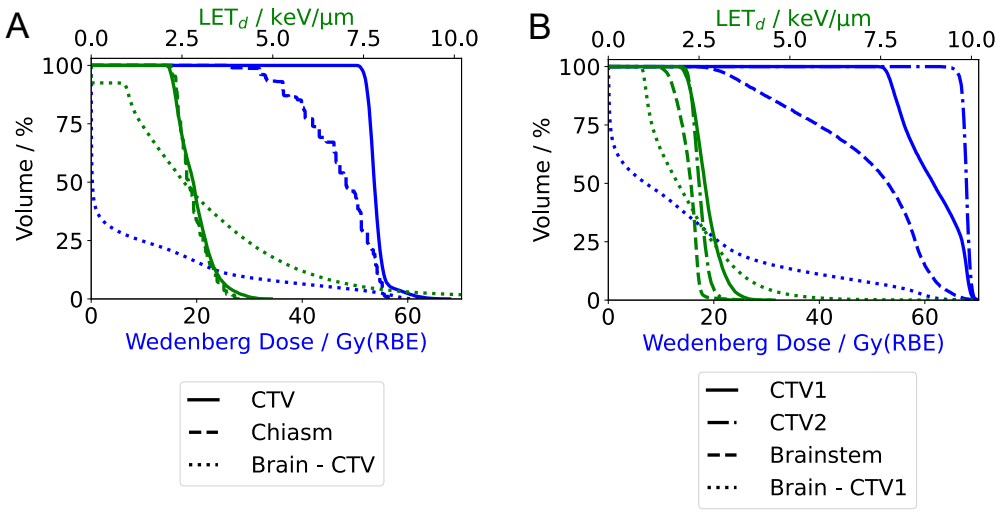

Figure 4.16: Dose volume histogram using the Wedenberg relative biological effectiveness model (blue) and linear energy transfer (LET) volume histogram (green) for the LET optimized treatment plans for patient 1 (A) and patient 2 (B) [101].

Table 4.2: Dose to 1% of the chiasm using the Wedenberg relative biological effectiveness model ($D_{wed,1}$), linear energy transfer (LET) to 1% of the chiasm (LET_1), 1.1-weighted dose to 95% (D_{95}) of the clinical target volume (CTV), homogeneity index (HI), conformity index (CI) and mean dose to the healthy brain tissue (D_{mean}) for the reference plan (RefPlan), the dirty dose optimized plans (DDopt) and the LET optimized plan of patient 1. For DDopt mean values (±standard deviation) over all DDopt plans are given.

Parameter	**RefPlan**	**DDopt**	**LETopt**
$D_{wed,1}$ (chiasm) / Gy(RBE)	58.46	56.98 (±1.05)	51.71
LET_1 (chiasm)/ keV/µm	7.80	4.06 (±0.49)	2.46
D_{95} (CTV) / Gy(RBE)	53.08	53.04 (±0.10)	52.64
HI (CTV)	0.92	0.92 (±0.01)	0.89
CI (CTV)	0.97	0.97 (±0.01)	0.93
D_{mean} (Brain-CTV) / Gy(RBE)	5.84	6.65 (±0.21)	7.05

variation of α/β from 2 Gy to 3 Gy led to a smaller $\Delta\text{NTCP}_{\text{wed}} = \text{NTCP}_{\text{wed}}(\alpha/\beta = 2Gy) - \text{NTCP}_{\text{wed}}(\alpha/\beta = 3Gy)$ for all DDopt plans compared to the RefPlan. For all DDopt plans and averaged over all considered critical OARs, a mean $\Delta\text{NTCP}_{\text{wed}}$ of 2 ($\pm$ 2) pp and 2 ($\pm$ 1) was found for patient 1 and patient 2, respectively. The corresponding values were 5 ($\pm$ 3) pp and 5 ($\pm$ 2) for the RefPlan of patient 1 and 2, respectively. When looking at the relative changes of NTCP_{wed} defined as $\Delta\text{NTCP}_{\text{wed}}/\text{NTCP}_{\text{wed}}(\alpha/\beta = 2Gy)$ and averaged over all OARs with $\text{NTCP}_{\text{wed}}(\alpha/\beta = 2Gy) > 0$ values of 0.5 and 0.3 were found for patient 1 and patient 2, respectively (Tab. 4.4).

Table 4.3: Dose to 1% of the brainstem using the Wedenberg relative biological effectiveness model ($D_{wed,1}$), linear energy transfer (LET) to 1% of the brainstem (LET_1), 1.1-weighted dose to 95% (D_{95}) of the clinical target volume (CTV), homogeneity index (HI), conformity index (CI) and mean dose to the healthy brain tissue (D_{mean}) for the reference plan (RefPlan), the dirty dose optimized plans (DDopt) and the LET optimized plan of patient 2. For DDopt mean values (±standard deviation) over all DDopt plans are given.

Parameter	**RefPlan**	**DDopt**	**LETopt**
$D_{wed,1}$ (brainstem) / Gy(RBE)	68.15	67.43 (±0.72)	67.05
LET_1 (brainstem)/ keV/µm	5.44	3.35 (±0.33)	2.83
D_{95} (CTV1) / Gy(RBE)	53.89	53.95 (±0.01)	53.9
D_{95} (CTV2) / Gy(RBE)	68.17	68.19 (±0.37)	68.12
HI (CTV2)	0.85	0.85 (±0.00)	0.85
CI (CTV2)	0.98	0.98 (±0.00)	0.98
D_{mean} (Brain-CTV) / Gy(RBE)	11.98	12.51 (±0.20)	12.6

Table 4.4: Normal tissue complication probability values resulting from the variable relative biological effectiveness (RBE)-weighted dose distribution using the Wedenberg RBE model $NTCP_{wed}$ for the reference plan (RefPlan) and dirty dose optimized plans (DDopt). For DDopt, the mean $NTCP_{wed}$ and standard deviation for all considered dirty dose optimization parameter combinations are shown. [101].

Organ at risk	**α/β**	**Patient 1**		**Patient 2**	
	in Gy	**RefPlan**	**DDopt**	**RefPlan**	**DDopt**
Brainstem	2	1%	0% ± 0%	17%	11% ± 2%
	3	0%	0% ± 0%	12%	8% ± 1%
Chiasm	2	20%	4% ± 2%	18%	6% ± 1%
	3	12%	2% ± 2%	13%	5% ± 1%
Right optical nerve	2	0%	0% ± 0%	18%	7% ± 2%
	3	0%	0% ± 0%	12%	5% ± 1%
Left optical nerve	2	27%	12% ± 3%	6%	2% ± 2%
	3	18%	8% ± 5%	4%	1% ± 1%

4.2.3 Discussion

The dirty & clean dose concept represents a novel tool to visualize and optimize vRBE-related quantities and is an innovative concept to account for the uncertainties introduced by the variability of the RBE. The basic idea is to divide the 1.1-weighted proton dose distribution into a clean dose and a dirty dose fraction based on the individual LET value of each proton and therefore without any averaging of the LET. The clean dose part is expected to have a biological dose-response similar to that of photons, while the biological response of the dirty part of the dose is expected to be non-photon-like. Thus, the uncertainties introduced by the use of a constant RBE together with tolerance doses based on photon data might be highest for the dirty part of the dose. With the dirty & clean dose concept a targeted optimization of the dirty dose is possible leading to treatment plans with a more photon-like dose response and making the use and photon-based tolerance doses for OAR more feasible.

When applying the dirty & clean dose concept, two parameters, namely the LET threshold and the dirty dose level, are needed for optimization. Following from the definition of the dirty dose, for low LET threshold values almost the whole dose was considered dirty. Therefore, the lower the LET threshold the more similar the dirty dose objective acts to a standard 1.1-weighted dose objective in plan optimization. On the other hand, the higher the LET threshold value the smaller the part of the dose considered during optimization. Thus, for too high LET threshold values nearly no influence on the resulting plan compared to the RefPlan was observed. Accordingly, the LET threshold determines to which extent the dose or the LET distribution gets optimized to achieve the desired dirty dose reduction. Since the biological dose is defined as the product of RBE and dose, a reduction of the biological dose can be achieved by either redistributing high LET-values and therefore reducing the RBE or by reducing the absorbed dose itself. With its two free parameters, the dirty & clean dose concept introduces an additional degree of freedom during optimization allowing for indirectly choosing between either redistributing more the dose or the LET.

Probably the best approach to determine suitable optimization parameters would be the analysis of correlations between toxicities and the corresponding dirty dose level and LET threshold values. Since these data are missing so far, maintaining the 1.1-weighted dose in the target volume while optimizing vRBE-related quantities in OARs in a two-step planning approach, as applied here, appears to be a practical alternative, which is also in line with current guidelines [106] as well as current research works on the optimization of vRBE-related quantities [22, 107–109]. This approach also corresponds to the current strategy in European proton therapy centers, since the majority of centers participating in the survey were considering RBE uncertainties only for critical OAR and not for the target volume. No relevant

effects on target dose coverage, homogeneity, and conformity were observed for any of the tested combinations of $\mathrm{LET}_{\mathrm{thres}}$ and max dirty dose level, while at the same time the dirty dose and therefore also D_{wed}, LET, and $\mathrm{NTCP}_{\mathrm{wed}}$ were reduced in critical OARs. Thus, the dirty & clean dose concept represents a practical approach allowing for reducing vRBE-related uncertainties while maintaining the 1.1-weighted dose distribution in the target volume and therefore ensuring tumor control.

The most pronounced reductions of D_{wed} in the OAR were found for $\mathrm{LET}_{\mathrm{thres}}$ values between 1.5 keV/µm and 2.5 keV/µm based on the parameter variation performed in the water phantom. Different studies [18, 21, 22, 112–114] analyzed the occurrence of unexpected side effects after proton therapy and found radiation-induced image changes to occur especially in voxels with a mean dose- or track-averaged LET higher than 2.5 keV/µm. Moreover, using the Wedenberg RBE model and assuming an α/β of 2 Gy, a dose per fraction of 2 Gy, and an LET of 1.5 keV/µm leads to an RBE of 1.1. Therefore, the parameter value range found in the water phantom study appears reasonable and compatible with different studies analyzing the occurrence of side effects after proton therapy as well as with calculated LET values resulting in an RBE of 1.1 as assumed in clinical practice.

The dirty & clean dose concept enabled more beneficial treatment plans in terms of D_{wed}. Most DDopt plans reduced $\mathrm{LET}_{\mathrm{d}}$ as well as D_{wed} in critical OARs resulting in lower $\mathrm{NTCP}_{\mathrm{wed}}$ values by reducing the number of high LET protons in the OARs. Furthermore, D_{wed} and $\mathrm{NTCP}_{\mathrm{wed}}$ of the DDopt plans showed a lower dependency on variations in the biological parameter α/β compared with the corresponding RefPlan, especially when looking at the absolute changes in $\mathrm{NTCP}_{\mathrm{wed}}$. The uncertainty in α/β is usually considered as a major source of uncertainty when calculating the vRBE-weighted dose [115, 116]. Therefore a smaller dependency on this parameter might be of particular relevance. The decreased dependency can be explained by the definition of the RBE in the Wedenberg model. The term depending on α/β is multiplied with $\mathrm{LET}_{\mathrm{d}}$ and the product decreases when DDopt reduces $\mathrm{LET}_{\mathrm{d}}$ in the OARs. Therefore, uncertainties in α/β introduce less effect on the vRBE and thus the $\mathrm{NTCP}_{\mathrm{wed}}$ in the DDopt plans.

Dirty dose optimization also comes with some risks. DDopt plans showed a higher absorbed 1.1-weighted dose in surrounding healthy tissue, where no dirty dose objective was applied, as well as a small increase of the near-maximum 1.1 weighted dose in the OARs which translated in a small $\mathrm{NTCP}_{1.1}$ increase by a maximum of 1 pp. However, clinically used tolerance doses of the 1.1-weighted dose for the OARs were never exceeded, and the resulting vRBE-weighted dose as well as $\mathrm{NTCP}_{\mathrm{wed}}$ were still reduced. This might be due to the two-step planning approach used here. Because of this approach, the standard max dose objective restricting the maximum 1.1-weighted dose in the OARs is also valid and maintained for the DDopt plans, preventing the 1.1-weighted dose from exceeding clinically used tolerance values.

A direct comparison between the DDopt and LETopt plans created in this thesis

showed a slightly higher reduction of near-maximum $D_{\mathrm{wed},1}$ in the OARs for patient 1 when using LETopt, while at the same time, LETopt reduced the dose coverage, homogeneity, and conformity of the target volume, which can lead to a reduced tumor control and contradicts current guidelines [106]. A prevention of dose changes in the target volume might be achieved by adjusting the objectives used in the LETopt plan, but this might, at the same time, reduce the achieved reduction in $D_{\mathrm{wed},1}$ and therefore might lead to comparable results between DDopt and LETopt, as found for patient 2. Therefore, when ensuring target dose coverage, the achieved benefits of DDopt and LETopt in terms of vRBE-weighted dose seem to be comparable. However, with LETopt, greater care must be taken to ensure tumor control. Since nearly no influence on the dose in the target volume was found by all tested dirty dose optimization parameter combinations, dirty dose appears less likely to result in target volume dose changes compared to the optimization of $\mathrm{LET_d}$.

The survey showed, that the most commonly treated entities for proton irradiation are cranial tumors. Therefore, here typical cranial tumor cases were used to confirm the basic findings of the water phantom studies. Because of the geometrical and anatomical conditions, irradiating cranial tumors might result in especially high RBE uncertainties in normal tissue [117, 118]. Thus, most clinical evidence for a variable RBE exists for these entities and cranial tumor patients might benefit most from the novel dirty & clean dose concept. Therefore, two different cranial patient cases with different prescribed doses to evaluate the feasibility of the concept for different dose regimes were analyzed. In silico patient studies with larger patient cohorts including other treatment sites, might be performed in the future to further confirm the obtained results in a more general way.

Most analyses of biological and clinical outcome data are based on averaged LET values [17–19, 52], although voxel-wise averaging the LET might introduce uncertainties [53]. Currently, the number of microdosimetry studies analyzing LET spectra and LET values of individual protons is increasing [51, 53, 119, 120] and novel techniques for calculating LET spectra and individual LET values were developed [121, 122]. Nevertheless, biological analysis and correlations between clinical outcome data and LET spectra or other microdosimetric quantities are still lacking. Therefore, here dose-averaged LET as well as vRBE-weighted dose values using the Wedenberg RBE model were calculated and analyzed to assess the benefits and risks of the dirty & clean dose concept. This allows for a comparison with other strategies optimizing RBE-related quantities [123–127], e.g., the optimization of the dose- or track-averaged LET, the track-end distribution optimizing the position of the stopping protons, the product of dose times averaged LET and a direct optimization of the vRBE-weighted dose using different RBE models. Some publications evaluated the same quantities as in the in silico patient study in this thesis, which allows for a direct comparison between the achieved results.

For example, the optimization of the vRBE-weighted dose using two different

RBE models [21,16] for an exemplary brain tumor case resulted in a reduction of about 3% of the maximum vRBE-weighted dose compared to a reference plan [127]. With dirty dose optimization, a reduction of the near-maximum Wedenberg dose of up to 11% was achieved. In contrast to the dirty & and clean dose concept, when applying a direct vRBE-weighted dose optimization approach, the choice of the RBE model is crucial. There are many different RBE models [49–51, 109, 128–132], most of them based on in vitro measurements. So far, most RBE calculations applying these models are only performed for research purposes, as stated by most centers in the questionnaire on the clinical consideration of the proton RBE. A clinically accepted RBE model for the use in treatment planning is still lacking. Moreover, all RBE models include biological parameters like α/β. These biological parameters usually have large uncertainties in a clinical environment. The dirty dose distribution, as well as the clean dose distribution, are each just another dose distribution and allow therefore the consideration of RBE uncertainties by optimizing purely physical parameters. Moreover, DDopt plans were found to be more robust against uncertainties in α/β than the corresponding RefPlan.

The optimization of the track-end distribution led to a reduced $\mathrm{NTCP}_{\mathrm{wed}}$ of up to 19 pp [123], which is in line with the achieved results when using dirty dose optimization. When applying different strategies to optimize the dose-averaged LET, a maximal reduction of the maximum $\mathrm{LET}_{\mathrm{d}}$ of up to approximately 2 keV/µm was achieved [125], while with dirty dose optimization a reduction of up to 4 keV/µm depending on the chosen optimization parameters was found. Strategies optimizing LET-related quantities usually optimize the dose- or track-averaged LET, which introduces ambiguities since different LET spectra in a voxel might lead to different biological effects, even though the averaged LET value is the same. Whether these uncertainties are of clinical relevance, is currently under debate, since some studies did not find a significant difference in RBE values based on averaged and not-averaged LET values [133], while others found the use of the individual LET value beneficial [53]. With the dirty & clean dose concept no averaging of the LET is necessary, instead, the individual LET value of each proton determines whether the dose contribution of this proton is considered as dirty or clean. Using the product of dose times $\mathrm{LET}_{\mathrm{d}}$ to account for RBE uncertainties tends to overestimate the influence of the $\mathrm{LET}_{\mathrm{d}}$, since both quantities are included equally in the optimization and therefore have the same effect on the optimization results. In contrast, the two different free parameters of the dirty & clean dose concept allow for indirectly influencing in which ratio dose and LET are considered in the optimization.

Hahn et al [134] recently published a comparison between different strategies, including the optimization of the vRBE-weighted dose, the track-end distribution, the $\mathrm{LET}_{\mathrm{d}}$ and the dirty dose, and showed a reduction of the vRBE-weighted dose in critical OARs while maintaining plan quality in terms of 1.1-weighted dose with all four tested strategies. The choice of only a single dose level and LET threshold value

during treatment planning was considered as the limiting factor to fully exploit the potential of dirty dose optimization. In contrast, the in silico analysis performed in this thesis systematically tested different parameter combinations. In this way, the range of suitable optimization parameters could be narrowed down to approximately 1.5 keV/µm to 2.5 keV/µm for the LET threshold and 40% to 60% of the DD_1 in the OAR of the corresponding RefPlan for the max dirty dose level. For these parameter combinations, the DDopt plans were found to be beneficial in terms of vRBE-weighted dose, while maintaining target dose distribution and at the same time being robust against changes in the optimization parameters. Therefore, these parameter combinations can be considered as a suitable choice. The study by Hahn et al used a parameter combination in this suitable range to create one dirty dose-optimized plan for each of the ten analyzed cranial patient cases. Therefore, the results of the in silico patient study obtained in this thesis are expected to also hold for a larger patient cohort.

In the current implementation, the separation of the 1.1-weighted dose in a clean and a dirty part is performed for primary and secondary protons. Since the uncertainties in the calculation of LET spectra of heavier secondary particles is currently under investigation, dose contributions of heavier particles are considered as clean dose at the moment. For the clinically used proton energy range, interactions creating heavy charged particles are rare. Therefore, only a small amount of the proton energy is deposited by heavy charged particles. In a future implementation, the separation in clean and dirty dose will be performed for all particles, which might further improve the achievable optimization results when applying the dirty & clean dose concept.

When creating the DDopt plans, all plan parameters of the RefPlan, including the optimization weights of the different objectives, were kept the same. For the newly added MaxDirtyDose objective, a weight of about 10% of the weight of the standard dose objectives used for OAR sparing was applied. With the development and implementation of multi-criteria optimization tools, a better understanding of the influence of individual weights might be possible in the future. Moreover, adding other clean or dirty dose-related objectives, e.g., different dirty dose volume histogram parameters or the mean dirty dose in an OAR, might further improve the achievable optimization results and might lead to treatment plans with an even more photon-like dose response in critical structures. Furthermore, the comparison between different numbers of treatment fields showed a redistribution of the stopping protons to normal tissue outside of the OAR to achieve the reduction of the dirty dose inside of the OAR, which was also found for other optimization strategies [123]. To limit the amount of dirty dose in healthy tissue, dirty and clean dose-related objectives for the normal tissue outside of the OAR could be included in future studies. Since the dirty & clean dose concept represents the optimization of just another dose distribution, this concept allows for the implementation of all objectives

used for standard 1.1-weighted dose optimization, as well as robust optimization and robustness analysis as performed for the 1.1-weighted dose distribution.

4.3 Conclusion

To gain deeper insight into the current clinical practice regarding the consideration of the relative biological effectiveness (RBE), a survey among all proton therapy centers in Europe was performed. Initial measures to counteract possible adverse effects of a variable RBE (vRBE), especially the arrangement of treatment fields, are already used by all European proton therapy centers while following current guidelines on prescribing a constant RBE. However, to change current guidelines in the future, centers call for more clinical data in the form of retrospective and prospective studies correlating clinical outcome with vRBE-related quantities. Enabling proton therapy centers to calculate and optimize these vRBE-related quantities in their clinical setting is considered the next crucial step.

Therefore, the dirty & clean dose concept, which separates the 1.1-weighted proton dose in a clean dose with a photon-like dose response and a dirty dose with a non-photon-like dose response, was introduced. The concept allows for the visualization and targeted optimization of the dirty part of the dose, which is associated with high RBE uncertainties. The biological effect of dirty dose optimized treatment plans is expected to be more similar to photon treatment plans and fewer uncertainties are introduced when applying dose threshold values for OAR sparing based on photon data. Thus, current clinical practice of prescribing a constant RBE, as done by all European proton therapy centers, might introduce fewer uncertainties for dirty dose-optimized treatment plans. Moreover, the novel concept was implemented into the research version of a clinical TPS allowing for future use in a clinical environment during treatment planning and therefore marking an important step towards novel and improved guidelines.

5 Summary and Conclusion

A precise estimate of the actual applied effective dose is crucial for optimally treating patients. However, different aspects of the planning and irradiation process, especially for specialized radiotherapy treatments, can make this precise knowledge of the actual applied effective dose difficult. For example, for some total body irradiation (TBI) techniques, no computed tomography (CT)-based dose calculations are performed, instead, the dose is calculated at individual dose reference points (usually 12) along the patient and these dose values are then used to describe the dose distribution in the entire body. Therefore, information about the exact applied 3D dose distribution is lacking. For proton therapy, a constant relative biological effectiveness (RBE) is applied clinically leading to uncertainties in the biological effective dose especially at the distal edge of a spread-out Bragg peak (SOBP) since the RBE is not constant but varies along the proton track. For both, TBI and RBE consideration in proton therapy, first a survey was performed providing detailed insight into the current clinical practice and future requirements for each topic. Based on the results of these surveys and the stated future requirements of the centers, novel workflows and concepts were introduced and used to create precise dose estimations of the applied effective dose in the patient.

For TBI, the survey showed that irradiation techniques that do not use 3D dose distributions are still most common in Germany. Moreover, a high heterogeneity in almost every aspect of the treatment process was found, caused by the lack of standardization. Thus, most centers considered performing retrospective analyses correlating 3D dose distributions of different techniques with clinical outcome data as the next important step towards standardization. Therefore, a novel Monte Carlo-based simulation workflow was developed and introduced in this thesis for creating 3D dose distributions for both most commonly used TBI techniques, the translational couch, and the extended source-to-surface-distance (SSD) technique. This workflow was then used for the validation of the beam-zone method, i.e., the treatment planning method used for dose calculation in individual dose reference points when applying the translational couch technique. Moreover, the novel workflow was used for a dosimetrical comparison of the dose distributions when performing the translational couch and extended SSD technique with helical tomotherapy for an exemplary patient case. The validation of the beam-zone method showed an overall sufficient agreement between the calculated and simulated dose values in the dose reference points considering clinically acceptable deviations ($\pm 10\%$). However, because of the dose inhomogeneities introduced by the use of lung blocks for dose

reduction, one individual dose point was, depending on the dose regime, not sufficient to characterize the dose in the corresponding anatomical region (sternum region) underlying the need for 3D dose calculation. The comparison between different TBI techniques also showed the highest dose deviations in the tissue surrounding the lung depending on whether a reduction of the lung dose is possible with or without additional shielding material. The use of helical tomotherapy led to an overall higher dose coverage and homogeneity, especially in the sternum region. To what extent this deviation in dose between techniques is of clinical relevance, is so far unknown due to the lack of studies comparing clinical outcome data of different TBI techniques. The novel simulation workflow introduced here allows for performing retrospective patient studies correlating 3D dose distributions with clinical outcome data, which was considered an important next step towards standardizing TBI in the corresponding survey.

The questionnaire regarding the RBE consideration in proton therapy showed that all centers in Europe were prescribing a constant RBE. However, at the same time, all centers were aware of the introduced uncertainties and were therefore applying some measures to counteract potential adverse effects. Most centers stated to not have the technical requirements to visualize or even optimize variable RBE-related quantities, which was considered the next important step towards formulating novel guidelines regarding the clinical use of RBE. Therefore, the novel dirty & clean dose concept was introduced in this thesis. This concept allows for the visualization and targeted optimization of the part of the dose having the highest uncertainties due to a variable RBE. This novel concept was used to create dirty dose optimized treatment plans by adding an additional dirty dose objective for all critical organs at risk (OAR) to the standard dose objectives of a reference plan for two exemplary patient cases. All dirty dose-optimized treatment plans showed a reduction of the variable RBE-weighted dose as well as the linear energy transfer (LET) in critical OARs, while at the same time maintaining dose coverage, homogeneity, and conformity of the target volume. Therefore, the novel dirty & clean dose concept allows to account for RBE uncertainties without compromising tumor control. The dirty & clean dose concept was implemented in a research version of a clinical treatment planning system (TPS) to enable future applications in clinical environments and thus the realization of retrospective and prospective patient studies, which was considered to be an important next step in the formulation of novel guidelines in the corresponding survey.

In conclusion, the conducted surveys in this thesis showed the urgent need for novel concepts and workflows to decrease the uncertainties in the applied effective dose in order to perform the next important steps towards new and improved guidelines for both, TBI and proton therapy. Potential tools allowing to decrease these uncertainties were introduced in this thesis and their efficiency was confirmed by performing different in silico patient studies. These tools now enable the realization

of important retrospective and prospective patient studies correlating the achieved clinical outcome with a precise estimate of the applied effective dose. The results of such studies are urgently needed to formulate novel guidelines and thus making the treatment of patients even more precise and safe in the future.

A Appendix

Questionnaire: RBE consideration in proton therapy

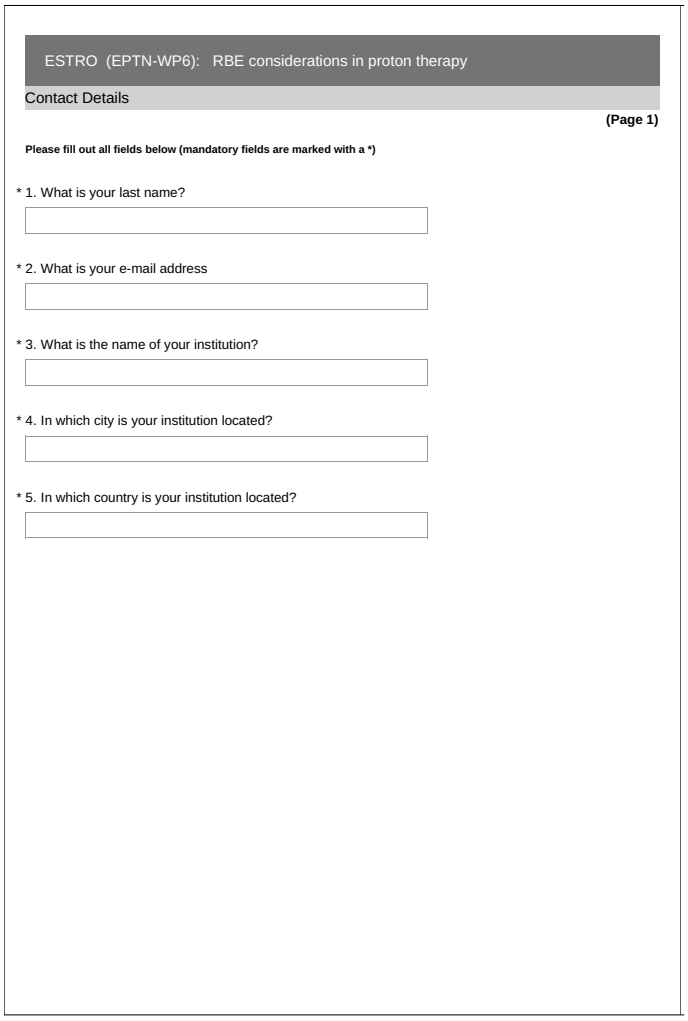

ESTRO (EPTN-WP6): RBE considerations in proton therapy

Contact Details

(Page 1)

Please fill out all fields below (mandatory fields are marked with a *)

* 1. What is your last name?

* 2. What is your e-mail address

* 3. What is the name of your institution?

* 4. In which city is your institution located?

* 5. In which country is your institution located?

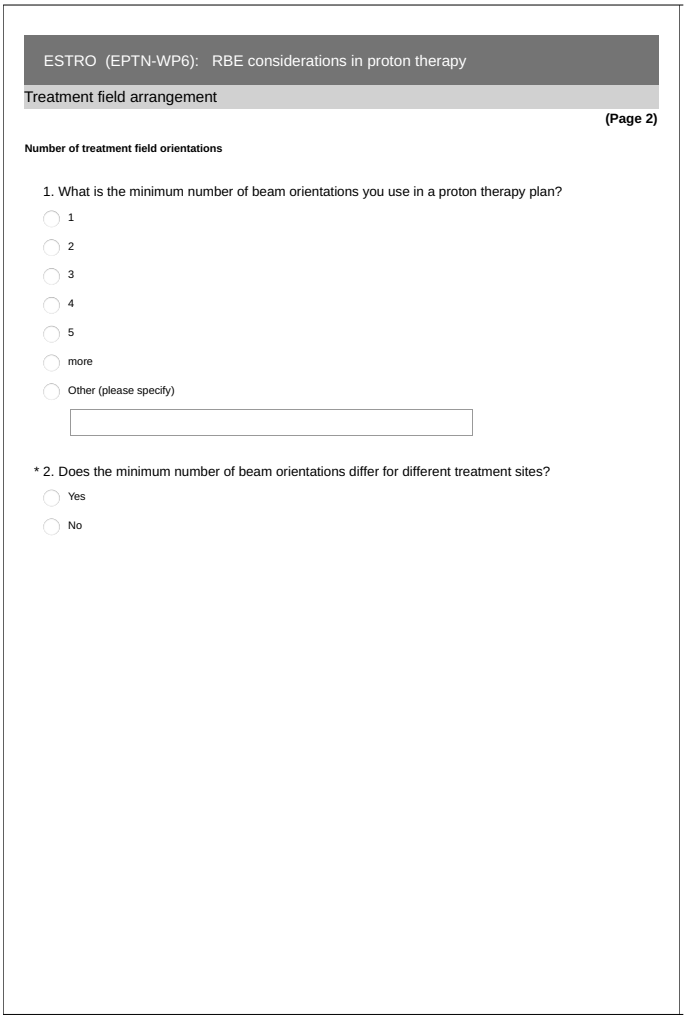

ESTRO (EPTN-WP6): RBE considerations in proton therapy

Treatment field arrangement

(Page 2)

Number of treatment field orientations

1. What is the minimum number of beam orientations you use in a proton therapy plan?

- 1
- 2
- 3
- 4
- 5
- more
- Other (please specify)

* 2. Does the minimum number of beam orientations differ for different treatment sites?

- Yes
- No

ESTRO (EPTN-WP6): RBE considerations in proton therapy

Number of fields

(Page 3)

Different treatment sites

1. What is the minimum number of treatment beam orientations ?

	1	2	3	4	5	more	rarly treated	not treated
Base of skul	○	○	○	○	○	○	○	○
Brain	○	○	○	○	○	○	○	○
Breast	○	○	○	○	○	○	○	○
Craniospinal irradiation	○	○	○	○	○	○	○	○
Head and neck	○	○	○	○	○	○	○	○
Liver	○	○	○	○	○	○	○	○
Lung	○	○	○	○	○	○	○	○
Oesophagus	○	○	○	○	○	○	○	○
Pancreas	○	○	○	○	○	○	○	○
Prostate	○	○	○	○	○	○	○	○

Other (please specify)

ESTRO (EPTN-WP6): RBE considerations in proton therapy

Treatment field arrangement (II/III)

(Page 4)

Beam angle selection

1. Do you apply restrictions on angles between proton beams?

- ○ No
- ○ Yes
- ○ Other (please specify)

2. Which restrictions do you apply on beam angles?

3. For which tumor entities do you apply restrictions on beam angles?

Field weights

4. Do you apply constraints regarding the relative field weights?

- ○ No constraints apply.
- ○ All fields should have comparable relative weight.
- ○ The following constraints apply for the relative field weight:

ESTRO (EPTN-WP6): RBE considerations in proton therapy

Treatment field arrangement (III/III)

(Page 5)

Beam stopping

1. Do you avoid field configurations where a beam stops in front of or inside an organ at risk (OAR)?

- ○ Yes
- ○ No
- ○ Other (please specify)

2. How do you avoid beams stopping in an OAR? [multiple answers possible]

- ☐ Field angles are avoided that result in beams stopping in an OAR.
- ☐ Fields stopping in or close to an OAR have a low weight.
- ☐ Field ranges are extended to place the end of range beyond an organ at risk ("shoot-through").
- ☐ Other:
  Please specify your strategy

ESTRO (EPTN-WP6): RBE considerations in proton therapy

Robust optimization

(Page 6)

Robust dose optimization

1. Do you apply robust optimization for dose planning?

- ○ Yes
- ○ No
- ○ Other (please specify)

2. What is considered for robustness in the optimization?

- ○ Target coverage.
- ○ Dose constraints for selected OAR and target coverage.
- ○ Dose constraints for all OAR and target coverage.
- ○ Dose constraints for OAR.
- ○ Other (please specify)

ESTRO (EPTN-WP6): RBE considerations in proton therapy

Variability of RBE in treatment planning (I/II)

(Page 7)

Active consideration of variable RBE

* 1. Do you consider the possibility during clinical treatment planning or plan approval that the proton RBE may be variable?

- ○ No, never.
- ○ In some cases.
- ○ Regularly.
- ○ Always.
- ○ Other (please specify)

2. When do you actively consider the possibility of a variable proton RBE? [multiple answers possible]

- ☐ Individual decision.
- ☐ For specific beam arrangements/treatment plans.
- ☐ For specific patient groups.
- ☐ For specific tumor sites.
- ☐ Never.
- ☐ Other (please specify)

3. Where do you actively consider the possibility of a variable RBE? [multiple answers possible]

- ☐ Organs at risk.
- ☐ Target volume.
- ☐ Organs at risk and target volume.
- ☐ Nowhere.
- ☐ Other (please specify)

4. What kind of measures do you apply to consider/counteract a potentially variable proton RBE? [multiple answers possible]

- ☐ Take special care about beam arrangements.
- ☐ Avoid proton beams to stop in or adjacent to organs at risk.
- ☐ Perform robust optimization.
- ☐ Consider the LET distribution for a treatment plan.
- ☐ Consider a variable RBE distribution for a treatment plan.
- ☐ Use LET or RBE for treatment plan optimization.
- ☐ Nothing.
- ☐ Other measures (please specify)

ESTRO (EPTN-WP6): RBE considerations in proton therapy

Variability of RBE in treatment planning (II/II)

(Page 8)

Prescription of a varible RBE

* 1. Do you prescribe anything else than a fixed RBE of 1.1 for patient treatment?

- ○ Yes
- ○ No

2. In which cases do you apply an RBE concept different from RBE = 1.1? [multiple answers possible]

- ☐ Never.
- ☐ Individual decision.
- ☐ For specific beam arrangements/treatment plans.
- ☐ For specific patient groups.
- ☐ For specific tumor sites.
- ☐ Within a clinical study on RBE.
- ☐ Always.
- ☐ Other (please specify)

3. If applicable: Please provide a short description of your RBE concept.

ESTRO (EPTN-WP6): RBE considerations in proton therapy

Estimation of LET and RBE for patient treatment (I/III)

(Page 9)

Frequency of LET or RBE calculation

1. Do you perform any patient-specific LET or RBE calculations to support treatment planning?

- ○ Yes
- ○ No

2. What is the frequency for performing patient-specific LET or RBE calculations?

- ○ Never.
- ○ Occasionally.
- ○ Regularly.
- ○ Always.
- ○ Other (please specify)

3. If applicable: What is triggering the calculation of LET or RBE?

Clinical workflow

4. Which quantities do you calculate for clinical treatments? [multiple answers possible]

- ☐ LET distribution.
- ☐ RBE distribution.
- ☐ Track-end distribution.
- ☐ Biological effect.
- ☐ NTCP with variable RBE.
- ☐ None of these.
- ☐ Other quantities (please specify)

ESTRO (EPTN-WP6): RBE considerations in proton therapy

Estimation of LET and RBE for patient treatment (II/III)

(Page 10)

Clinical workflow

1. How do results of these calculations enter clinical practice? [multiple answers possible]

- [ ] Never used.
- [ ] During the treatment planning process.
- [ ] For plan evaluation or plan approval.
- [ ] In the course of robust optimization.
- [ ] For documentation.
- [ ] For retrospective analysis to support patient follow-up.
- [ ] For clinical research purposes.
- [ ] Other (please specify)

2. Who initiates the calculation of LET or RBE in clinical praxis? [multiple answers possible]

- [ ] Treating physician.
- [ ] Physicist.
- [ ] Dosimetrist.
- [ ] Standard procedure.
- [ ] Never performed.
- [ ] Other (please specify)

3. Who performs the calculation of LET or RBE in clinical praxis? [multiple answers possible]

- [ ] Treating physician.
- [ ] Physicist.
- [ ] Dosimetrist.
- [ ] Research staff.
- [ ] Never performed.
- [ ] Other (please specify)

ESTRO (EPTN-WP6): RBE considerations in proton therapy

Estimation of LET and RBE for patient treatment (III/III)

(Page 11)

Specification of LET or RBE calculation

1. If applicable: Please specify the software you use to perform these calculations.

2. If applicable: Please specify the tumor entities for which you perform these calculations.

3. If applicable: Please provide additional specification to better characterize the calculations.

ESTRO (EPTN-WP6): RBE considerations in proton therapy

RBE consideration for patient follow-up

(Page 12)

Consideration of RBE in follow-up

1. Do you consider RBE in any way during patient follow-up? [multiple answers possible]

- ☐ No.
- ☐ Yes, in an attempt to better understand individual radiation response.
- ☐ Yes, within a (retrospective) study to estimate clinical RBE data.
- ☐ Yes, but in another way. (please specify)

2. If applicable: How do you consider RBE in follow-up?

3. If applicable: For which tumor sites do you consider RBE in follow-up?

Implementation of other RBE measures

4. Have you implemented any other measure at your clinic in connection with RBE which has not been considered in this questionnaire?

ESTRO (EPTN-WP6): RBE considerations in proton therapy

Future improvements

(Page 13)

Your wish list concerning proton RBE

1. What would you like to change in your treatment workflow with respect to RBE?

2. What kind of evidence should be generated to consider variable proton RBE in patient treatment?

3. What kind of treatment planning tools should be developed by vendors to consider variable proton RBE in patient treatment?

4. Which kind of guidelines do you miss in the context of a variable proton RBE?

5. What kind of publications are you missing?

6. What else are you missing or wish to see in the future concerning the proton RBE?

ESTRO (EPTN-WP6): RBE considerations in proton therapy

Comments

(Page 14)

1. Add any additional comments below

Thank you very much for your kind participation!

Your valuable contribution is highly appreciated.

Questionnaire: Current clinical practice of TBI

Umfrage Ganzkörperbestrahlung - AK Großfeldtechniken

Ziel der Umfrage ist eine Bestandsaufnahme der aktuell verwendeten Großfeldtechniken (Hier: Ganzkörperbestrahlung) in Deutschland. Die Umfrage richtet sich primär an physikalisch tätige Personen, wobei bei einzelnen Punkten auch medizinisches Personal zur Rate gezogen werden kann/sollte. Die Beantwortung der Fragen dauert ca. 15 Minuten und kann jeder Zeit unterbrochen und zu einem späteren Zeitpunkt fortgesetzt werden. Einzelne Fragen können übersprungen werden.

Vielen Dank, dass Sie sich die Zeit nehmen an dieser Umfrage teilzunehmen.

In dieser Umfrage sind 58 Fragen enthalten.

Allgemeine Fragen

1 Name des Zentrums

Bitte geben Sie Ihre Antwort hier ein:

2 Berufliche Tätigkeit

Bitte wählen Sie die zutreffenden Antworten aus:
Bitte wählen Sie alle zutreffenden Antworten aus:

- [ ] MPE
- [ ] MPE in Ausbildung
- [ ] Wissenschaftlicher Mitarbeiter/-in
- [ ] Doktorand/-in
- [ ] Student/-in
- [ ] Arzt/Ärztin
- [ ] Sonstiges:

3 E-Mail Adresse (für mögliche Rückfragen)

Bitte geben Sie Ihre Antwort hier ein:

4 Welche Großfeldtechniken werden in Ihrer Klinik durchgeführt?

Bitte wählen Sie die zutreffenden Antworten aus:
Bitte wählen Sie alle zutreffenden Antworten aus:

- [ ] Ganzkörperbestrahlung
- [ ] Ganzhautbestrahlung
- [ ] Bestrahlung der Craniospinalen Achse
- [ ] Keine der genannten

Ganzkörperbestrahlung - Allgemeine Fragen

5 Wie viele Patienten pro Jahr werden in Ihrer Klinik mit einer Ganzkörperbestrahlung behandelt?

Bitte geben Sie Ihre Antwort hier ein:

6
Wie viel Prozent der mit einer Ganzkörperbestrahlung behandelten Pateinten in Ihrer Klinik sind Kinder?

Bitte geben Sie Ihre Antwort hier ein:

7 Bei welchen Erkrankungen wird eine Ganzkörperbestrahlung verschrieben?

Bitte wählen Sie die zutreffenden Antworten aus:
Bitte wählen Sie alle zutreffenden Antworten aus:

- [ ] Leukämie
- [ ] Lymphome
- [ ] Multiple Myelome
- [ ] Plasmozytome
- [ ] Neuroblastome
- [ ] Sonstiges:

8 Zu welchem Zeitpunkt wird die Ganzkörperbestrahlung durchgeführt?

Bitte wählen Sie die zutreffenden Antworten aus:
Bitte wählen Sie alle zutreffenden Antworten aus:

- [ ] Vor der Chemotherapie
- [ ] Nach der Chemotherapie
- [ ] Zeitgleich mit der Chemotherapie
- [ ] Sonstiges:

Ganzkörperbestrahlung - Bestrahlungsgerät

9 Mit welcher Bestrahlungsanlage führen Sie die Ganzkörperbestrahlung durch?

Bitte wählen Sie die zutreffenden Antworten aus:
Bitte wählen Sie alle zutreffenden Antworten aus:

- [ ] Linac
- [ ] Cobalt-Gerät
- [ ] Tomotherapie
- [ ] Sonstiges:

10 Falls Sie die Bestrahlung an einem Linac durchführen, welchen Linac verwenden Sie?

Kommentieren wenn eine Antwort gewählt wird
Bitte wählen Sie die zutreffenden Punkte aus und schreiben Sie einen Kommentar dazu:

- [ ] Varian
- [ ] Elekta
- [ ] Tomotherapie-Gerät
- [ ] Es wird kein Linac verwendet
- [ ] Sonstiges:

11 Welche Photonenenergie verwenden Sie für die Ganzkörperbestrahlung?

Bitte geben Sie Ihre Antwort hier ein:

12 Führen Sie eine Brustwandaufsättigung mit Elektronen durch?

Bitte wählen Sie eine der folgenden Antworten:
Bitte wählen Sie nur eine der folgenden Antworten aus:

- ◯ Ja
- ◯ Nein
- ◯ Sonstiges

13 Falls Sie eine Brustwandaufsättigung mit Elektronen durchführen, welche Energie verwenden Sie?

Bitte geben Sie Ihre Antwort hier ein:

14 Welche Dosisrate des Bestrahlungsgeräts verwenden Sie für die Ganzkörperbestrahlung? (falls möglich bitte in cGy/min angeben)

Bitte geben Sie Ihre Antwort hier ein:

15 Welche Dosisrate liegt am Patienten vor? (falls möglich bitte in cGy/min angeben)

Bitte geben Sie Ihre Antwort hier ein:

Ganzkörperbestrahlung - Bestrahlungstechnik

16
Mit welcher Technik werden die Patienten bestrahlt?

Bitte wählen Sie die zutreffenden Antworten aus:
Bitte wählen Sie alle zutreffenden Antworten aus:

- [ ] Sweeping Beam
- [ ] Translationsliege
- [ ] Stark vergrößerter Abstand zwischen Quelle und Patient
- [ ] VMAT/IMRT
- [ ] Tomotherapie
- [ ] Sonstiges:

17 Falls Sie die Bestrahlung mittels VMAT/IMRT durchführen, wie viele Felder und wie viele Patientenpositionen verwenden Sie?

Bitte geben Sie Ihre Antwort hier ein:

18 Welchen Abstand zwischen Quelle und Patient verwenden Sie?

Bitte geben Sie Ihre Antwort hier ein:

19 Welche Feldorientierung verwenden Sie?

Bitte wählen Sie die zutreffenden Antworten aus:
Bitte wählen Sie alle zutreffenden Antworten aus:

- [ ] ap/pa
- [ ] RL/LR
- [ ] Beides (ap/pa und RL/LR)
- [ ] Keine der geannten
- [ ] Sonstiges:

20 In welcher Position befindet sich der Patient während der Bestrahlung?

Bitte wählen Sie die zutreffenden Antworten aus:
Bitte wählen Sie alle zutreffenden Antworten aus:

- [ ] Bauchlage
- [ ] Rückenlage
- [ ] Seitenlage
- [ ] Sitzend
- [ ] Stehend
- [ ] Keine der genannten
- [ ] Sonstiges:

21 Wie erfolgt die Positionierung des Patienten?

Bitte geben Sie Ihre Antwort hier ein:

22 Wie erfolgt die Kontrolle der Positionierung?

Bitte wählen Sie die zutreffenden Antworten aus:
Bitte wählen Sie alle zutreffenden Antworten aus:

- [ ] EPID
- [ ] Filme
- [ ] CBCT
- [ ] Sonstiges:

23 Wird der Patient auf der Standardliege des Beschleunigers bestrahlt?

Bitte wählen Sie die zutreffenden Antworten aus:
Bitte wählen Sie alle zutreffenden Antworten aus:

- [ ] Ja
- [ ] Nein
- [ ] Sonstiges:

24 Wie lange ist die durchschnittliche Behandlungszeit (inkl. Positionierung, Bestrahlung)?

Bitte geben Sie Ihre Antwort hier ein:

25 Wie lange ist die reine Bestrahlungszeit?

Bitte geben Sie Ihre Antwort hier ein:

26 Bitte beschreiben Sie ihre Bestrahlungstechnik.

Bitte geben Sie Ihre Antwort hier ein:

Ganzkörperbestrahlung - Bestrahlungsplanung

27 Wie hoch ist die Verschreibungsdosis?

Bitte geben Sie Ihre Antwort hier ein:

28 In wie vielen Fraktionen wird die Verschreibungsdosis appliziert?

Bitte geben Sie Ihre Antwort hier ein:

29 Wie viele Fraktionen werden pro Tag appliziert?

Bitte geben Sie Ihre Antwort hier ein:

30 Wie wird die Verschreibungsdosis definiert?

Bitte wählen Sie die zutreffenden Antworten aus:
Bitte wählen Sie alle zutreffenden Antworten aus:

- [ ] Mittlere Dosis im Zielvolumen
- [ ] Minimale Dosis im Zielvolumen
- [ ] Dosis an einem bestimmten Punkt (z.B. Mittelpunkt des Abdomen)
- [ ] Gemittelte Dosis über mehrere Punkte
- [ ] Sonstiges:

31 Wie wird das Zielvolumen definiert?

Bitte geben Sie Ihre Antwort hier ein:

32 Erfolgt die Bestrahlungsplanung auf Basis von einem CT?

Bitte wählen Sie die zutreffenden Antworten aus:
Bitte wählen Sie alle zutreffenden Antworten aus:

- [ ] Es efolgt eine 3D Bestrahlungsplanung auf einem CT
- [ ] Es erfolgt eine "manuelle" Bestrahlungsplanung mithilfe von aus einem CT ermittelten Daten (z.B. Dicken)
- [ ] Nein
- [ ] Sonstiges:

33 Falls die Bestrahlungsplanung auf Basis eines Ganzkörper-CTs erfolgt, beschreiben Sie bitte, wie das Ganzkörper-CT aufgenommen und erstellt wird.

Bitte geben Sie Ihre Antwort hier ein:

34 Welches Equipment wird während der Bestrahlung verwendet?

Bitte wählen Sie die zutreffenden Antworten aus:
Bitte wählen Sie alle zutreffenden Antworten aus:

- [ ] Beamspoiler/Plexiglasplatte
- [ ] Abschirmblöcke
- [ ] Sonstiges:

35 Wie lange dauert durchschnittlich die Erstellung eines Bestrahlungsplans?

Bitte geben Sie Ihre Antwort hier ein:

36 Wie lange dauern die Vorbereitungen vor der ersten Bestrahlung (inkl. Bestrahlungsplanung, Erstellen individueller Komponenten, ...)?

Bitte geben Sie Ihre Antwort hier ein:

37 Bitte beschreiben Sie, wie die Bestrahlungsplanung abläuft.

Bitte geben Sie Ihre Antwort hier ein:

Ganzkörperbestrahlung - Risikoorgane

38 Welche Risikoorgane/-strukturen werden geschont?

❗ Bitte wählen Sie die zutreffenden Antworten aus:
Bitte wählen Sie alle zutreffenden Antworten aus:

- [ ] Lunge
- [ ] Nieren
- [ ] Linsen
- [ ] Gar keine
- [ ] Sonstiges:

39 Welche Dosisgrenzwerte werden für die einzelnen Risikoorgane verwendet?

Bitte geben Sie Ihre Antwort hier ein:

40 Wie werden die Risikoorgane geschont?

❗ Bitte wählen Sie die zutreffenden Antworten aus:
Bitte wählen Sie alle zutreffenden Antworten aus:

- [ ] Absorptionsblöcke / Transmissionsblöcke
- [ ] Verwendung des MLC
- [ ] Gar nicht
- [ ] Sonstiges:

Ganzkörperbestrahlung - Qualitätssicherung

41 Welches Ausfallkonzept haben Sie?

Bitte wählen Sie die zutreffenden Antworten aus:
Bitte wählen Sie alle zutreffenden Antworten aus:

- [ ] Identisches Bestrahlungsgerät in der Klinik
- [ ] Identisches Bestrahlungsgerät in anderer, nahegelegender Klinik
- [ ] Anderes Bestrahlungsgerät, an dem die gleiche Bestrahlungstechnik angewendet wird
- [ ] Komplett andere Bestrahlungstechnik
- [ ] Sonstiges:

42 Ist bei Ausfall des Bestrahlungsgeräts eine Neuplanung nötig?

Bitte wählen Sie die zutreffenden Antworten aus:
Bitte wählen Sie alle zutreffenden Antworten aus:

- [ ] Ja
- [ ] Nein
- [ ] Sonstiges:

43 Welche Methoden/Messungen zusätzlich zur Standard-Qualitätssicherung führen Sie noch für die Ganzkörperbestrahlung durch?

Bitte geben Sie Ihre Antwort hier ein:

44 Führen Sie eine Dosismessung während der Bestrahlung durch?

Bitte wählen Sie die zutreffenden Antworten aus:
Bitte wählen Sie alle zutreffenden Antworten aus:

- [ ] Ja
- [ ] Nein
- [ ] Sonstiges:

45 Welche Messgeräte werden für die Dosismessungen während der Bestrahlung verwendet?

Bitte geben Sie Ihre Antwort hier ein:

46 Wo werden die Messgeräte während der Bestrahlung platziert?

Bitte geben Sie Ihre Antwort hier ein:

47 Welche Risikoanalysen werden durchgeführt?

Bitte wählen Sie die zutreffenden Antworten aus:
Bitte wählen Sie alle zutreffenden Antworten aus:

- [ ] FMEA
- [ ] Risikomatrix
- [ ] Gar nicht
- [ ] Sonstiges:

48 Falls Sie Risikoanalysen durchführen, beschreiben Sie diese bitte.

Bitte geben Sie Ihre Antwort hier ein:

49 Folgen Sie bei Ihrer Bestrahlung bestimmten Richtlinien/Protokollen?

❗ Bitte wählen Sie die zutreffenden Antworten aus:
Bitte wählen Sie alle zutreffenden Antworten aus:

- [ ] Leitlinien der DGMP, 2003
- [ ] AAPM Report Nr. 17
- [ ] Richtlinien der ILROG, 2018
- [ ] Sonstiges:

Ganzkörperbestrahlung - Allgemeine Einschätzungen

50 Welche Vorteile sehen Sie bei der von Ihnen verwendeten Technik im Vergleich zu anderen Techniken?

Bitte geben Sie Ihre Antwort hier ein:

51 Welche Nachteile sehen Sie bei der von Ihnen verwendeten Bestrahlungstechnik im Vergleich zu anderen Techniken?

Bitte geben Sie Ihre Antwort hier ein:

52 Was sehen Sie als die größte Herrausforderung bei der von Ihnen verwendeten Technik?

Bitte geben Sie Ihre Antwort hier ein:

53 Platz für zusätzliche Kommentare.

Bitte geben Sie Ihre Antwort hier ein:

Zukunft

54 Welche Forschungsfragen sollten Ihrer Meinung nach zukünftig zum Thema Ganzkörperbestrahlungen untersucht werden?

Bitte geben Sie Ihre Antwort hier ein:

55
Wären Sie prinzipielle interessiert daran, an einer in silico Patientenstudie teilzunehmen, bei der Sie einen Datensatz von einem Beispielpatienten erhalten würden und Sie einen Bestrahlungsplan für diesen Patienten erstellen müssten?

Bitte wählen Sie nur eine der folgenden Antworten aus:

◯ Ja

◯ Nein

Wir würden zukünftig, im Rahmen des AKs, gerne weiterführende Studien durchführen um die Unterschiede und Gemeinsamkeiten der einzelnen Techniken besser vergleichen zu können. Deswegen planen wir eine in silico Patientenstudie, bei der der Datensatz eines Beispielpatienten an verschiedene Zentren verteilt wird und diese eine Bestrahlungsplan nach Ihrer Technik erstellen. Auf dem nächsten AK Treffen werden wir hierauf noch detaillierter eingehen, dennoch würden wir gerne schon einmal abfragen, ob prinzipilles Interesse am Mitwirken an einer solchen Studie besteht.

56 Wären Sie prinzipiell interessiert daran, an einer dosimetrischen Studie teilzunehmen, bei der Sie die Dosis während der Bestrahlung an definierten Positionen entlang des Patienten messen müssten?

Bitte wählen Sie nur eine der folgenden Antworten aus:

◯ Ja

◯ Nein

Wir würden zukünftig, im Rahmen des AKs, gerne weiterführende Studien durchführen um die Unterschiede und Gemeinsamkeiten der einzelnen Techniken besser vergleichen zu können. Deswegen planen wir eine dosimetrische Studie, bei der die Dosis an definierten Punkten entlang des Patienten während der Bestrahlung gemessen werden soll. Auf dem nächsten AK Treffen werden wir hierauf noch detaillierter eingehen, dennoch würden wir gerne schon einmal abfragen, ob prinzipilles Interesse am Mitwirken an einer solchen Studie besteht.

57 Sind Sie damit einverstanden, dass ihr Zentrum inklusive der an Ihrem Zentrum durchgeführten Bestrahlungstechnik auf der Website des AKs gelistet wird?

Bitte wählen Sie nur eine der folgenden Antworten aus:

◯ Ja

◯ Nein

References

[1] B. Baskar, K. A. Lee, R. Yeo, and K. W. Yeoh, "Cancer and radiation therapy: Current advances and future directions," *International Journal of Medical Sciences*, vol. 9, pp. 193–199, 3 Feb. 2012. DOI: 10.7150/IJMS.3635.

[2] J. van Dyk, J. M. Galvin, G. P. Glasgow, and E. B. Podgorsak, "The physical aspects of total and half body photon irradiation: Report of the AAPM TG-29," 1986.

[3] U. Quast, "Whole body radiotherapy: A TBI-guideline," *Journal of medical physics*, vol. 31, pp. 5–12, 1 2006. DOI: 10.4103/0971-6203.25664.

[4] I. Sakellari *et al.*, "Long-term outcomes of total body irradiation plus cyclophosphamide versus busulfan plus cyclophosphamide as conditioning regimen for acute lymphoblastic leukemia: A comparative study," *Annals of hematology*, vol. 97, pp. 1987–1994, 10 2018. DOI: 10.1007/S00277-018-3383-9.

[5] M. E. U. Rehman *et al.*, "Total body irradiation versus chemotherapy conditioning in pediatric acute lymphoblastic leukemia patients undergoing hematopoietic stem cell transplant: A systematic review and meta-analysis," *Clinical Lymphoma, Myeloma and Leukemia*, vol. 23, pp. 249–258, 4 2023. DOI: 10.1016/J.CLML.2023.01.004.

[6] F. Khimani *et al.*, "Impact of total body irradiation-based myeloablative conditioning regimens in patients with acute lymphoblastic leukemia undergoing allogeneic hematopoietic stem cell transplantation: Systematic review and meta-analysis," *Transplantation and Cellular Therapy*, vol. 27, 620.e1–620.e9, 7 2021. DOI: 10.1016/J.JTCT.2021.03.026.

[7] G. Pierce, A. Balogh, R. Frederick, D. Gordon, A. Yarschenko, and A. Hudson, "Extended SSD VMAT treatment for total body irradiation," *Journal of Applied Clinical Medical Physics*, vol. 20, pp. 200–211, 1 2019. DOI: 10.1002/ACM2.12519.

[8] M. Cananoglu, P. Hurmuz, M. Yeginer, and G. Ozyigit, "Planning and dosimetric evaluation of three total body irradiation techniques: Standard SSD VMAT, extended SSD VMAT and extended SSD field-in-field," *Radiation and Environmental Biophysics*, vol. 62, pp. 73–81, 1 2023. DOI: 10.1007/S00411-022-00999-X.

[9] A. H. Zhuang, A. Liu, T. E. Schultheiss, and J. Y. C. Wong, "Dosimetric study and verification of total body irradiation using helical tomotherapy and its comparison to extended SSD technique," *Medical Dosimetry*, vol. 35, pp. 243–249, 4 2010. DOI: 10.1016/j.meddos.2009.07.001.

[10] B. Umek, M. Zwitter, and H. Habič, "Total body irradiation with translation method," *Radiotherapy and Oncology*, vol. 38, pp. 253–255, 3 1996. DOI: 10.1016/0167-8140(95)01697-X.

[11] M. Sarfaraz, C. Yu, D. J. Chen, and L. Der, "A translational couch technique for total body irradiation," *Journal of Applied Clinical Medical Physics*, vol. 2, pp. 201–209, 4 2001. DOI: 10.1120/JACMP.V2I4.2597.

[12] H. H. Chen, J. Wu, K. S. Chuang, J. F. Lin, J. C. Lee, and J. C. Lin, "Total body irradiation with step translation and dynamic field matching," *BioMed research international*, vol. 2013, p. 216 034, Jul. 2013. DOI: 10.1155/2013/216034.

[13] U. Quast, "Physical treatment planning of total-body irradiation: Patient translation and beam-zone method," *Medical Physics*, vol. 12, pp. 567–574, 5 1985. DOI: 10.1118/1.595677.

[14] J. A. Pĕagarícano, M. Chao, F. Van Rhee, E. G. Moros, P. M. Corry, and V. Ratanatharathorn, "Clinical feasibility of TBI with helical tomotherapy," *Bone Marrow Transplantation*, vol. 46, pp. 929–935, 7 2010. DOI: 10.1038/bmt.2010.237.

[15] T. Wilhelm-Buchstab *et al.*, "Total body irradiation: Significant dose sparing of lung tissue achievable by helical tomotherapy," *Zeitschrift für Medizinische Physik*, vol. 30, pp. 17–23, 1 2020. DOI: 10.1016/J.ZEMEDI.2019.05.002.

[16] M. Köksal *et al.*, "Whole body irradiation with intensity-modulated helical tomotherapy prior to haematopoietic stem cell transplantation: Analysis of organs at risk by dose and its effect on blood kinetics," *Journal of Cancer Research and Clinical Oncology*, vol. 149, pp. 7007–7015, 10 2023. DOI: 10.1007/S00432-023-04657-7.

[17] J. Eulitz *et al.*, "Predicting late magnetic resonance image changes in glioma patients after proton therapy," *Acta Oncologica*, vol. 58, pp. 1536–1539, 10 2019. DOI: 10.1080/0284186X.2019.1631477.

[18] E. Bahn, J. Bauer, S. Harrabi, K. Herfarth, and M. Alber, "Late contrast enhancing brain lesions in proton-treated patients with low-grade glioma : Clinical evidence for increased periventricular sensitivity and variable RBE," *International Jounral of Radiation, Oncology, Biology, Physics*, vol. 107, pp. 571–578, 3 2020. DOI: 10.1016/j.ijrobp.2020.03.013.

[19] C. R. Peeler *et al.*, "Clinical evidence of variable proton biological effectiveness in pediatric patients treated for ependymoma," *Radiotherapy and Oncology*, vol. 121, pp. 395–401, 3 2016. DOI: 10.1016/j.radonc.2016.11.001.

[20] G. M. Engeseth *et al.*, "Mixed effect modeling of dose and linear energy transfer correlations with brain image changes after intensity modulated proton therapy for skull base head and neck cancer," *International Journal of Radiation Oncology, Biology, Physics*, vol. 111, pp. 684–692, 3 2021. DOI: 10.1016/J.IJROBP.2021.06.016/ATTACHMENT/0CFDD7F6-3752-4CFD-AC3C-327B4BE291B1/MMC1.DOCX.

[21] A. Bertolet *et al.*, "Correlation of LET with MRI changes in brain and potential implications for normal tissue complication probability for patients with meningioma treated with pencil beam scanning proton therapy," *International Journal of Radiation Oncology, Biology, Physics*, vol. 112, pp. 237–246, 1 2022. DOI: 10.1016/J.IJROBP.2021.08.027.

[22] J. Ödén, I. Toma-Dasu, P. Witt Nyström, E. Traneus, and A. Dasu, "Spatial correlation of linear energy transfer and relative biological effectiveness with suspected treatment-related toxicities following proton therapy for intracranial tumors," *Medical Physics*, vol. 47, pp. 342–351, 2 2021. DOI: 10.1002/mp.13911.

[23] T. S. A. Underwood *et al.*, "Asymptomatic late-phase radiographic changes among chest-wall patients are associated with a proton RBE exceeding 1.1," *International Journal of Radiation Oncology, Biology, Physics*, vol. 101, pp. 809–819, 4 2018. DOI: 10.1016/j.ijrobp.2018.03.037.

[24] C. C. Wang *et al.*, "End-of-range radiobiological effect on rib fractures in patients receiving proton therapy for breast cancer," *International Journal of Radiation Oncology, Biology, Physics*, vol. 107, pp. 449–454, 3 2020. DOI: 10.1016/j.ijrobp.2020.03.012.

[25] A. Lühr *et al.*, "Radiobiology of proton therapy: Results of an international expert workshop," *Radiotherapy and Oncology*, vol. 128, pp. 56–67, 1 2018.

[26] H. Paganetti, "Proton relative biological effectiveness-uncertainties and opportunities," *International Journal of Particle Therapy*, vol. 5, pp. 2–14, 1 2019. DOI: 10.14338/IJPT-18-00011.1.

[27] H. Paganetti, "Relative biological effectiveness (RBE) values for proton beam therapy. variations as a function of biological endpoint, dose, and linear energy transfer," *Physics in Medicine and Biology*, vol. 59, R419–R472, 22 2014. DOI: 10.1088/0031-9155/59/22/R4190.

[28] ICRU, "ICRU report 19: Radiation quantaties and units," *Journal of the ICRU*, 1971.

[29] U. Oelfke, "Physikalische Wechselwirkungen ionisierender Strahlung mit Materie," in *Medizinische Physik 2 - Medizinische Strahlenphysik*, W. Schlegel, Ed., Springer, 2002.

[30] S. M. Seltzer, D. T. Bartlett, D. T. Burns, G. Dietze, H. G. Menzel, and A. Wambersie, "ICRU report 85: Fundamental quantities and units for ionizing radiation," *Journal of the ICRU*, 2011. DOI: 10.1093/jicru/ndr011.

[31] F. H. Attix, "Charged-particle interactions in matter," in *Introduction to radiological physics and radiation dosimetry*, Wiley-VCH, 1986.

[32] W. D. Newhauser and R. Zhang, "The physics of proton therapy," *Physics in Medicine and Biology*, vol. 60, R155–R209, 8 2015. DOI: 10.1088/0031-9155/60/8/R155.

[33] H. Bethe, "Zur Theorie des Durchgangs schneller Korpuskularstrahlen durch Materie," *Annalen der Physik*, vol. 397, pp. 325–400, 3 1930. DOI: 10.1002/andp.19303970303.

[34] F. Bloch, "Zur Bremsung rasch bewegter Teilchen beim Durchgang durch Materie," *Annalen der Physik*, vol. 408, pp. 285–320, 3 1933. DOI: 10.1002/andp.19334080303.

[35] M. J. Berger *et al.*, "ICRU report 49: Stopping powers and ranges for protons and alpha particles," *Journal of the ICRU*, 1993. DOI: 10.1093/jicru/os25.2.Report49.

[36] B. Gottschalk, "Physics of proton interactions in matter," in *Proton therapy physics*, H. Paganetti, Ed., CRC Press, 2012.

[37] L. H.-M. and J. Flanz, "Characteristics of clinical proton beams," in *Proton therapy physics*, H. Paganetti, Ed., CRC Press, 2012.

[38] F. Guan *et al.*, "Analysis of the track- and doseaveraged LET and LET spectra in proton therapy using the geant4 Monte Carlo code," *Medical Physics*, vol. 42, pp. 6234–6247, 11 2015. DOI: 10.1118/1.4932217.

[39] H. Paganetti, "Particle beam scanning," in *Proton therapy physics*, H. Paganetti, Ed., CRC Press, 2012.

[40] A. M. Kellerer and H. D. Rossi, "Theory of dual radiation action," *Current Topics in Radiation Research Quarterly*, vol. 8, pp. 85–158, 2 1972.

[41] K. H. Chadwick and H. P. Leenhouts, "A molecular theory of cell survival," *Physics in Medicine and Biology*, vol. 18, pp. 78–87, 1 1973. DOI: 10.1088/0031-9155/18/1/007.

[42] S. J. McMahon, "The linear quadratic model: Usage, interpretation and challenges," *Physics in Medicine and Biology*, vol. 64, pp. 1–24, 1 2018. DOI: 10.1088/1361-6560/aaf26a.

[43] G. V. Dalrymple *et al.*, "Some effects of 138-MeV protons on primates," *Radiation Research*, vol. 28, pp. 471–488, 2 1966.

[44] G. V. Dalrymple *et al.*, "The relative biological effectiveness of 138-MeV protons as compared to cobalt-60 gamma radiation," *Radiation Research*, vol. 28, pp. 489–506, 2 1966.

[45] J. Tepper, L. Verhey, M. Goitein, and H. D. Suit, "In vivo determinations of rbe in a high energy modulated proton beam using normal tissue reactions and fractionated dose schedules," *International Journal of Radiation Oncology, Biology, Physics*, vol. 2, pp. 1150–1122, 11-12 1977. DOI: 10.1016/0360-3016(77)90118-3.

[46] M. Urano, M. Goitein, L. Verhey, O. Mendiondo, H. D. Suit, and A. Koehler, "Relative biological effectiveness of a high energy modulated proton beam using a spontaneous murine tumor in vivo," *International Journal of Radiation Oncology, Biology, Physics*, vol. 6, pp. 1187–1193, 9 1980. DOI: 10.1016/0360-3016(80)90172-8.

[47] A. Lühr, C. von Neubeck, M. Krause, and E. G. C. Troost, "Relative biological effectiveness in proton beam therapy – currentknowledge and future challenges," *Clinical and Translational Radiation Oncology*, vol. 9, pp. 35–41, 1 2018. DOI: 10.1016/j.ctro.2018.01.006.

[48] P. Chaudhary *et al.*, "Relative biological effectiveness variation along monoenergetic and modulated Bragg peaks of a 62-MeV therapeutic proton beam: A preclinical assessment," *International Journal of Radiation Oncology, Biology, Physics*, vol. 90, pp. 27–35, 1 2014. DOI: 10.1016/j.ijrobp.2014.05.010.

[49] M. Wedenberg, B. K. Lind, and B. Hårdemark, "A model for the relative biological effectiveness of protons: The tissue specific parameter α/β of photons is a predictor for the sensitivity to LET changes," *Acta Oncologica*, vol. 52, pp. 580–588, 3 2014. DOI: 10.3109/0284186X.2012.705892.

[50] A. L. McNamara, J. Schuemann, and H. Paganetti, "A phenomenological relative biologicaleffectiveness (RBE) model for proton therapy based on all published in vitro cell survival data," *Physics in Medicine and Biology*, vol. 60, pp. 8399–8416, 21 2015. DOI: 10.1088/0031-9155/60/21/8399.

[51] E. Rørvik, S. Thörnqvist, C. H. Stokkevåg, T. J. Dahle, L. F. Fjaera, and K. S. Ytre-Hauge, "A phenomenological biological dose model for proton therapy based on linear energy transfer spectra," *Medical Physics*, vol. 44, pp. 2586–2594, 6 2017. DOI: 10.1002/mp.12216.

[52] J. Eulitz *et al.*, "Increased relative biological effectiveness and periventricular radiosensitivity in proton therapy of glioma patients," *Radiotherapy and Oncology*, vol. 178, p. 109 422, Jan. 2023. DOI: 10.1016/j.radonc.2022.11.011.

[53] R. Grün, T. Friedrich, E. Traneus, and M. Scholz, "Is the dose-averaged LET a reliable predictor for the relative biological effectiveness?" *Medical Physics*, vol. 46, pp. 1064–1074, 2 2019. DOI: 10.1002/MP.13347.

[54] L. Brualla, M. Rodriguez, J. Sempau, and P. Andreo, "PENELOPE/PRIMO-calculated photon and electron spectra from clinical accelerators," *Radiation Oncology*, vol. 14, 1 Jan. 2019. DOI: 10.1186/S13014-018-1186-8.

[55] W. Schlegel, "Bestrahlungsgeräte der Teletherapie," in *Medizinische Physik 2 - Medizinische Strahlenphysik*, W. Schlegel, Ed., Springer, 2002.

[56] T. Bortfeld, "IMRT: A review and preview," *Physics in Medicine and Biology*, vol. 51, R363–79, 13 2006. DOI: 10.1088/0031-9155/51/13/R21.

[57] M. Teoh, C. H. Clark, K. Wood, S. Whitaker, and A. Nisbet, "Volumetric modulated arc therapy: A review of current literature and clinical use in practice," *The British Journal of Radiology*, vol. 84, pp. 967–96, 1007 2011. DOI: 10.1259/BJR/22373346.

[58] T. R. Mackie, "History of tomotherapy," *Physics in Medicine and Biology*, vol. 51, R427–453, 13 2006. DOI: 10.1088/0031-9155/51/13/R24.

[59] U. Quast and A. Hoederath, "Strahlentherapie - Radiologische Onkologie," in *Ganzkörperbestrahlung*, E. Scherer and H. Sack, Eds., 4th, Springer, 1996.

[60] U. Quast, "Strahlentherapie - Radiologische Onkologie," in *Ganzkörperbestrahlung bei der Therapie maligner Systemerkrankungen*, E. Scherer, Ed., 3rd, Springer, 1987.

[61] U. Quast, "Total body irradiation–review of treatment techniques in europe," *Radiotherapy and Oncology*, vol. 9, pp. 91–106, 2 1987. DOI: 10.1016/S0167-8140(87)80197-4.

[62] Y. Bentele, "Ganzkörperbestrahlung in a.p.–p.a. Stehfeldtechnik mit Translation," *Radiopraxis*, vol. 8, pp. 161–174, 03 2015. DOI: 10.1055/S-0041-103068.

[63] J. Flanz, "The physics of proton biology," in *Proton therapy physics*, H. Paganetti, Ed., CRC Press, 2012.

[64] M. Krämer and M. Durante, "Ion beam transport calculations and treatment plans in particle therapy," *The European Physical Journal D*, vol. 60, pp. 195–202, 1 2010. DOI: 10.1140/EPJD/E2010-00077-8.

[65] U. Schneider, E. Pedroni, and A. Lomax, "The calibration of CT Hounsfield units for radiotherapy treatment planning," *Physics in Medicine and Biology*, vol. 41, pp. 111–124, 1 1996. DOI: 10.1088/0031-9155/41/1/009.

[66] W. Schneider, T. Bortfeld, and W. Schlegel, "Correlation between CT numbers and tissue parameters needed for Monte Carlo simulations of clinical dose distributions," *Physics in Medicine and Biology*, vol. 45, pp. 459–478, 2 2000. DOI: 10.1088/0031-9155/45/2/314.

[67] D. Jones, "ICRU report 50: Prescribing, recording and reporting photon beam therapy," *Medical Physics*, vol. 21, pp. 833–834, 6 1994. DOI: 10.1118/1.597396.

[68] ICRU, "ICRU report 62: Prescribing, recording and reporting photon beam therapy (supplement to ICRU 50)," 1999.

[69] B. Emami *et al.*, "Tolerance of normal tissue to therapeutic irradiation," *International Journal of Radiation Oncology, Biology, Physics*, vol. 21, pp. 109–22, 1 1991. DOI: 10.1016/0360-3016(91)90171-Y.

[70] S. M. Bentzen *et al.*, "Quantitative analyses of normal tissue effects in the clinic (QUANTEC): An introduction to the scientific issues," *International Journal of Radiation Oncology, Biology, Physics*, vol. 76, S3–9, 3 Suppl 2010. DOI: 10.1016/J.IJROBP.2009.09.040.

[71] V. Hernandez *et al.*, "What is plan quality in radiotherapy? The importance of evaluating dose metrics, complexity, and robustness of treatment plans," *Radiotherapy and Oncology*, vol. 153, pp. 26–33, Dec. 2020. DOI: 10.1016/J.RADONC.2020.09.038.

[72] R. E. Drzymala *et al.*, "Dose-volume histograms," *International journal of radiation oncology, biology, physics*, vol. 21, pp. 71–78, 1 1991. DOI: 10.1016/0360-3016(91)90168-4.

[73] P. Källman, A. Ågren, and A. Brahme, "Tumour and normal tissue responses to fractionated non-uniform dose delivery," *International Journal of Radiation Biology*, vol. 62, pp. 249–262, 2 1992. DOI: 10.1080/09553009214552071.

[74] A. Ågren Cronqvist, "Quantification of the response of heterogeneous tumours and organized normal tissues to fractionated radiotherapy," 1995.

[75] T. Bortfeld, W. Schlegel, R. Bendl, U. Oelfke, G. Küster, and W. Schneider, "Bestrahlungsplanung," in *Medizinische Physik 2 - Medizinische Strahlenphysik*, W. Schlegel, Ed., Springer, 2002.

[76] A. Ahnesjö, "Collapsed cone convolution of radiant energy for photon dose calculation in heterogeneous media," *Medical Physics*, vol. 16, pp. 577–592, 4 1989. DOI: 10.1118/1.596360.

[77] T. Bortfeld, W. Schlegel, and B. Rhein, "Decomposition of pencil beam kernels for fast dose calculations in three-dimensional treatment planning," *Medical Physics*, vol. 20, pp. 311–318, 2 Pt 1 1993. DOI: 10.1118/1.597070.

[78] I. J. Chetty *et al.*, "Report of the AAPM task group no. 105: Issues associated with clinical implementation of monte carlo-based photon and electron external beam treatment planning," *Medical Physics*, vol. 34, pp. 4818–53, 12 2007. DOI: 10.1118/1.2795842.

[79] P. W. Koken and L. H. P. Murrer, "Total body irradiation and total skin irradiation techniques in Belgium and the Netherlands: Current clinical practice," *Advances in Radiation Oncology*, vol. 6, p. 100 664, 4 2021. DOI: 10.1016/J.ADRO.2021.100664.

[80] H. Kawaguchi *et al.*, "National survey on total-body irradiation prior to reduced-intensity stem cell transplantation in Japan: The Japanese Radiation Oncology Study Group," *Journal of Radiation Research*, vol. 60, pp. 579–585, 5 2019. DOI: 10.1093/JRR/RRZ028.

[81] N. Ishibashi *et al.*, "National survey of myeloablative total body irradiation prior to hematopoietic stem cell transplantation in Japan: survey of the Japanese Radiation Oncology Study Group (JROSG)," *Journal of Radiation Research*, vol. 59, pp. 477–483, 4 2018. DOI: 10.1093/JRR/RRY017.

[82] R. C. N. Studinski, D. J. Fraser, R. S. Samant, and M. S. Macpherson, "Current practice in total-body irradiation: Results of a Canada-wide survey," *Current Oncology*, vol. 24, pp. 181–186, 3 2017. DOI: 10.3747/CO.24.3484.

[83] P. Rassiah *et al.*, "Practice patterns of pediatric total body irradiation techniques: A children's oncology group survey," *International Journal of Radiation Oncology, Biology, Physics*, vol. 111, pp. 1155–1164, 5 2021. DOI: 10.1016/J.IJROBP.2021.07.1715.

[84] L. S. Fog *et al.*, "Total body irradiation in Australia and New Zealand: Results of a practice survey," *Physical and Engineering Sciences in Medicine*, vol. 43, pp. 825–835, 3 2020. DOI: 10.1007/S13246-020-00878-Z.

[85] B. A. W. Hoeben *et al.*, "Towards homogenization of total body irradiation practices in pediatric patients across SIOPE affiliated centers. A survey by the siope radiation oncology working group," *Radiotherapy and Oncology*, vol. 155, pp. 113–119, Feb. 2021. DOI: 10.1016/J.RADONC.2020.10.032.

[86] S. Giebel *et al.*, "Extreme heterogeneity of myeloablative total body irradiation techniques in clinical practice: A survey of the acute leukemia working party of the european group for blood and marrow transplantation," *Cancer*, vol. 120, pp. 2760–2765, 17 2014. DOI: 10.1002/cncr.28768.

[87] M. Pla, S. G. Chenery, and E. B. Podgorsak, "Total body irradiation with a sweeping beam," *International Journal of Radiation Oncology, Biology, Physics*, vol. 9, pp. 83–89, 1 1983. DOI: 10.1016/0360-3016(83)90214-6.

[88] P. M. Härtl *et al.*, "Total body irradiation-an attachment free sweeping beam technique," *Radiation Oncology*, vol. 11, p. 81, 10 2016. DOI: 10.1186/S13014-016-0658-Y.

[89] I. Bratova, P. Paluska, J. Grepl, I. Sirak, J. Petera, and M. Vosmik, "Total body irradiation for standard treatment rooms: A robust sweeping beam technique with respect to the body shape," *Reports of Practical Oncology and Radiotherapy*, vol. 27, pp. 268–274, 2 2022. DOI: 10.5603/RPOR.A2022.0039.

[90] U. Quast and H. Sack, *Ganzkörper-Strahlenbehandlung: Leitlinien in der Radioonkologie*, 2003.

[91] N. Hodapp, "The ICRU report 83: Prescribing, recording and reporting photon-beam intensity-modulated radiation therapy (IMRT)," *Strahlentherapie und Onkologie*, vol. 188, pp. 97–99, 1 2012. DOI: 10.1007/S00066-011-0015-X.

[92] J. Perl, J. Shin, J. Schümann, B. Faddegon, and H. Paganetti, "TOPAS: An innovative proton monte carlo platform for research and clinical applications," *Medical Physics*, vol. 39, pp. 6818–6837, 11 2012. DOI: 10.1118/1.4758060.

[93] H. Shimizu *et al.*, "Interfacility variation in treatment planning parameters in tomotherapy: Field width, pitch, and modulation factor," *Journal of Radiation Research*, vol. 59, pp. 664–668, 5 2018. DOI: 10.1093/jrr/rry042.

[94] S. L. Wolden *et al.*, "American college of radiology (ACR) and american society for radiation oncology (ASTRO) practice guideline for the performance of total body irradiation (TBI)," *American Journal of Clinical Oncology*, vol. 36, pp. 97–101, 1 2013. DOI: 10.1097/COC.0B013E31826E0528.

[95] P. Lonski, M. MacManus, B. A. Campbell, G. Wheeler, E. Ungureanu, and T. Kron, "Assessment of lung doses in patients undergoing total body irradiation for haematological malignancies with and without lung shielding," *Journal of Medical Imaging and Radiation Oncology*, vol. 67, pp. 684–690, 6 2023. DOI: 10.1111/1754-9485.13550.

[96] M. C. Lavalle, L. Gingras, M. Chrtien, S. Aubin, C. Ct, and L. Beaulieu, "Commissioning and evaluation of an extended SSD photon model for PINNACLE3: An application to total body irradiation," *Medical Physics*, vol. 36, pp. 3844–3855, 8 2009. DOI: 10.1118/1.3171688.

[97] A. Hussain, E. Villarreal-Barajas, D. Brown, and P. Dunscombe, "Validation of the Eclipse AAA algorithm at extended SSD," *Journal of Applied Clinical Medical Physics*, vol. 11, pp. 90–100, 3 2010. DOI: 10.1120/JACMP.V11I3.3213.

[98] N. Lamichhane, V. N. Patel, and M. T. Studenskia, "Going the distance: Validation of Acuros and AAA at an extended SSD of 400 cm," *Journal of Applied Clinical Medical Physics*, vol. 17, pp. 63–73, 2 2016. DOI: 10.1120/JACMP.V17I2.5913.

[99] M. C. Lavallée, S. Aubin, M. Larochelle, I. Vallières, and L. Beaulieu, "3D heterogeneous dose distributions for total body irradiation patients," *Journal of Applied Clinical Medical Physics*, vol. 12, pp. 205–214, 3 2011. DOI: 10.1120/JACMP.V12I3.3416.

[100] L. Heuchel, C. Hahn, J. Pawelke, B. Singers Sørensen, M. Dosanjh, and A. Lühr, "Clinical use and future requirements of relative biological effectiveness: Survey among all European proton therapy centres," *Radiotherapy and oncology*, vol. 172, pp. 134–139, Jul. 2022. DOI: 10.1016/J.RADONC.2022.05.015.

[101] L. Heuchel *et al.*, "The dirty and clean dose concept: Towards creating proton therapy treatment plans with a photon-like dose response," *Medical Physics*, Oct. 2023. DOI: 10.1002/MP.16809.

[102] ICRU, "Icru report 78: Prescribing, recording, and reporting proton-beam therapy," *Journal of the ICRU*, vol. 7, pp. 1–8, 2 2007. DOI: 10.1093/JICRU_NDM021.

[103] J. Bauer, E. Bahn, S. Harrabi, K. Herfarth, J. Debus, and M. Alber, "How can scanned proton beam treatment planning for low-grade glioma cope with increased distal rbe and locally increased radiosensitivity for late MR-detected brain lesions?" *Medical Physics*, vol. 48, pp. 1497–1507, 4 2021. DOI: 10.1002/mp.14739.

[104] D. Giantsoudi, J. Adams, S. M. MacDonald, and H. Paganetti, "Proton treatment techniques for posterior fossa tumors: Consequences for linear energy transfer and dose-volume parameters for the brainstem and organs at risk," *International Journal of Radiation Oncology, Biology, Physics*, vol. 97, pp. 401–410, 2 2017. DOI: 10.1016/J.IJROBP.2016.09.042.

[105] M. Tambas *et al.*, "Current practice in proton therapy delivery in adult cancer patients across europe," *Radiotherapy and Oncology*, vol. 167, pp. 7–13, Feb. 2022. DOI: 10.1016/J.RADONC.2021.12.004.

[106] H. Paganetti *et al.*, "Report of the AAPM TG-256 on the relative biological effectiveness of proton beams in radiation therapy," *Medical Physics*, vol. 46, e53–e78, 3 2019. DOI: 10.1002/MP.13390.

[107] D. Sánchez-Parcerisa, M. López-Aguirre, A. Dolcet Llerena, and J. M. Udías, "MultiRBE: Treatment planning for protons with selective radiobiological effectiveness," *Medical Physics*, vol. 46, pp. 4276–4284, 9 2019. DOI: 10.1002/mp.13718.

[108] Y. An *et al.*, "Robust intensity-modulated proton therapy to reduce high linear energy transfer in organs at risk," *Medical Physics*, vol. 44, pp. 6138–6147, 12 2017. DOI: 10.1002/MP.12610.

[109] J. Unkelbach, P. Botas, D. Giantsoudi, B. L. Gorissen, and H. Paganetti, "Reoptimization of intensity modulated proton therapy plans based on linear energy transfer," *International Journal of Radiation Oncology, Biology, Physics*, vol. 96, pp. 1097–1106, 5 2016. DOI: 10.1016/J.IJROBP.2016.08.038.

[110] L. De Roeck *et al.*, "The european particle therapy network (EPTN) consensus on the follow-up of adult patients with brain and skull base tumours treated with photon or proton irradiation," *Radiotherapy and Oncology*, vol. 168, pp. 241–249, Mar. 2022. DOI: 10.1016/J.RADONC.2022.01.018.

[111] C. Hahn *et al.*, "Towards harmonizing clinical linear energy transfer (LET) reporting in proton radiotherapy: A european multi-centric study," *Acta Oncologica*, vol. 61, pp. 206–214, 2 2021. DOI: 10.1080/0284186X.2021.1992007.

[112] A. Niemierko *et al.*, "Brain necrosis in adult patients after proton therapy: Is there evidence for dependency on linear energy transfer?" *International Journal of Radiation Oncology, Biology, Physics*, vol. 109, pp. 109–119, 1 2021. DOI: 10.1016/J.IJROBP.2020.08.058.

[113] M. Garbacz *et al.*, "Study of relationship between dose, let and the risk of brain necrosis after proton therapy for skull base tumors," *Radiotherapy and Oncology*, vol. 163, pp. 143–149, Oct. 2021. DOI: 10.1016/J.RADONC.2021.08.015.

[114] D. Giantsoudi *et al.*, "Incidence of CNS injury for a cohort of 111 patients treated with proton therapy for medulloblastoma: LET and RBE associations for areas of injury," *International Journal of Radiation Oncology, Biology, Physics*, vol. 95, pp. 287–296, 1 2016. DOI: 10.1016/J.IJROBP.2015.09.015.

[115] H. Paganetti, "Relating the proton relative biological effectiveness to tumor control and normal tissue complication probabilities assuming interpatient variability in α/β," *Acta Oncologica*, vol. 56, pp. 1379–1386, 11 2017. DOI: 10.1080/0284186X.2017.1371325.

[116] S. J. McMahon, "Proton RBE models: Commonalities and differences," *Physics in Medicine and Biology*, vol. 66, 04NT02, 4 2021. DOI: 10.1088/1361-6560/abda98.

[117] C. Hahn *et al.*, "Impact of range uncertainty on clinical distributions of linear energy transfer and biological effectiveness in proton therapy," *Medical Physics*, vol. 47, pp. 6151–6162, 12 2020. DOI: 10.1002/MP.14560.

[118] R. Grün *et al.*, "Physical and biological factors determining the effective proton range," *Medical Physics*, vol. 40, p. 111 716, 11 2013. DOI: 10.1118/1.4824321.

[119] G. Magrin, H. Palmans, M. Stock, and D. Georg, "State-of-the-art and potential of experimental microdosimetry in ion-beam therapy," *Radiotherapy and Oncology*, vol. 182, p. 109 586, May 2023. DOI: 10.1016/J.RADONC.2023.109586.

[120] A. Lühr, C. von Neubeck, S. Helmbrecht, M. Baumann, W. Enghardt, and M. Krause, "Modeling in vivo relative biological effectiveness in particle therapy for clinically relevant endpoints," *Acta Oncologica*, vol. 56, pp. 1392–1398, 11 2017. DOI: 10.1080/0284186X.2017.1356468.

[121] J. M. DeCunha, M. Newpower, and R. Mohan, "GPU-accelerated calculation of proton microdosimetric spectra as a function of target size, proton energy, and bounding volume size," *Physics in Medicine and Biology*, vol. 68, 2023. DOI: 10.1088/1361-6560/ACE60A.

[122] L. Tian, C. Hahn, and A. Lühr, "An ion-independent phenomenological relative biological effectiveness (RBE) model for proton therapy," *Radiotherapy and Oncology*, vol. 174, pp. 69–76, Sep. 2022. DOI: 10.1016/J.RADONC.2022.06.023.

[123] E. Traneus and J. Öden, "Introducing proton track-end objectives in intensity modulated proton therapy optimization to reduce linear energy transfer and relative biological effectiveness in critical structures," *International Journal of Radiation Oncology, Biology, Physics*, vol. 103, pp. 747–757, 3 2019. DOI: 10.1016/j.ijrobp.2018.10.031.

[124] D. Giantsoudi, C. Grassberger, D. Craft, A. Niemierko, A. Trofimov, and H. Paganetti, "Linear energy transfer-guided optimization in intensity modulated proton therapy: Feasibility study and clinical potential," *International Journal of Radiation Oncology, Biology, Physics*, vol. 87, pp. 216–222, 1 2013. DOI: 10.1016/J.IJROBP.2013.05.013.

[125] C. Liu *et al.*, "Robust optimization for intensity modulated proton therapy to redistribute high linear energy transfer from nearby critical organs to tumors in head and neck cancer," *International journal of radiation Oncology, Biology, Physics*, vol. 107, pp. 181–193, 1 2020. DOI: 10.1016/J.IJROBP.2020.01.013.

[126] W. Gu, D. Ruan, W. Zou, L. Dong, and K. Sheng, "Linear energy transfer weighted beam orientation optimization for intensity-modulated proton therapy," *Medical Physics*, vol. 48, pp. 57–70, 1 2021. DOI: 10.1002/MP.14329.

[127] H. Henjum *et al.*, "The organ sparing potential of different biological optimization strategies in proton therapy," *Advances in Radiation Oncology*, vol. 6, 6 2021. DOI: 10.1016/J.ADRO.2021.100776.

[128] J. J. Wilkens and U. Oelfke, "A phenomenological model for the relative biological effectiveness in therapeutic proton beams," *Physics in Medicine and Biology*, vol. 49, p. 2811, 13 2004. DOI: 10.1088/0031-9155/49/13/004.

[129] A. Mairani *et al.*, "A phenomenological relative biological effectiveness approach for proton therapy based on an improved description of the mixed radiation field," *Physics in Medicine and Biology*, vol. 62, pp. 1378–1395, 4 2017. DOI: 10.1088/1361-6560/AA51F7.

[130] M. Belli, A. Campa, and I. Ermolli, "A semi-empirical approach to the evaluation of the relative biological effectiveness of therapeutic proton beams: The methodological framework," *Radiation Research*, vol. 148, pp. 592–598, 6 1997. DOI: 10.2307/3579735.

[131] Y. Chen and S. Ahmad, "Empirical model estimation of relative biological effectiveness for proton beam therapy," *Radiation Protection Dosimetry*, vol. 149, pp. 116–123, 2 2012. DOI: 10.1093/RPD/NCR218.

[132] B. Jones, "Towards achieving the full clinical potential of proton therapy by inclusion of LET and RBE models," *Cancers*, vol. 7, pp. 460–480, 1 2015. DOI: 10.3390/CANCERS7010460.

[133] M. Newpower *et al.*, "Using the proton energy spectrum and microdosimetry to model proton relative biological effectiveness," *International Journal of Radiation Oncology, Biology, Physics*, vol. 104, pp. 316–324, 2 2019. DOI: 10.1016/J.IJROBP.2019.01.094.

[134] C. Hahn *et al.*, "Comparing biological effectiveness guided plan optimization strategies for cranial proton therapy: Potential and challenges," *Radiation Oncology*, vol. 17, pp. 1–13, 1 2022. DOI: 10.1186/S13014-022-02143-X.

List of Publications

Journal Articles

L. Heuchel et al, "Clinical use and future requirements of relative biological effectiveness: Survey among all European proton therapy centers", Radiotherapy and Oncology, vol. 172, pp. 134-139, 2022, DOI: 10.1016/J.RADONC.2ß22.05.015.

L. Heuchel et al, "The dirty and clean dose concept: Towards creating proton therapy treatment plans with a photon-like dose response", Medical Physics, Oct 2023, DOI: 10.1002/mp.16809.

Conference Contributions

L. Heuchel et al, "Is a variable proton RBE considered in clinical practice? ESTRO survey among proton therapy centers", ESTRO annual meeting, Madrid (virtual) 2021 (Talk).

L. Heuchel et al, "Does reduction of variable RBE-weighted dose in organs at risk impact clinical proton plan quality?", AAPM annual meeting, Washington 2022 (Talk).

L. Heuchel et al, "Dirty Dose/Clean Dose – A novel concept to reduce uncertainty in proton relative biological effectiveness by optimizing high-LET dose contributions", PTCOG annual meeting, Madrid 2023 (Talk).

L. Heuchel et al, "Ganzkörperbestrahlungsplanung für die Translationsmethode: Monte-Carlo-Validierung des Feldzonenverfahrens", DGMP annual meeting, Magdeburg 2023 (Talk).

L. Heuchel et al, "Umfrage: Großfeldbestrahlungstechniken in Deutschland", DGMP annual meeting, Meeting of the working group on large field irradiation techniques, Magedburg 2023 (Talk).

Journal Articles in Preparation

L. Heuchel et al, "Monte-Carlo dose calculation for total body irradiation: dosimetric validation of the beam-zone method and comparison of different techniques", submitted: Medical Physics, November 2023.

L. Heuchel et al, "Large field irradiation techniques (total body irradiation, total skin irradiation and cranio-spinal irradiation) in Germany: Survey on the current clinical practice", in preparation.

Journal Articles not directly related to this Thesis

C. Hahn, L. Heuchel et al, "Comparing biological effectiveness guided plan optimization strategies for cranial proton therapy: potential and challenges", Radiation Oncology, vol. 17, issue 1, pp. 169-182, 2022, DOI: https://doi.org/10.1186/s13014-022-02143-x.

M. Schneider,..., L. Heuchel et al, "Combined proton radiography and irradiation for high-precision preclinical studies in small animals", Frontiers in Oncology, Aug 2022, DOI: 10.3389/FONC.2022.982417.

Danksagung

An dieser Stelle möchte ich mich bei allen bedanken, die mich in unterschiedlicher Form während meiner Promotion unterstützt haben.

Zunächst geht mein Dank an Prof. Dr. Armin Lühr für die Betreuung dieser Arbeit und die Möglichkeit diese Projekte durchführen und auch eigene Ideen verwirklichen zu können. Mein Dank gilt außerdem PD Dr. Christian Bäumer für die Ermöglichung der Zusammenarbeit mit dem WPE und der Übernahme des Zweitgutachtens dieser Arbeit.

Ich möchte mich bei allen Kollegen an der TU Dortmund bedanken, die für eine angenehme Arbeitsatmosphäre während meiner Promotion gesorgt haben. Insbesondere möchte ich mich bei Dr. Abdelkhalek Hammi für seine immerwährende Hilfsbereitschaft, bei Dr. Christian Hahn für die gute Zusammenarbeit in Lehre und Forschung sowie das kritische Lesen dieser Arbeit und bei Lisa-Marie Meier für die Beantwortung von allen meinen (noch so dummen) Fragen bedanken.

Herzlich danke ich außerdem meiner Familie und meinen Freunden, die mich während der gesamten Promotionszeit unterstütz haben, und für ihre Rücksichtnahme insbesondere in den sehr arbeitsintensiven Phasen.

Zu guter Letzt möchte ich mich bei Dr. Frank Schümann bedanken, meinem Physik-Lehrer in der Oberstufe und der erste, der mich ermutigt hat in die Physik zu gehen. Seine Begeisterung für die Physik war einfach ansteckend und ohne seine Worte (”Ich erwarte von dir, dass du einen Physik-LK belegst und danach Physik studieren gehst.”) hätte ich wahrscheinlich niemals Medizinphysik studiert.